

**An exploratory study into the effects of DNA and protein degradation in a laboratory based model and naturally aged porcine (*S scrofa*) teeth.**

by

Rene Human

Supervisor: Prof MJ Bester

Co-supervisor: Dr EN L'Abbe

Submitted in fulfillment of the requirements for the degree

**MSc. (Anatomy)**

In the School of Medicine, Faculty of Health Sciences,

University of Pretoria. South Africa

© University of Pretoria

2011

## **ABSTRACT**

In forensic anthropology, laboratory-based (LBM) and field-based (FM) models can be used to develop new methods and to research the stability and rate at which bio-molecules degrade. In this study, both these methods were used to investigate the effects that temperature, time after death (TAD) and other environmental factors had on the concentration of and change in molecular structure (increase in free pyrrole content, ninhydrin reactive nitrogen (NRN) and iron). of collagen, haemoglobin(Hb)and DNA in porcine teeth

For the LBM, porcine teeth were heated at 90<sup>0</sup>C for 0-4 hours, 1 hour intervals, (total number of teeth n=35). A porcine FM was established at the Miertjie Le Roux Experimental Farm of the University of Pretoria. From the decomposing pigs, teeth were collected at TAD intervals of 20 days (n=35). The morphology of the teeth were evaluated and recorded. Methods for collagen and DNA isolation, quantification of protein, collagen, haemoglobin (Hb), free pyrrole content (FPC), ninhydrin reactive nitrogen (NRN), total iron, Fe<sup>2+</sup> and Fe<sup>3+</sup> as well as a real-time PCR method for the detection of mitochondrial *cytb* gene in porcine teeth were established. These methods were used to determine the concentration and structural integrity of these molecules in the LBM and FM teeth.

The morphology of the LBM teeth was regular with only minor changes in colour with time heated. The collagen and Hb concentration did not change with time. A decrease in total iron (not statistically significant) and Fe<sup>3+</sup> (p=0.014; R<sup>2</sup>=0.74) was found and was associated with an increase in Fe<sup>2+</sup> (p=0.014; R<sup>2</sup>=0.965). No change in free pyrrole content was found. The total protein concentration determined using the Biuret method showed a decrease with time (p=0.009; R<sup>2</sup>=0.99). For DNA, a linear decrease in concentration (p=0.00; R<sup>2</sup>=0.93) was found. This DNA could still be used for the successful amplification of the *cytb* gene. As for DNA a similar decrease in NRN (p=0.00; R<sup>2</sup>=0.99) was also found whether this is related to protein or DNA degradation is unknown. From this data the total protein, DNA and NRN showed a definite time related change in concentration.

For the field model the teeth were brown, cracked, weathered and corroded. As for LBM, there were no time related changes in mass and collagen content. A significant decrease in total protein concentration (p=0.00; R<sup>2</sup>=0.52) and FPC (p=0.01; R<sup>2</sup>=0.98) was observed. Hb, FPC and iron levels (total iron, Fe<sup>3+</sup> and Fe<sup>2+</sup>) did not change with time but concentrations FPC and iron were higher than those found in the LBM. Also total protein concentration

although it decreases with time was also increased when compared to the LBM (sentence is awkward, re-word). This could be due to increase bacteria activity that results in an increase in protein biomass, iron accumulation and pyrolle synthesis. In contrast Hb levels were the same as LBM and are species specific and not related to increased bacterial activity. NRN showed a time related decrease in concentration ( $p=0.09$ ;  $R^2=0.99$ ) and was also twice that found in the LBM. This is related to decomposition of porcine protein and DNA as well as that derived from bacteria. A decrease in DNA concentration with time was found ( $p=0.00$ ;  $R^2=0.88$ ). DNA from all samples and could be used for the amplification of *cytb*.

In conclusion the LBM allows for rapid method development and the investigation of the effect of single factors on the integrity of bio-molecules such as protein and DNA. The FM can then be used to further investigate the effect of many additional environmental factors on the concentration and structure of the same bio-molecules. Using both models, it was found that total protein, DNA and NRN showed a time related change in concentration while the concentration of collagen and Hb remained constant.

## **DECLARATION**

I, Rene Human, declare that this dissertation is my own work except for the help from my supervisors. The thesis will be submitted for the degree Master of Science in Anatomy at the University of Pretoria. I has not been previously submitted for any other degree or examination at this or any other University.

Sign \_\_\_\_\_

This \_\_\_\_\_ day of \_\_\_\_\_ 2011.

## **ACKNOWLEDGEMENTS**

Firstly I would like to thank my supervisor Prof MJ Bester for her guidance, understanding and vital contributions to this project. Without your knowledge this would have been impossible. I would like to thank my co-supervisor Dr EN L'Abbé for your patience, all the editing and financial contribution to the project. Many thanks goes out to Ms Natalie Keough and Jolandie Myburgh for the use of the pigs from the Body Farm and for providing photos and any extra data.

I would like to thank the Department of Pharmacology and Chemical Pathology for the use of their equipment. Sincere thanks to Chantelle from Chemical Pathology for help with the PCR and gels.

Special thanks to Ms June Serem for her help in the laboratory, with all the writing and for lending a ear when I needed it.

A sincere token of appreciation to my father Mr Hugo Human, my mother Mrs Heather Human and especially my fiancé Mr A Baron for their unconditional love and support. To all my friends and family

Lastly I would like to dedicate this dissertation to my beloved brother Juan Human. May you lie safely in God's hands.

## TABLE OF CONTENTS

<b>TABLE OF CONTENTS</b>	i
<b>LIST OF TABLES</b>	iv
<b>LIST OF FIGURES</b>	vi
<b>LIST OF ABBREVIATIONS</b>	ix
<b>CHAPTER 1: INTRODUCTION</b>	1
1.1. Aims of the study	3
<b>CHAPTER 2: LITERATURE REVIEW</b>	5
2.1. Decomposition	5
2.1.1. Experimental models used to study the process of decomposition	7
2.1.2. The use of pigs in decomposition studies	9
2.1.3. Protein decomposition	10
2.1.4. Decomposition of fats	11
2.1.5. Decomposition of carbohydrates	13
2.1.6. Decomposition of DNA	14
2.2. Decomposition of bone and teeth	16
2.2.1. Acellular components	18
2.2.1.1. Specialised acellular tissue, cementum, enamel and dentine	18
2.2.1.2. Structure of collagen, biosynthesis and biochemical and microbial degradation of collagen	19
2.2.1.2.1. Structure of collagen	20
2.2.1.2.2. Biosynthesis of collagen	20
2.2.1.2.3. Biochemical degradation of collagen	21
2.2.1.2.4. Degradation of collagen during decomposition	22
2.2.2. Cellular components	24
2.2.2.1. Structure, biosynthesis, biochemical and microbial degradation of Hb	25
2.2.2.1.1. Structure of Hb	25
2.2.2.1.2. Biosynthesis of Hb	25
2.2.2.1.3. Biochemical degradation of Hb	26
2.2.2.1.4. Blood and the decomposition of Hb	26
2.2.2.2. Structure, biosynthesis, biochemical and microbial degradation of DNA	27
2.2.2.2.1. Structure of DNA	27
2.2.2.2.2. Biosynthesis of DNA	28
2.2.2.2.3. Biochemical degradation of DNA	29

2.2.2.2.4. Decomposition related changes to DNA structure	30
2.2.2.2.5. Amplification of mitochondrial DNA	32
<b>CHAPTER 3: MATERIALS AND METHODS</b>	<b>36</b>
3.1. Materials	36
3.1.1. Teeth	36
3.1.2. Reagents	36
3.1.3. Equipment	37
3.2. Methods	37
3.2.1. <i>In vitro</i> aging	37
3.2.2. Naturally aged teeth, field model	37
3.2.3. Experimental design	38
3.2.3.1. Collagen concentration	43
3.2.3.1.1. Isolation of collagen from the insoluble tooth fraction	43
3.2.3.2. Analysis of water soluble constituents	43
3.2.3.2.1. Determination of total protein content	43
3.2.3.2.2. Determination of total haemoglobin (Hb) content	44
3.2.3.2.3. Determination of pyrrole ring content	44
3.2.3.2.4. Determination of total iron content	44
3.2.3.2.5. Determination of ninhydrin reactive nitrogen (NRN)	45
3.2.3.2.6. Determination of DNA concentration, structure and integrity	45
3.2.3.2.6.1. DNA isolation	45
3.2.3.2.6.2. Analysis DNA quantity and quality	46
3.2.3.2.6.3. Agarose gel electrophoresis (AGE)	46
3.2.3.2.6.4. Detection of the $\beta$ -actin and cytochrome <i>b</i> gene	47
3.2.3.2.6.5. Agarose gel electrophoresis of PCR products	48
3.3. Data management	49
3.4. Statistical analysis	49
3.5. Ethical considerations	50
<b>CHAPTER 4: RESULTS AND DISCUSSION</b>	<b>51</b>
4.1 <i>In vitro</i> model	51
4.1.1. Water insoluble fraction	56
4.1.1.1. Collagen content of the teeth	56



4.1.2. Water soluble fraction	59
4.1.2.1. Protein, haemoglobin, pyrrole, iron and NRN present in the pulp cavity.	59
4.1.2.1.1. Protein	59
4.1.2.1.2. Heamoglobin	61
4.1.2.1.3. Pyrrole concentration	62
4.1.2.1.4. Iron content	63
4.1.2.1.5. Ninhydrin reactive nitrogen	65
4.1.2.1.6. DNA content	67
4.1.2.1.6.1. PCR amplification	70
4.1.3. Identification of bio-molecules as indicators of heating time	73
4.2. Field study	73
4.2.1. Water insoluble fraction	81
4.2.1.1. Collagen content	81
4.2.2. Water soluble fraction	83
4.2.2.1. Protein, haemoglobin, pyrrole, iron and NRN present in the pulp cavity.	83
4.2.2.1.1. Protein content	83
4.2.2.1.2. Heamoglobin content of the teeth	85
4.2.2.1.3. Pyrrole content	86
4.2.2.1.4. Iron content	87
4.2.2.1.5. Ninhydrin reactive nitrogen	88
4.2.2.1.6. DNA content	89
4.2.2.1.6.1. PCR amplification	92
4.2.3. Identification of bio-molecules as indicators of heating time	94
4.3 Comparison between <i>in vitro</i> and field models	95
<b>CHAPTER 5: CONCLUDING DISCUSSION</b>	96
<b>CHAPTER 6: REFERENCES</b>	98



## LIST OF TABLES

<b>Table 2.1</b>	Parameters for which can and cannot be controlled in each model	9
<b>Table 3.1</b>	A representation of the teeth collected from the field teeth. The coloured blocks indicate which teeth were used for the study. P= Pig number T= tooth number and PN= Pig nigella	40
<b>Table 3.2</b>	Parameters evaluated and techniques used	42
<b>Table 3.3</b>	Primer sequences from Bellis and associates (Bellis 2003., <i>et al</i> 2003)	48
<b>Table 4.1.1</b>	Mass of all teeth, <i>in vitro</i> study before and after freeze-drying.	55
<b>Table 4.1.2</b>	Percentage loss in mass of all teeth, <i>in vitro</i> study with freeze-drying.	56
<b>Table 4.1.3</b>	Collagen content, <i>in vitro</i> model	57
<b>Table 4.1.4</b>	Protein content, <i>in vitro</i> study	59
<b>Table 4.1.5</b>	Hb content, <i>in vitro</i> model	62
<b>Table 4.1.6</b>	Pyrrole content, <i>in vitro</i> model	63
<b>Table 4.1.7</b>	Total iron, Fe <sup>3+</sup> and Fe <sup>2+</sup> concentrations, <i>in vitro</i> model	64
<b>Table 4.1.8</b>	The ratio of Fe <sup>3+</sup> :Fe <sup>2+</sup> of all teeth in the <i>in vitro</i> model	64
<b>Table 4.1.9</b>	Ninhydrin positive components, <i>in vitro</i> model	65
<b>Table 4.1.10</b>	DNA content, <i>in vitro</i> study	67
<b>Table 4.1.11</b>	Summary: Line equations, R <sup>2</sup> and p-values of all the parameters measured	73
<b>Table 4.2.1</b>	Mass of all teeth collected from field study before and after freeze-drying	80
<b>Table 4.2.2</b>	Loss in mass of all teeth used in the field study with freeze-drying. (n=45)	81
<b>Table 4.2.3</b>	Collagen content, field model	81
<b>Table 4.2.4</b>	Protein concentration, field study	83
<b>Table 4.2.5</b>	Hb content, field study	86
<b>Table 4.2.6</b>	Pyrrole content, field study	87
<b>Table 4.2.7</b>	Total iron, Fe <sup>3+</sup> and Fe <sup>2+</sup> content, field study.	88
<b>Table 4.2.8</b>	The ratio of Fe <sup>3+</sup> :Fe <sup>2+</sup> , field study.	88
<b>Table 4.2.9</b>	Ninhydrin positive components, field study.	89
<b>Table 4.2.10</b>	DNA content, field study.	91
<b>Table 4.2.11</b>	Summary of line equations, R <sup>2</sup> and p-values of all the parameters measured	95

## LIST OF FIGURES

<b>Figure 2.1</b>	Summary of the different stages of human and animal decomposition. Intervals determined by data from Myburgh (2010).	7
<b>Figure 2.2</b>	The process and the products that form with protein decomposition. Adapted from Vass <i>et al.</i> , (2002).	11
<b>Figure 2.3</b>	The process and the products that form with fat decomposition. Adapted from Vass <i>et al.</i> , (2002).	13
<b>Figure 2.4</b>	The process and the products that form with carbohydrate decomposition. Adapted from Vass <i>et al.</i> , (2002).	14
<b>Figure 2.5</b>	The process and the products that form with DNA and RNA decomposition.	16
<b>Figure 2.6</b>	Structure of a typical tooth	18
<b>Figure 2.7</b>	Summary of the biosynthesis and the process and the products that form with collagen degradation/decomposition.	24
<b>Figure 2.8</b>	The physiological and post-mortem degradation of Hb.	27
<b>Figure 2.9</b>	Biochemical pathways initiated by oxygen, serum and glucose deprivation leading to nuclease activation and cell death. AIF: apoptosis initiating factor. Adapted from Alaeddini <i>et al.</i> , (2010).	29
<b>Figure 2.10</b>	Oxidation, hydrolytic and enzymatic attacks associated with DNA degradation. A: adenine, G: guanine, C: cytosine, T: thymine. Adapted from Alaeddini <i>et al.</i> , (2010).	31
<b>Figure 3.1</b>	A timeline indicating the collection periods of the teeth from the field study with Blue = 20-40 days, Orange = 40-60 days, Green = 60-80 days, Pink = 80-100 days and Yellow = 100+ days.	39
<b>Figure 4.1.1</b>	Typical morphology of porcine teeth heated for 0, 1, 2, 3 and 4 hours.	54
<b>Figure 4.1.2</b>	Mass of teeth after heating for 0-4 hours, before and after freeze-drying. Each data point is a mean $\pm$ SEM of three separate experiments, total number of teeth (n)=45. Average of three independent experiments. Samples with the same letters are statistically similar.	55
<b>Figure 4.1.3</b>	Collagen concentration <i>in vitro</i> model, after heating for 0-4 hours, demineralisation and solubilisation (A) determined by the Bradford method and (B) 230nm absorbance, (C) after desalting, absorbance 230nm absorbance and (D) then freeze-drying. Each data point is a mean $\pm$ SEM of three separate experiments, total population size (n)=45. Samples with the same letters are statistically similar.	58
<b>Figure 4.1.4</b>	Average protein content of the pulp cavity of the teeth, <i>in vitro study</i> , after heating for 0-4 hours determined using the (A) Bradford and (B) Biuret assay. Each data point is a mean $\pm$ SEM of three separate experiments, n=45. Samples with the same letters are statistically similar.	60

<b>Figure 4.1.5</b>	Hb content (mg/g) of the pulp cavity of the teeth used in the <i>in vitro</i> model determined using the Drabkin method. Each data point is a mean $\pm$ SEM of three separate experiments, n=45. Samples with the same letters are statistically similar.	62
<b>Figure 4.1.6</b>	Pyrrrole concentration (mg/g), model the pulp cavity of the teeth used in the <i>in vitro</i> model determined with fluorescence (Ex <sub>404nm</sub> and Em <sub>624nm</sub> ). Each data point is a mean $\pm$ SEM of three separate experiments, n=45. Samples with the same letters are statistically similar.	63
<b>Figure 4.1.7</b>	Total iron, Fe <sup>3+</sup> and Fe <sup>2+</sup> concentration of the pulp cavity of the teeth used in the <i>in vitro</i> model determined using Xylenol Orange. Each data point is a mean $\pm$ SEM of three separate experiments, n=45. Samples with the same letters are statistically similar.	64
<b>Figure 4.1.8</b>	NRN present in the pulp cavity after heating for 0-4 hours. Each data point is a mean $\pm$ SEM of three separate experiments, n=45. Samples with the same letters are statistically similar.	66
<b>Figure 4.1.9</b>	DNA concentration of the pulp cavity of the teeth heated 0-4 hours determined (A) from the 260 nm absorbance readings and (B) fluorescence following Hoechst binding. Each data point is a mean $\pm$ SEM of three separate experiments, n=45. Samples with the same letters are statistically similar.	68
<b>Figure 4.1.10</b>	Agarose gel electrophoresis (AGE) of the isolated DNA from samples heated for 0-4 hours. (10 $\mu$ l), Lane 1=236 $\mu$ g, lane 2=115 $\mu$ g, lane 3=188 $\mu$ g and lane 4=95 $\mu$ g and lane 5=135 $\mu$ g calculated from Hoe determination respectively.	70
<b>Figure 4.1.11</b>	RT-PCR amplification of 1) no template control, 2) human DNA (positive control 1, 3) porcine DNA (positive control 2), T0 and samples 4) T1, 5) T2, 6) T3 and 7) T4	72
<b>Figure 4.1.12</b>	Agarose gel electrophoresis, of PCR products derived from PCR amplification of DNA isolated from teeth that were heated for 0-4 hours. Lane 1: 100bp ladder, lane 2: human DNA, used as control, lane 3-7 contains T0, T1, T2, T3 and T4 respectively.	72
<b>Figure 4.2.1</b>	Decomposition of pig carcasses representing time intervals 20-40, 40-60, 60-80, 80-100 and 100+ days.	76
<b>Figure 4.2.2</b>	Typical tooth morphology found in field samples. Tooth descriptions according to Fernandez, Jalvo <i>et al.</i> , (2010).	78
<b>Figure 4.2.3</b>	Mass of teeth collected in field study, (a) before and (b) after freeze-drying. Each data point is a mean $\pm$ SEM of three separate experiments, n=45. Samples with the same letters are statistically similar.	80

<b>Figure 4.2.4</b>	Collagen concentration field model, after heating for 0-4 hours, demineralisation and solubilisation (A) determined by the Bradford method and (B) Absorbance at 230nm, (C) after desalting 230nm absorbance and (D) then freeze-drying. Each data point is a mean $\pm$ SEM of three separate experiments, n=45. Samples with the same letters are statistically similar.	82
<b>Figure 4.2.5</b>	Protein content of the pulp cavity of the teeth collected in the field study determined using the (a) Bradford and (b) Biuret assay. Each data point is a mean $\pm$ SEM of three separate experiments, n=45. Samples with the same letters are statistically similar.	84
<b>Figure 4.2.6</b>	Hb content (mg/g) of the pulp cavity of the teeth collected in the field study determined using the Drabkin method. Each data point is a mean $\pm$ SEM of three separate experiments, n=45. Samples with the same letters are statistically similar.	86
<b>Figure 4.2.7</b>	Pyrrole concentration of the pulp cavity of the teeth collected in the field study determined with fluorescence (Ex $_{404nm}$ and Em $_{624nm}$ ). Each data point is a mean $\pm$ SEM of three separate experiments, n=45. Samples with the same letters are statistically similar.	87
<b>Figure 4.2.8</b>	Total iron, Fe $^{3+}$ and Fe $^{2+}$ concentration of the pulp cavity of the teeth collected in the field study determined using Xylenol Orange. Each data point is a mean $\pm$ SEM of three separate experiments, n=45. Samples with the same letters are statistically similar.	88
<b>Figure 4.2.9</b>	NRN present in the pulp cavity of teeth collected in the field study. Each data point is a mean $\pm$ SEM of three separate experiments, n=45. Samples with the same letters are statistically similar.	89
<b>Figure 4.2.10</b>	DNA concentration of the pulp cavity of the teeth collected in the field study determined (A) from the 260 nm absorbance readings and (B) fluorescence following Hoechst binding. Each data point is a mean $\pm$ SEM of three separate experiments, n=45. Samples with the same letters are statistically similar.	91
<b>Figure 4.2.11</b>	Agarose gel electrophoresis (AGE) of the isolated DNA from samples collected in the field study. (20 $\mu$ l), Lane 1 =20.3 $\mu$ g, lane 2= 32.2 $\mu$ g, lane 3= 14.01 $\mu$ g and lane 4=21.29 $\mu$ g and lane 5=14.32 ug calculated from Hoe determination.	92
<b>Figure 4.2.12</b>	RT-PCR amplification of 1) no template control, 2) human DNA (positive control 1, 3) porcine DNA (positive control 2) and samples 8) 20-40, 9) 40-60, 10) 60-80, 11) 80-100 and 12) 100+ field samples.	93

**Figure 4.2.13** Agarose gel electrophoresis, of PCR products derived from amplification 94  
of DNA isolated from teeth that collected at 0-20, 20-40, 40-60, 60-80 and  
100+ days. Lane 1: 100bp ladder, lane 2: Hu=human DNA, used as  
control, lane 3-7 contains 20-40, 40-60, 60-80, 80-100, 100+ respectively



## LIST OF ABBREVIATIONS

$\mu\text{g/ml}$	Microgram per millilitre
<b>A</b>	Adenine
<b>AAR</b>	Aspartic acid racemisation
<b>CH<sub>3</sub>COOH</b>	acetic acid
<b>ACTB</b>	Beta-actin gene
<b>AGE</b>	Agarose gel electrophoresis
<b>ANOVA</b>	Analysis of variance
<b>AUCC</b>	Animal Use and Care Committee
<b>BP</b>	Before present
<b>bp</b>	Base pair
<b>BPB</b>	Bromophenol blue
<b>BSA</b>	Bovine serum albumin
<b>C=C</b>	Carbon carbon double bond
<b>CBB</b>	Coomassie Brilliant Blue
<b>cDNA</b>	Copy deoxyribonucleic acid
<b>CH<sub>3</sub>)<sub>2</sub>CHCH<sub>2</sub>CH<sub>2</sub>OH</b>	Isoamylalcohol
<b>CH<sub>3</sub>COOH</b>	Acetic acid
<b>CHCl<sub>3</sub></b>	Chloroform
<b>Cu<sup>2+</sup></b>	Copper ions
<b>CuSO<sub>4</sub></b>	Copper sulphate
<b>cyt <i>b</i></b>	Cytochrome <i>b</i> gene
<b>ddH<sub>2</sub>O</b>	Double distilled water
<b>DMT</b>	Dried mass of teeth
<b>DNA</b>	Deoxyribonucleic acid
<b>DPD</b>	Deoxypyridinoline
<b>EDTA,</b>	Ethylenediaminetetraacetic acid
<b>ELISA</b>	Enzyme-linked immunosorbent assay
<b>ER</b>	Endoplasmic reticulum
<b>EtBr</b>	Ethidium bromide
<b>EtOH</b>	Ethanol
<b>FABF</b>	Forensic Anthropology Body Farm
<b>Fe</b>	Iron
<b>Fe<sup>3+</sup></b>	Ferric iron
<b>Fe<sup>2+</sup></b>	Ferrous iron
<b>g</b>	Gram



<b>g/g</b>	Gram per gram
<b>GIT</b>	Gastrointestinal tract
<b>Gly</b>	Glycine
<b>GuaHCl</b>	Guanidine-HCl
<b>h</b>	Hour
<b>H<sub>2</sub>SO<sub>4</sub></b>	Sulphuric acid
<b>Hb</b>	Haemoglobin
<b>H-bonds</b>	Hydrogen bonds
<b>HCl</b>	Hydrochloric acid
<b>HMW</b>	High Molecular weight
<b>Hoe</b>	Hoechst
<b>HV2</b>	Hypervariable region 2
<b>HVR1</b>	Hypervariable region 1
<b>IDT</b>	Integrated DNA Technologies
<b>K<sub>3</sub>Fe(CN)<sub>6</sub></b>	Potassium ferricyanide
<b>KCN,</b>	Potassium cyanide
<b>KI</b>	Potassium iodide
<b>LDH</b>	Lactate dehydrogenase
<b>LMW</b>	Low molecular weight
<b>LSD</b>	Fisher's least significant difference
<b>Lys-OH</b>	Hydroxylysine
<b>M</b>	Molar
<b>m<sup>2</sup></b>	Square meters
<b>mg</b>	Milligram
<b>mg/g</b>	Milligram per gram
<b>MgCl<sub>2</sub></b>	Magnesiumchloride
<b>ml</b>	Millilitre
<b>mM</b>	Micromolar
<b>MMPs</b>	Matrix metalloproteinases
<b>mRNA</b>	Messenger ribonucleic acid
<b>mtDNA</b>	Mitochondrial deoxyribonucleic acid
<b>MT-MMPs</b>	Membrane type-MMPs
<b>Na<sub>2</sub>CO<sub>3</sub></b>	Sodium carbonate
<b>NaCl</b>	Sodium chloride
<b>NaClO<sub>4</sub></b>	Sodium perchlorate
<b>NADPH</b>	Nicotinamide adenine dinucleotide phosphate hydrogen



<b>NaHCO<sub>3</sub></b>	Sodium bicarbonate
<b>NaKC<sub>4</sub>H<sub>4</sub>O<sub>6</sub></b>	Sodium potassium tartrate
<b>NaOH</b>	Sodium hydroxide
<b>nDNA</b>	Nuclear deoxyribonucleic acid
<b>ng</b>	Nanogram
<b>nm</b>	Nanometer
<b>nm</b>	Nanometer
<b>NRN</b>	Ninhydrin reactive nitrogen
<b>NTx</b>	N-terminal telopeptide of type 1 collagen
<b>O<sub>2</sub></b>	Oxygen
<b>°C</b>	Celsius
<b>PCR</b>	Polymerase chain reaction
<b>pg</b>	Picogram
<b>pg/μl</b>	Picogram per microliter
<b>PMI</b>	Post-mortem interval
<b>PMSF</b>	Phenylmethanesulfonylfluoride
<b>Pro</b>	Proline
<b>Pro-OH</b>	Hydroxyproline
<b>qPCR</b>	Real-time quantitative PCR
<b>RFLP</b>	Restriction fragment length polymorphism
<b>RNA</b>	Ribonucleic acid
<b>rpm</b>	Revolutions per minute
<b>rRNA</b>	Ribosomal ribonucleic acid
<b>SAWS</b>	South African weather station
<b>SBS</b>	Solubilising buffer solution
<b>SD</b>	Standard deviation
<b>SDS</b>	Sodium dodecyl sulphate
<b>SDS-PAGE</b>	Sodiumdodecyl sulphate polyacryl gel electrophoresis
<b>SEM</b>	Scanning electron microscopy
<b>SEM</b>	Standard error of mean
<b>STR</b>	Short tandem repeats
<b>T</b>	Thymidine
<b>TAD</b>	Time after death
<b>TAE</b>	Tris base, acetic acid and EDTA
<b>Taq</b>	<i>Thermus aquaticus</i>
<b>TFe</b>	Total iron



<b>TLC</b>	Thin-layer chromatography
<b>T<sub>m</sub></b>	Melting temperature
<b>USA</b>	United States of America
<b>UV</b>	Ultraviolet
<b>V</b>	Volt
<b>VNTRs</b>	Variable number of tandem repeats
<b>XO</b>	Xylenol Orange
<b>α</b>	Alpha
<b>β</b>	Beta
<b>β-actin</b>	Beta actin gene
<b>γ</b>	Gamma
<b>μl</b>	Microliter
<b>μm</b>	Micrometer

## **CHAPTER 1: INTRODUCTION**

The estimation of the date of death from skeletal remains has important medico-legal implications (Prieto-Castello *et al.*, 2007). The need for the estimation of time since death requires information regarding decomposition. Decomposition is a complex process largely influenced by temperature and to a lesser extent by enzymatic digestion, bacterial action, environmental conditions (Vass *et al.*, 2002); and intrinsic factors that may alter the course of postmortem change (Prieto-Castello *et al.*, 2007). It is possible that the survival of certain biomolecules may aid in the investigation of the decomposition process and estimation of the postmortem interval (Vass *et al.*, 2002). Few scientific methods based on chemical measurements that can be used to provide information on the postmortem interval (PMI) exist (Vass *et al.*, 2002). Currently PMI estimation is based on visual assessment of the remains, determination of core body temperature, potassium contents of the vitreous humor and measurement of volatile fatty acids, and forensic entomology (Vass *et al.*, 2002). During decomposition large biomolecules are broken down into their building blocks and the presence of these smaller constituent units can be assessed and analysed (Vass *et al.*, 2002). Decay of bone and teeth releases simple chemical substances that have been studied by many researchers (Vass *et al.*, 2002; Dent *et al.*, 2004; Prieto-Castello 2007). Teeth can be used as a reliable indicator of age and several methods such as chemical, histological, morphological techniques have been employed (Ferreira *et al.*, 2008).

In many cases, human remains are severely decomposed or completely skeletonized (Von Wurmb-Schwark *et al.*, 2003; Dobberstein *et al.*, 2008) and an associated lengthy PMI, environmental conditions and degradation processes can alter the integrity of biomolecules and the reliability of molecular anthropological methods.

Teeth are the most durable structures of the human body and stay intact long after death even as other tissues disintegrate. For this reason teeth prove to be useful for both morphological and molecular studies and can reveal relevant information regarding the identification of unknown corpses through DNA analysis and time since death by the analysis of bio-molecules such as collagen (Evison *et al.*, 1997; Baker *et al.*, 2001; Von Wurmb-Schwark *et al.*, 2003; Budowle *et al.*, 2005; Dobberstein *et al.*, 2008).

Teeth consist of dentine, enamel, cementum and a pulp cavity that contains pulp, blood vessels and nerves. Enamel is the hardest substance in the body and consists of 96% inorganic material. Dentine calcifies similar to bone but it is much harder as it consists of 72% inorganic material (Ten Cate, 1994; Sweet and Hildebrand, 1998; Presecki *et al.*, 2000;

Malaver and Yunis, 2003). Furthermore the increased hydroxyapatite crystal content of teeth contributes to the greater stability of DNA found in teeth when compared to bone (Ten Cate, 1994). Due to hardness, stability and inertness of dentine the pulp content of the teeth is in a relatively isolated and sterile environment and therefore is an attractive system to use to assess the effects of environmental factors such as time and temperature on decomposition of biochemical constituents of tissue such as protein and DNA (Potsch *et al.*, 1992; Presecki *et al.*, 2000; Von Wurmb-Schwark *et al.*, 2003; Shiroma *et al.*, 2004; Da Silva and De Oliveira, 2008; Dobberstein *et al.*, 2008). The protein and DNA is derived from soft connective tissue, blood vessels, nerves and odontoblasts found within the pulp. Decomposition results in the degradation of tissue structure and the proteins and DNA contained within. Biomolecules will degrade at different rates depending on their structure and composition. The extraction of DNA from teeth can provide information regarding the rate or extent of decomposition as well as information regarding the identification of an individual.

Teeth provide an enclosed sterile environment which is an excellent source of biomolecules such as DNA, structural and functional proteins. With aging of bone many of these molecules will either denature or degrade (Malaver and Yunis, 2003). Researchers have endeavoured to identify biomolecules that can be used to determine the PMI especially in skeletal remains. In order to develop and standardize protocols to identify the PMI a simple reproducible model is required (Potsch *et al.*, 1992; Presecki *et al.*, 2000; Von Wurmb-Schwark *et al.*, 2003; Shiroma *et al.*, 2004; Da Silva and De Oliveira, 2008; Dobberstein *et al.*, 2008). For this reason many researchers use the *in vitro* bone model. The *in vitro* bone model, is a laboratory based model in which bone or teeth are artificially aged by heating the samples to 90°C for short time intervals. From this material the biomolecules such as DNA and collagen is isolated and the concentration and structural integrity of these biomolecules is determined. However this model does not into account the effect of environmental factors that contribute to natural aging but does provide an excellent system for the development new methods and furthermore to optimize, validate and standardize all methodologies (Von Wurmb-Schwark *et al.*, 2003; Dobberstein *et al.*, 2008).

The criteria used for further evaluation in a field model will be on the basis of (i) reproducibility, (ii) stability, (iii) variability with time. In a field model other factors such as such as temperature, humidity, rainfall, soil, bacteria will also contribute to aging are included. A field model usually consists of animals such as pigs which are of the same species and are similar in age and masses are place in a field and are exposed to the same

environmental conditions which are carefully recorded. A field model consisting of 40 pigs placed at different times during September 2008 to March 2009 has been established at the Miertjie le Roux experimental farm outside Pretoria. The pigs are of known weight, sex and age and were obtained from a local pig farmer and the pigs all died of a common bacterial infection.

Other than degradation of DNA and biomolecules, the environment alters the morphology of teeth during decomposition. The teeth become discoloured and brittleness increases. These changes can be accounted for by the changes in collagen content and total protein present in the sample. Thus a morphological study on teeth of decomposed teeth can aid even more in the assessment of decomposed remains and the integrity of such tissues. (Dobberstein *et al.*, 2008).

Several studies regarding the investigation of the degradation of DNA and other biomolecules have been conducted. Most studies, however focus on either mummified teeth, burned remains, ancient remains, buried remains, routine casework cases or drowned bodies (Hagelberg and Clegg, 1991; Richards and Sykes, 1995; Bender *et al.*, 2000; Baker *et al.*, 2001; Von Wurmb-Schwark *et al.*, 2003; Shiroma *et al.*, 2004; Von Wurmb-Schwark *et al.*, 2004; Ye *et al.*, 2004; Mitchell *et al.*, 2005; Nelson and Melton, 2007; Dobberstein *et al.*, 2008). These studies were, however, limited as the circumstances under which the samples were collected, were not controlled. Little information on the postmortem conditions of these cases was also known and a well established field model were lacking in all cases.

Therefore the aims of this study are to develop methodologies for the isolation of several biomolecules that alter in abundance and composition with aging. For this the *in vitro* aging model will be used. These molecules will then be measured in a field model to confirm their possible use as indicators of aging.

## **1.1 Aims**

To determine if the concentration of several major constituent bio-molecules found in decomposing porcine teeth changes with time.

The objectives of this study is to:

### 1. Establish methodologies

- (i) to determine the concentration of collagen, protein, haemoglobin, pyrroles, iron, ninhydrin reactive nitrogen and DNA,

- (ii) to isolate collagen and DNA, and
- (iii) to amplify the nuclear *ACTB* and mitochondrial *cytb* genes.

2. Use the abovementioned methods to determine if the concentration of these macromolecules change in porcine teeth using a laboratory based model (heating for 0-4 hours at 90°C) and a porcine field model (decomposition over a period of 100+ days).
3. Determine if the DNA isolated from both models is usable for PCR amplification of the nuclear *ACTB* and the mitochondrial *cytb* genes.
4. In both models identify bio-molecules that show a significant decrease in concentration with time, which is measured as induced heating or decomposition.

## **CHAPTER 2: LITERATURE REVIEW**

### **2.1. Decomposition**

Decomposition is the breakdown of an organism and it involves several processes which begin immediately after death. A summary of these processes are depicted in Figure 2.1 (Haglund and Sorg 1999; Dent *et al.*, 2004; Byers, 2008). Following death, cells are deprived of oxygen which causes them to rupture and release nutrient rich fluids. This process spreads to all tissues and eventually to the entire body. Autolysis (Vass *et al.*, 2002); which is initiated by digestive fluids residing in the intestinal tract, follows cellular damage and causes a general destruction of internal organs and a breakdown of carbohydrates, fat and protein by hydrolytic enzymes.

Putrefaction commences about 48 to 72 hours after autolysis and is dependent on environmental factors. Micro-organisms and bacteria present in the body degrade these soft tissues. In addition to the enzymes present in the soil, bacteria and fungi also contribute to soft tissue decay. Utilization and eventual depletion of the body's oxygen occurs and the environment changes from aerobic to anaerobic. The latter depletion favours anaerobic bacterial activity derived from the intestinal canal and the environment. Putrefaction is followed with liquefaction and disintegration of the body until skeletal material is left. Taphonomic factors such as animals, plants and chemical weathering also contributes to the degradation of a body (Haglund and Sorg, 1999; Vass *et al.*, 2002; Dent *et al.*, 2004; Byers, 2008).

Decomposition is described in five general stages namely fresh, bloat, active decay, advanced decay and dry (Payne, 1965; Haglund and Sorg, 1997; Haglund and Sorg, 2000). The fresh stage begins shortly after death (Carter *et al.*, 2007); and includes livor mortis (overall discolouration), rigor mortis (rigidity) and algor mortis (cooling) (Janaway *et al.*, 2009). Autolysis occurs in this stage. This involves chemical changes within the body, changes in pH and loss of the structural integrity of cells. Cellular enzymes are released which leads to the breakdown of surrounding cells and tissues. Putrefaction is initiated during this stage as aerobic bacteria deplete oxygen; anaerobic bacteria transform carbohydrates; and lipids, proteins and microbial proliferation takes place (Carter *et al.*, 2007). Organic acids such as propionic acid and lactic acid are formed and gases such as methane, hydrogen sulfide and ammonia are released (Carter *et al.*, 2007).

These actions lead to the bloating stage where gases accumulate within the body cavity and cause distension of the abdomen (Carter and Tibbett, 2008). Liquefaction of tissue and natural liquids take place and escape via the orifices (Janaway *et al.*, 2009). Haemoglobin is converted to sulfhaemoglobin within the intestine and is transported throughout the body via these gases (Pinheiro, 2006). The presence of maggot activity (Payne, 1965) is seen in this stage and, when combined with the accumulation of gases, leads to the release of fluids into the surrounding environment (Carter *et al.*, 2007). The next stage of decomposition involves active decay during which the greatest tissue mass loss is observed. Fluids and gases continue to purge from the body (Carter and Tibbett, 2008). Maggots and insects migrate away at the end of this stage to pupate (Carter *et al.*, 2007).

Active decay is followed with advanced decay and decomposition slows down (Carter and Tibbett, 2008). The loss of available soft tissue characterizes this stage (Carter and Tibbett, 2008) and insect activity is greatly reduced (Janaway *et al.*, 2009). The soil surrounding the decomposing remains presents with an increase in soil carbon and nutrients (phosphorous, potassium, calcium and magnesium) (Carter *et al.*, 2007); a change in soil pH; and an increase in soil nitrogen (Vass 1992). The last phase of decomposition involves skeletonization where bone, cartilage and dry skin are present (Payne, 1965; Haglund and Sorg, 1997; Haglund and Sorg, 2000). Taphonomic factors such as bleaching and chemical weathering of bone is seen during the later phases of this stage (Haglund and Sorg, 1997; Haglund and Sorg, 2000; Dent *et al.*, 2004).

Extrinsic and intrinsic factors such as temperature, availability of oxygen, prior embalming, burial, accessibility of remains to scavengers, trauma, humidity, rainfall, body size and weight, clothing, surface on which the body rests and food or objects within the digestive system largely affect the rate of decomposition (Haglund and Sorg, 1997; Haglund and Sorg, 2000; Dent *et al.*, 2004).

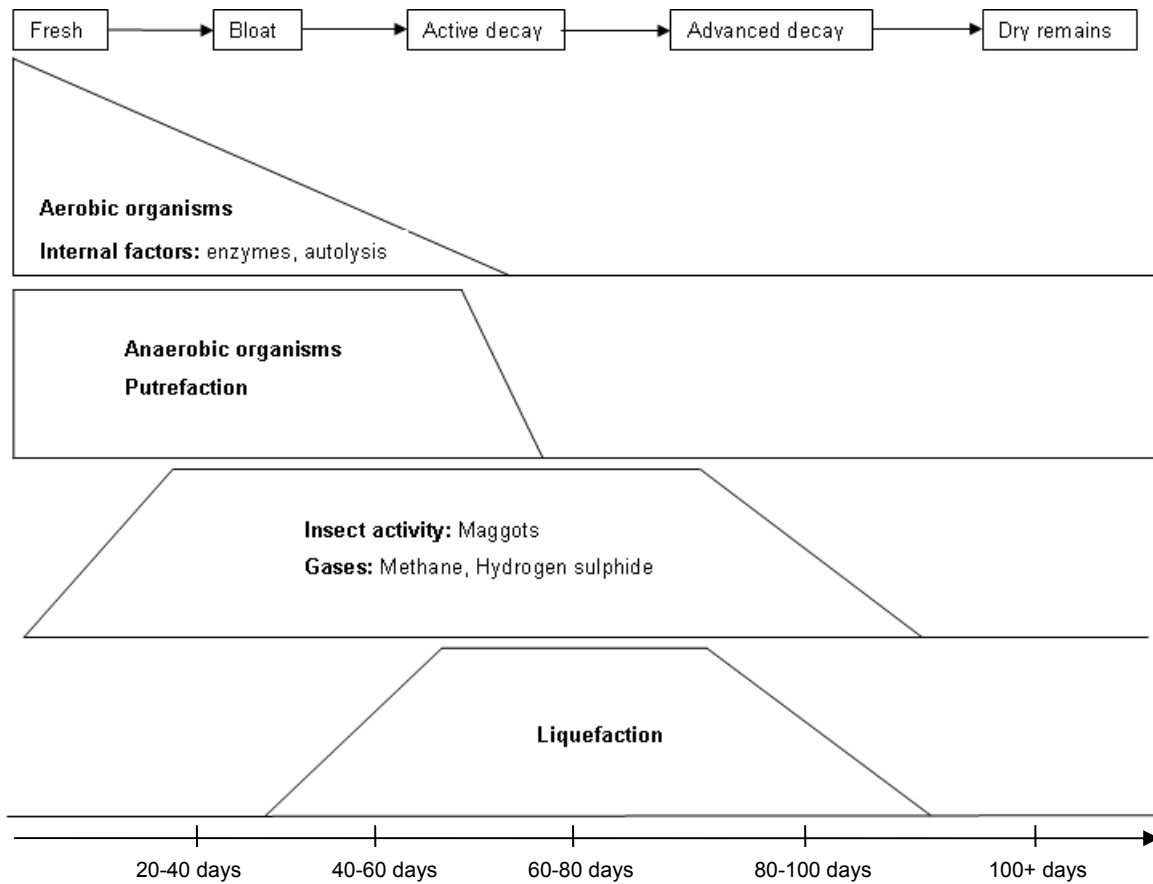


**Figure 2.1.** Summary of the different stages of human and animal decomposition. Intervals determined by data from Myburgh (2010).

### **2.1.1. Experimental models used to study the process of decomposition**

To investigate the processes involved in decomposition, human bodies or animal carcasses are placed in a field (field model) or are used in a laboratory based model (*in vitro* model), where many of the above-mentioned extrinsic factors can be controlled.

In field models, the post-mortem process is studied within a natural environment in which decomposition is monitored but not controlled. These research facilities, or body farms, are used to study the decomposition process in a variety of settings and circumstances.

Many universities in the USA have established decomposition facilities. The University of Tennessee in Knoxville started the first body farm in 1981. The farm comprises of a 10 000 m<sup>2</sup> or 2.5-acre wooded plot and contains numerous decomposing cadavers. The bodies are often exposed to different settings such as emersion in water or in a car trunk. Careful record, such as speed of decomposition and insect activity, are kept of all decomposition



processes. The cadavers are either donated bodies or unclaimed bodies (Bass and Jefferson, 2007).

The Western Carolina University has a similar facility in a mountain habitat (Cross *et al.*, 2009); although this facility is much smaller (Cross *et al.*, 2009); it is also used for cadaver dog training (Perotti *et al.*, 2009). Researchers at the Texas State University's Forensic Anthropology Research Facility investigate the decomposition of human remains under different topographical and climate conditions (Cross *et al.*, 2009); as well as the effect of vulture scavenging (Reeves, 2009). The facility further assists in medico-legal investigations (Reeves, 2009).

Sam Houston State University has a state-of-the-art research and training facility that is a 247-acre plot with a variety of environmental conditions and web cams that monitor post-mortem activities. The facility also provides training for forensic specialists, students, law enforcement and academicians (Bass and Jefferson, 2003).

California University of Pennsylvania recently established a body farm but it is not yet operational. Other facilities such as Roma Khan India have proposed creating such a body farm in India (Bass and Jefferson, 2003). In the United Kingdom, the University of Lancashire has an established body farm where cadavers dogs are used to smell out bodies, DNA research is conducted and the influence of decomposition on soil is investigated. A major limitation of body farms is that no two bodies are identical regarding factors such as age, weight and sex and this makes the reproducibility of experiments difficult.

Using a field model where animals such as pigs are used makes it possible to control for these differences and subsequently the effect of environmental factors alone can be studied. In many countries such as South Africa and the United Kingdom it is not feasible or permitted to use human material and pigs provide an easy solution. Such a facility has been established at the University of Pretoria by the Forensic Anthropology Research Centre of the Department of Anatomy (Myburgh, 2010).

A laboratory based model, or an *in vitro* model, has been used by several authors (Von Wurmb-Schwark *et al.*, 2003; Dobberstein *et al.*, 2008). In this model the decomposition process is further simplified and the effect of single parameters such as heat, alone, or heat and temperature in combination can be investigated. This laboratory based model has been

used to study the effect of storage, temperature, humidity on tooth morphology, extractable DNA, amplifiable DNA content, protein content as well as collagen content and structure (Garcia *et al.*, 1996; Pfeiffer *et al.*, 1999; Gotherstrom *et al.*, 2002; Von Wurmb-Schwark *et al.*, 2003; Dobberstein *et al.*, 2008; Rubio *et al.*, 2009). The greatest benefit of laboratory models is that they can be used to identify factors that may hamper DNA extraction and amplification and are useful for the development of techniques and optimisation of methodologies (Von Wurmb-Schwark *et al.*, 2003). But, a major limitation of these models is that they only take the effect of temperature on time after death into account and not other environmental factors such as soil composition and pH or humidity and rainfall. Also, the number of teeth used in these studies is small and comparisons with other projects are difficult. A better way to determine the effect of all environmental factors on bone decomposition is to use a field model (Von Wurmb-Schwark *et al.*, 2003; Dobberstein *et al.*, 2008; Rubio *et al.*, 2009).

Other models include the use of samples originating from forensic case works or archaeological collections. The origin and circumstances of these samples are often limited or unknown (Dobberstein *et al.*, 2008). A body represents one sample in a particular condition and circumstance. Therefore, the data that is generated is insufficient for statistical analysis.

There are considerable differences between these models (summarized in Table 2.1) and these factors must be taken into account when designing experiments and in analysing and interpreting data.

**Table 2.1: Parameters for which can and cannot be controlled in each model**

<u>Experimental system</u>	<u>Physiological factors</u>			<u>Environmental factors</u>	<u>Reproducibility of experiments</u>	<u>Microbial activity</u>
	<u>Age</u>	<u>Mass</u>	<u>Sex</u>			
<b>Naturally decomposing body/animal</b>	X	X	X	Usually unknown	Insufficient number of samples for meaningful reproducibility	Normal natural process has occurred
<b>Field model</b>	√	√	√	Recorded	Limited reproducibility	Reflects above
<b><i>In vitro</i> model</b>	√	√	√	Controlled	All parameters are controlled excellent reproducibility	Absent

### **2.1.2. The use of pigs in decomposition studies**

Pigs are frequently used and are considered excellent models for human decomposition studies (Anderson and Hobischak, 2004). Pigs and humans have similar skin, muscle and

hair structure (Campobasso *et al.*, 2001; Anderson and Hobischak, 2004). Pigs are omnivores with similar intestinal fauna. The stomachs of both animals are glandular and are lined with cardiac, pyloric and gastric mucosa. Both humans and pigs have long small intestine and the colon is sacculated with haustrae. The pH values of the gastrointestinal tract (GIT) of humans and pigs are similar. For pigs, these are stomach pH of 2.2-4.3, small intestine pH of 6.0-6.9 and colon, pH=6.8. While for the human the pH of the stomach is 1.5-3.5, the small intestine is pH of 5-7 and the colon, pH of 5.5-7.0. Humans and pigs contain similar gut flora such as *E. coli* (Kararli, 1995).

The progression of human and pig decomposition is similar (Campobasso *et al.*, 2001). Decomposition studies show that decomposing human and pig carcasses attract similar taxa of carrion and other insects (Schoenly and Hall, 2002). Iris discolouration and pigmentation is used for the estimation of the PMI in humans. Pigs have a similar eye structure and are used in such cases to study this taphonomic artefact (Abraham *et al.*, 2008). In many situations where an ethical restriction limits the use of human cadavers in decomposition studies, pigs have been found to be a reliable alternative (Voss *et al.*, 2008). In addition pigs are genetically homologous and there is not much variation between the species. In these studies the size, mass, age and sex of the pigs used can also be selected.

### **2.1.3. Protein decomposition**

Degradation is a function of the localisation, physiological function and structure of the protein. Epithelial cells of the GIT mucosa and closely associated neurons are the first to be degraded as these cells are in close contact with the proteolytic enzymes and intestinal bacteria present in the GIT. In contrast, the more resistant proteins to degradation are found in the epidermis of the skin and bone. The resistance of the skin to degradation is related to the structure and proteins present in the stratum corneum. The stratum corneum consists of layers of flattened fused cell remnants containing fibrous protein such as collagen and keratin which are highly resistant to proteolytic digestion. Both collagen and keratin have a high glycine or/and proline content, have a secondary helix structure with strong inter and intramolecular bonds which contributes to the stability of these molecules and a resistance to proteolytic digestion (Vass *et al.*, 2002; Dent *et al.*, 2004).

During decomposition, proteins are broken down by proteases. Proteolysis does not occur at a constant rate and this may be a function of structure but also localisation. For example, the degradation rate of albumin in the liver will differ from that found in the skin. Proteolysis results in protein fragmentation and further digestion causes the release of protein peptones,

proteoses, polypeptides and amino acids as summarised in Figure 2.2 (Vass *et al.*, 2002; Dent *et al.*, 2004).

Phenolic substances such as skatole and indole are released with continuing proteolysis. Gases; carbon dioxide, hydrogen sulphide, methane and ammonia are eventually released. With further decomposition sulphur containing amino acids undergo desulphurhydratation and yield hydrogen sulphide gas, sulphides, ammonia, thiols and pyruvic acid. Decarboxylation occurs during proteolysis and this process leads to the evolution of two gases known as putrescine and cadaverine. Putrescine is derived from ornithine while cadaverine is derived from lysine. These gases, together with hydrogen sulphide and methane, are present in soils where bodies are decomposing (Vass *et al.*, 2002; Dent *et al.*, 2004). According to Vass *et al.*, (2002), putrescine and cadaverine are not suitable as biomarkers while amino acids are significant post-mortem interval (PMI) indicators.

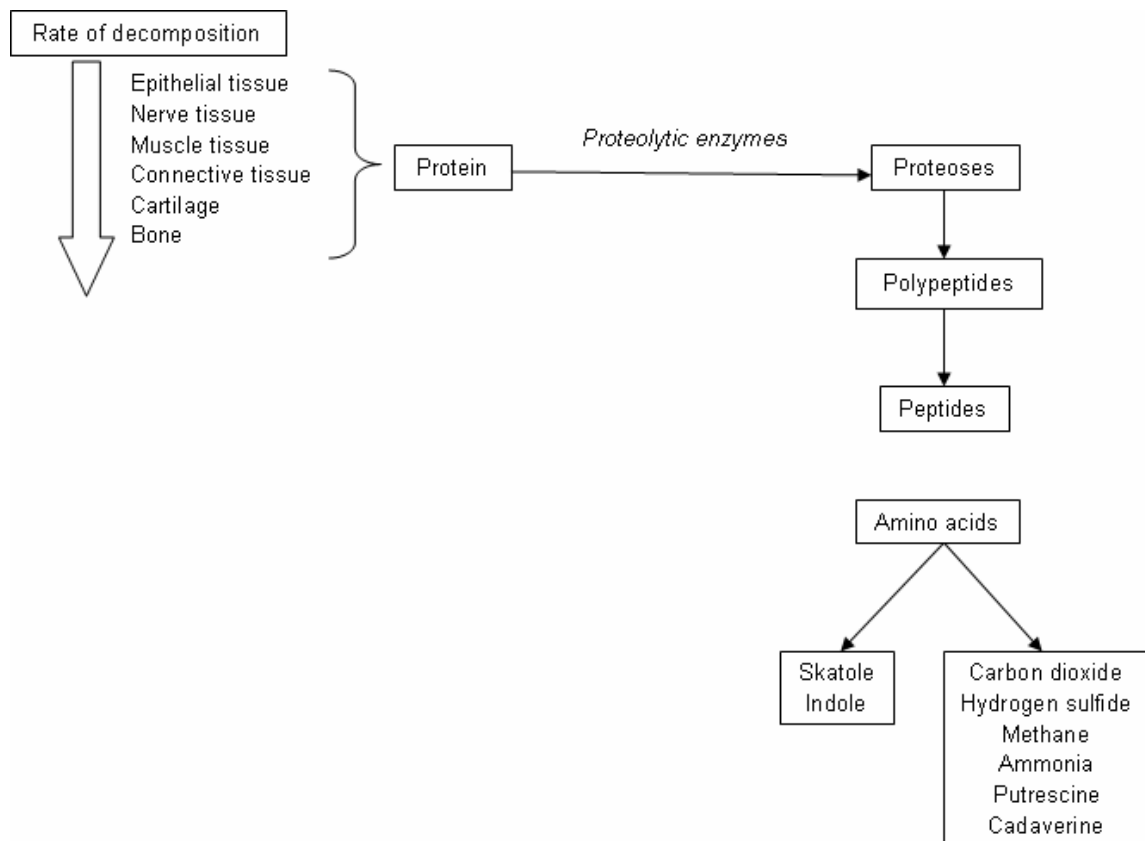


**Figure 2.2.** The process and the products that form with protein decomposition. Adapted from Vass *et al.*, (2002).

#### **2.1.4.Fat decomposition**

Lipids occur as fats found mainly in adipose tissue or as structural components of membranes. The basic structure of lipids is triacylglycerol bonded by ester linkages to three fatty acids. The most abundant fatty acids in adipose tissue are mono-unsaturated oleic acid

followed by linoleic, palmitoleic and palmitic acid. During decomposition of adipose tissue, the triglycerides undergo hydrolysis to yield free triacylglycerol and the fatty acids. Intrinsic lipase activity and bacterial activity cause the formation of stearic, oleic and palmitic acids. Fatty acids salts are formed through the reaction of these fatty acids with potassium and sodium present in tissue fluids. Potassium and sodium are then replaced with magnesium and calcium ions and form water and insoluble soaps known as adipocere (Figure 2.3). Small amounts of hydroxy-fatty acids may be formed that are hydrolysed to oxy-fatty acids. Alternatively these fatty acids can undergo oxidation due to aerobic metabolism by bacteria, fungi and atmospheric oxygen. This leads to the formation of ketones and aldehydes. Further degradation of fatty acids and glycerol leads to the release of water and carbon dioxide (Vass *et al.*, 2002; Dent *et al.*, 2004).

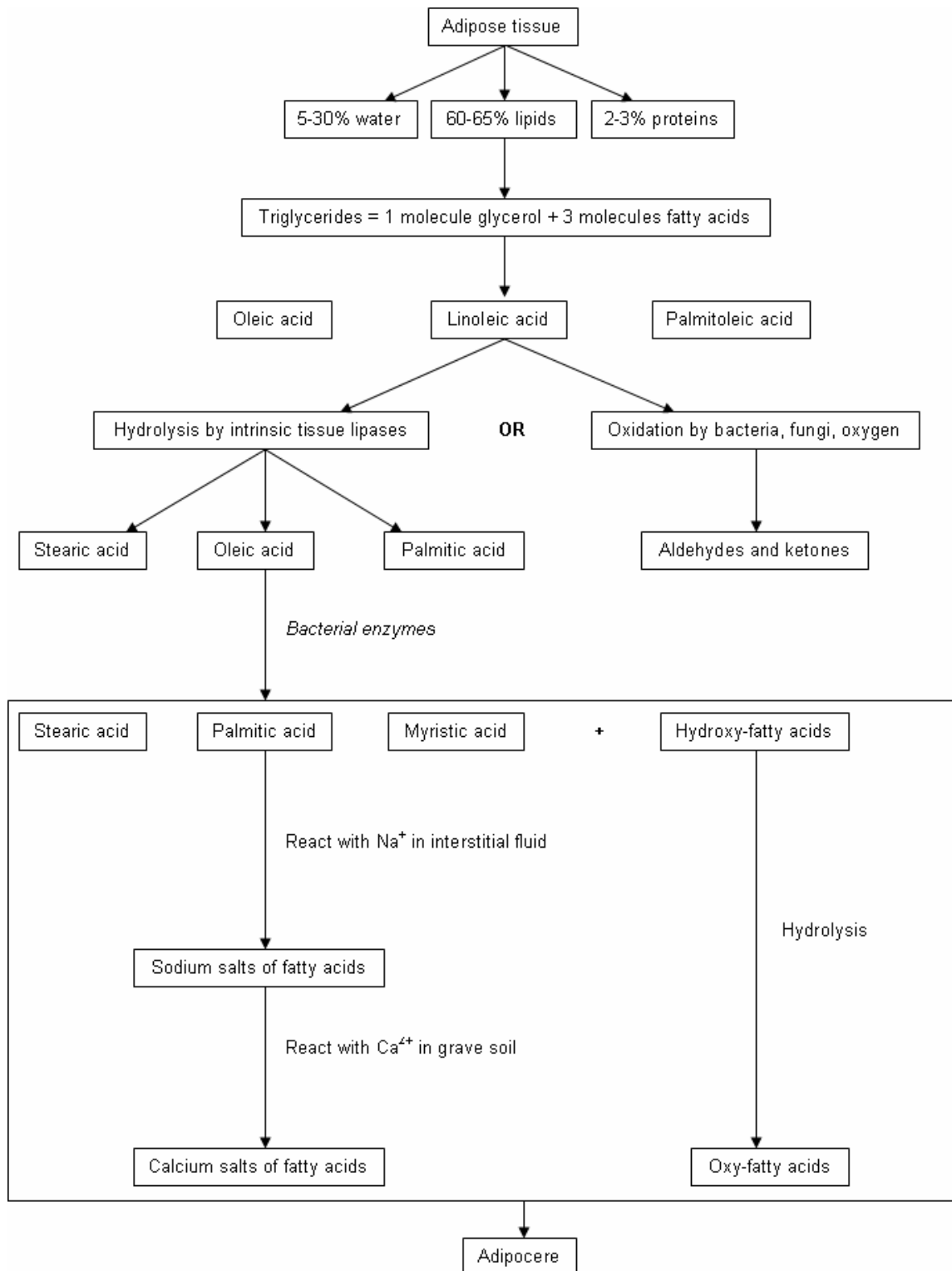


**Figure 2.3.** The process and the products that form with fat decomposition. Adapted from Vass *et al.*, (2002).

**2.1.5. Decomposition of carbohydrates**

Carbohydrates are polymers that consist of several monomers and during the early stages of decomposition, polysaccharides, such as glycogen found in the liver, are broken down to

sugars or glucose monomers. These sugars can be completely oxidized into carbon dioxide and water or may form organic acids and alcohols. Organic acids formed by the decomposition of fungi include glycuronic acid, citric acid and oxalic acid. Bacteria decompose carbohydrates either anaerobically or aerobically. Lactic acid, butyric acid, acetic acid and alcohols (butyl alcohol, ethyl alcohol and acetone) are produced under anaerobic conditions. Aerobic decomposition of carbohydrates by bacteria produces carbon dioxide and water through the citric acid cycle. Methane, hydrogen and hydrogen sulphide are also produced via bacterial carbohydrate fermentation. These processes are summarized in Figure 2.4 (Vass *et al.*, 2002; Dent *et al.*, 2004).

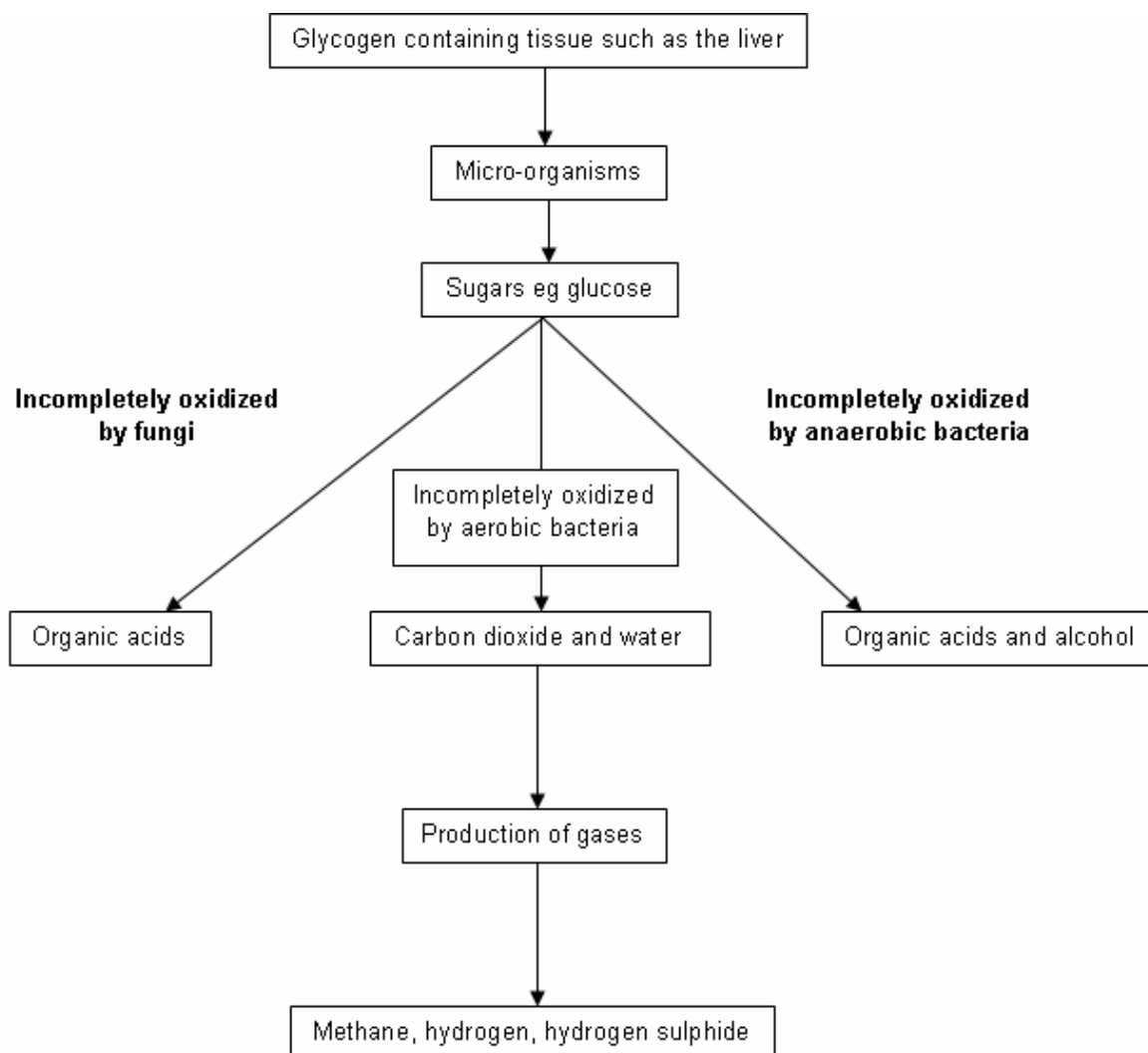


**Figure 2.4.** The process and the products that form with carbohydrate decomposition. Adapted from Vass *et al.*, (2002).

### **2.1.6. Decomposition of DNA**

The thermodynamic degradation of DNA involves the breaking of the double-stranded helix by the disintegration of the hydrogen bonds between the duplex. Stacking energies exist

between the purine and pyrimidine bases which are less for A:T rich regions. Therefore, these regions denature more readily. DNA denaturation occurs when DNA is heated above its melting temperature but also biologically when DNA replication and transcription occurs and is initiated at the TATA box region (Ussery, 2000).

DNA degradation in bones and teeth is not fully understood as DNA degradation is linked to the crystallinity (hydroxyapatite) and to the collagen content of teeth. In contrast, DNA degradation in other soft tissue types is well understood. DNA degradation in forensic or archaeological bone and tooth samples are the result of UV-light, humidity, elevated temperatures as well as bacterial and fungal contamination (Dobberstein 2008; Rubio *et al.*, 2009). After death oxidative processes, cellular nucleases and hydrolytic enzymes cause chromosomal DNA degradation. Hydrolytic enzymes are released when cellular and subcellular membranes decay during autolysis (Kaiser *et al.*, 2008). The process of DNA cleavage by nucleases specifically endonucleases is activated following the proteolytic removal of histone proteins during cell death. Direct hydrolysis or destabilisation cause single strand breaks due to the cleavage of the phosphate sugar backbone. Double strand breaks is the result of the cleavage of both strands. These strand breaks can be identified by the presence of low molecular weight DNA fragments. Hydrolytic damage causes deamination of cytosine and 5-methylcytosine into uracil and thymine residues, respectively (Mitchell *et al.*, 2005). Other changes to the nucleotide residues include the modification of pyrimidines and sugar residues, the formation of abasic sites and interstrand cross-links as well as methylation, hydroxylation and thymindimerisation (Dobberstein *et al.*, 2008).



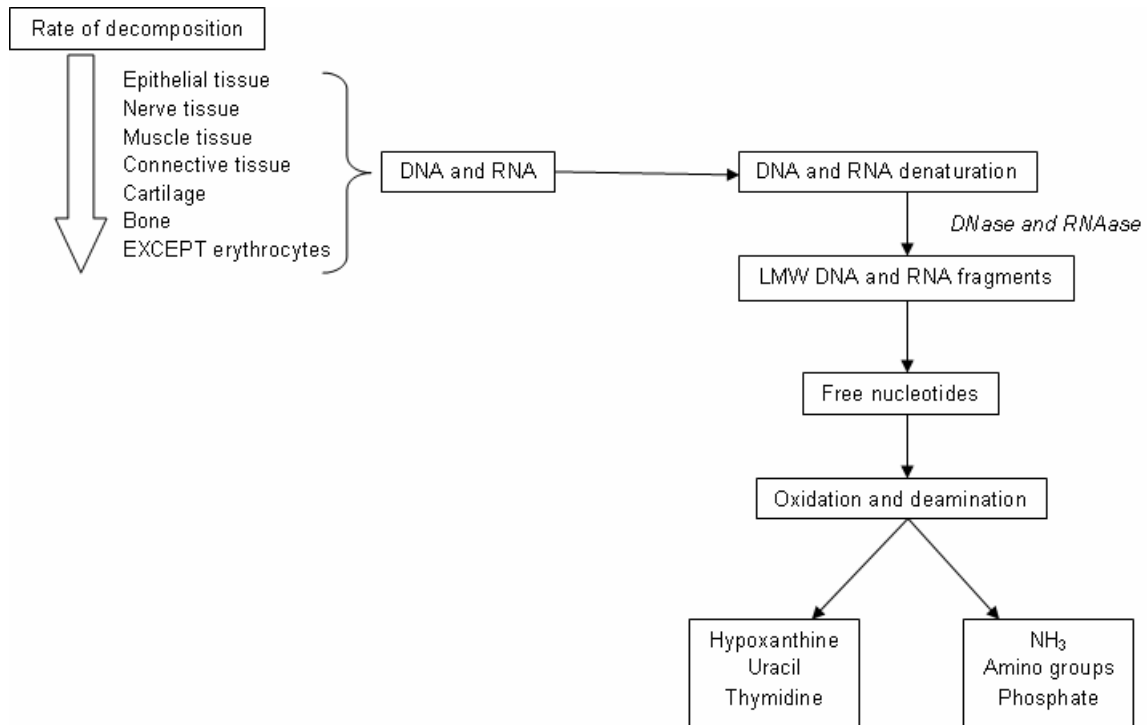


**Figure 2.5.**The process and the products that form with DNA and RNA decomposition.

## **2.2. Decomposition of bone and teeth**

The skeleton is often the only material that remains of an individual that can be used for identification. Using these skeletal remains in most instances only the sex, age, stature, probable age (child, adolescent, adult or elderly) and ancestry of the individual can be determined. Cause of death may be ascertained from fracture patterns, however, this is far more tricky. The teeth are the most resistant to decomposition and this is often the only remaining material from which DNA can be isolated and be used for specific identification of an individual (Dobberstein *et al.*, 2008).

As this study focuses on changes in the concentration and structural integrity of major bio-molecules found in teeth, the change of this structure of these bio-molecules will be described in more detail. The anatomical, tissue and cellular structure will also be described. In addition a short description of the structure, biosynthesis and degradation of the most abundant proteins, namely collagen and haemoglobin as well as DNA will be included.

Bones and teeth are composed of a protein fraction (mainly collagen), a mineral component (hydroxyapatite) and ground substance (mucopolysaccharides and glycoproteins). Bacterial action degrades collagen. Bacteria that produce collagenases degrade the collagen into peptides and then into amino acids which leach away. The inorganic mineral,

hydroxyapatite, is lost by inorganic mineral weathering in which calcium ions are replaced by protons. The ions are also substituted, infiltrated and absorbed and the bone becomes more susceptible to breaking, fragmentation and eventual disintegration (Dent *et al.*, 2004).

In living tissue there is a continuous turnover of bio-molecules. Understanding these biosynthesis pathways provides information as to the types of building blocks of bio-molecules that are found in tissue. In contrast, degradation pathways provide information on the breakdown products as well as clues regarding the mechanisms in which microbes degrade bio-molecules. For this reason the biosynthesis, normal biochemical as well as microbial degradation will be discussed.

Four types of teeth can be differentiated and are the incisors, canines, premolars and molars. All teeth exhibit the same basic structure and consist of the crown, neck and root as shown in Figure 2.6. The anatomical crown covered with enamel extends above the jaw while the anatomical root covered with cementum is located within the jaw. Between the anatomical crown and the anatomical root is the neck section. The bulk of the tooth is made up of dentine, a tissue type similar to bone. Contained within the dentine layer is the pulp cavity which follows the shape of the tooth. The pulp cavity is made up of soft connective tissue which contains blood vessels and nerves that enter the tooth through the apical foramen (Ten Cate, 1992; Coetzee *et al.*, 2003, 282-4; Ross *et al.*, 2003). Three specialized acellular tissues types make up teeth and these are the cementum, enamel and dentine.

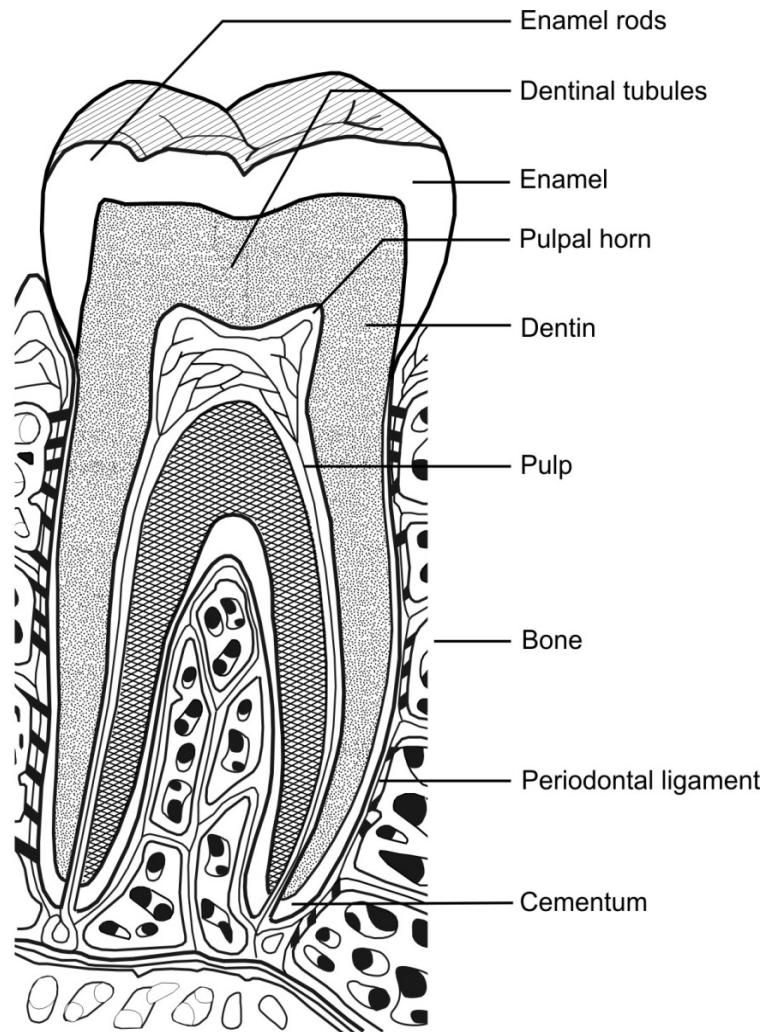


**Figure 2.6.** Structure of a typical tooth

## **2.2.1.Acellular components**

### **2.2.1.1.Specialised acellular tissue, cementum, enamel and dentine**

Dentine is a hard, yellowish white avascular tissue that forms the bulk of the tooth and is more resilient than enamel. Approximately 70% of dentine is mineralized with hydroxyapatite. The organic component of dentine consists mainly of fibrous protein collagen. Dentine is permeated by closely packed tubules that traverse the entire thickness and contain the cytoplasmic extensions of the odontoblasts. The cell bodies of the odontoblasts are aligned along the inner edge of the dentine to form the peripheral boundary of the dental pulp. Dentine is a sensitive tissue and capable of repair.

Three types of dentin can be recognized namely primary, secondary and tertiary dentine. The primary dentine forms most of the tooth and outlines the pulp chamber. Primary dentine has an outer layer that is called the mantle dentine and is the first layer that is formed by

newly differentiated odontoblasts. The layer consists of ground substance that contains no phosphophoryn and loosely packed collagen fibrils. The rest of the dentine is the circumpulpal dentine. Secondary dentine forms after the completion of root formation and represent the continuing but slower process of dentine deposition by odontoblasts. Secondary dentine is a tubular structure that has an incremental pattern and is continuous with primary dentine. The secondary dentine is deposited in an uneven manner around the periphery of the pulp space. Secondary dentine scleroses more easily than primary dentine thereby reducing the permeability of the dentine and protecting the pulp. Tertiary dentine is also known as reactive, reparative or irregular secondary dentine and is produced in response to noxious stimuli such as caries. Tertiary dentine is produced by cells that are directly affected by the stimulus. Tertiary dentine displays a sparse, irregular tubular pattern with many cellular inclusions, osteodentine that contain cells that secrete collagen type I and III (Ten Cate, 1994).

The enamel is the hardest substance found in teeth and consists of approximately 96% inorganic salts of which 90% consists of calcium phosphate in the form of apatite or hydroxyapatite. Hydroxyapatite is arranged in rods 4µm wide and 8µm high. Enamel crystals can be found in the spaces between the enamel rods. Adult enamel is acellular and contains very little organic material(Ten Cate, 1994; Coetzee *et al.*, 2003, 282-4; Ross *et al.*, 2003).

Cementum is a hard, bone-like tissue that covers the dentin on the roots of the teeth. It is avascular and consists largely of collagen. Two types of cementum are differentiated. Acellular cementum covers the root dentin from the cervical margin to the root apex; whereas cellular cementum covers the acellular cementum that contains the cementoblasts. The cementoblasts lie in lacunae in a similar way in which osteocytes lie in bone lacunae. The cementum anchors the fibers of the periodontal ligament to the roots of the teeth (Ten Cate, 1994).

#### **2.2.1.2. Structure of collagen, biosynthesis, biochemical and microbial degradation**

Proteins present in the acellular fraction such as collagen, albumin and alpha-2HS-glycoprotein has a high affinity for hydroxyapatite (Grupe, 1995; Dent *et al.*, 2004). Collagen is the major fibrous protein present in teeth. It is water insoluble and provides strength and flexibility to tissue (Higham and Petchey, 2000). To date at least 27 types of collagen have been identified (Lui *et al.*, 2007) and are classified according to the degree of helical and non-helical structures, the amount of hydroxylysine and the monomer combinations present within them (Balzer *et al.*, 1997; Coetzee *et al.*, 2003; Ross *et al.*, 2003).

#### **2.2.1.2.1. Structure of collagen**

Collagen fibres have a high tensile strength and consist of fibres that are 1-12 $\mu$ m thick. Each fibre consists of parallel, longitudinal collagen fibrils that are approximately 0.2-0.5 $\mu$ m in diameter (Coetzee *et al.*, 2003, 74-5; Ross *et al.*, 2003). These fibrils are divided further into parallel, longitudinal microfibrils which are 20 to 100nm thick. Each microfibril in turn is composed of collagen molecules or tropocollagen. A microfibril is formed when collagen molecules align head to tail in overlapping rows. A collagen molecule measures 300nm long and 1.5nm thick and is a triple helix composed of three spiralling polypeptide chains. The polypeptide chains,  $\alpha$ -chains are composed of proline (Pro), glycine (Gly), hydroxyproline (Pro-OH) and hydroxylysine (Lys-OH) molecules. A Gly molecule is always the third molecule in the  $\alpha$  chain except at the ends of the chain. Each Gly in the  $\alpha$ -chain is usually preceded by a Pro-OH or Lys-OH molecule and followed by a Pro molecule. Therefore, they are repeated as x-Pro-Gly or x-Hyp-Gly where Pro and Pro-OH make up 30% of the total amino acid composition of collagen (Lui *et al.*, 2007).

Gly, Pro and Pro-OH are responsible for the structural integrity of the alpha chain (Coetzee *et al.*, 2003, 74-5; Ross *et al.*, 2003; Lui *et al.*, 2007). The secondary structure namely hydrogen bonds involving Pro-OH and the tertiary electrostatic interactions between Lys-OH and Lys impart stability to the collagen molecule. Sugar groups can also bind to the Lys-OH residues (Coetzee *et al.*, 2003, 74-5; Ross *et al.*, 2003; Lui *et al.*, 2007). Cross-linking also occurs between Lys and histidine (His) residues and the amount of these bonds increase with age of the organism (Campbell and Farrell, 2006). Intramolecular cross-links occur between two  $\alpha$ -chains in the non-helical section of the same molecule by means of aldol condensation of two aldehydes. Intermolecular cross-linking, on the other hand, takes place between the telopeptide region of one molecule and the helical region of a quarterly staggered, adjacent molecule. Dimers of  $\alpha$ -chains are designated beta ( $\beta$ ) components while trimers of three  $\alpha$ -chains are designated gamma ( $\gamma$ ) components (Lui *et al.*, 2007).

Different types of collagen can be identified according to the combinations of  $\alpha$ -chains found within their collagen structure. Teeth consist of dense connective tissue and is thus composed of type I collagen. Type I collagen consists of two similar alpha chains ( $\alpha$ 1) and a third different alpha chain ( $\alpha$ 2) (Ross *et al.*, 2003); therefore collagen is a triple helix.

#### **2.2.1.2.2. Biosynthesis of collagen**

Several intracellular and extracellular steps are involved in the synthesis of collagen. Intracellular biosynthesis within the osteoblast involves DNA transcription to mRNA and then

the translation to form polypeptides of 1400 amino acids that serve as the precursors for the  $\alpha$ -chain. The latter step occurs in the polysomes that are bound to the endoplasmic reticulum (ER). The polypeptide chain then passes through the ribosomal membrane and enters into the cisternae of the ER. The peptidyl Pro and Lys residues then undergo hydroxylation followed by the formation of the helix structure. Inter and intramolecular cross-links are established and glycosylation of collagen is initiated. This is followed by the formation of interchain disulfide bonds required for helix formation. A triple helix is formed by three  $\alpha$  subunits. This final intracellular step and the completion of glycosylation, which started within the cisternae of the ER, are completed in the Golgi vacuoles. Collagen is released from the cell as procollagen, which after several enzymatic changes ends in the formation of tropocollagen. Tropocollagen is an insoluble monomer which precipitates as a unit component of the collagen fibrils (Perez-Tamayo, 1978; Campbell and Farrell, 2006).

#### **2.2.1.2.3. Biochemical degradation of collagen**

During normal bone turnover and bone resorption, for example fractures and osteoporosis, the matrix metalloproteinases (MMPs), which are zinc-dependent endopeptidases, are responsible for the degradation of collagens. MMPs are grouped into collagenases, gelatinases, stromelysins and stromelysin-like MMPs, membrane type-MMPs (MT-MMPs), and novel MMPs. Collagenase types 1-3 can cleave fibrillar collagens at about three fourths of the way from the aminoterminal end that results in two separate fragments susceptible to denaturation and further proteolysis. Following cleavage by collagenase, the gelatinases digest the N-terminal non-helical telopeptide. The stromelysins and stromelysin-like MMPs are able to degrade a wide range of substrates in the extracellular matrix, including some of the collagens, but not type I and III collagens in their native form. Of the membrane-type MMPs, MT1-MMP degrades the native collagens I, II and III and activates gelatinases and MMP-13. Collagen fibers can also be endocytosed and degraded within the lysosomes (Garnero and Delmas, 2003).

In addition to extracellular collagen degradation by specific endoproteinases such as MMPs, fragments of collagen fibers can be endocytosed and degraded within the lysosomes. Once degraded into smaller fragments, the usual abundant cellular proteases will further digest the collagen and results in the formation of smaller unique fragments that are often used in the diagnosis of diseases such as osteoporosis. These include telopeptide (N-terminal telopeptide of type 1 collagen (NTx)), a peptide fragment from the amino terminal end of the protein matrix as well as deoxypyridinoline (DPD), a collagen breakdown product with a ring structure and pyridinium cross-links. The analysis of DPD is widely used by pathologists to

evaluate the degree and effectiveness of therapy in patients with osteoporosis (Garnero and Delmas, 2003).

#### **2.2.1.2.4. Degradation of collagen during decomposition**

Due to its stability over-time, collagen type I (found in bone and teeth) is especially suited for radiocarbon dating and stable isotope analysis for the reconstruction of palaeodiet (Balzer *et al.*, 1997; Stevens and Hedges, 2004). Filtered collagen is collected and lyophilized and stable isotope analysis of carbon and nitrogen is performed. But, several factors, including climate and local environment, can result in variation in the data (Stevens and Hedges, 2004).

Little is known about the precise mechanisms involved in the degradation of collagen in dentine (Komsa-Penkova *et al.*, 1996; Dobberstein *et al.*, 2008). Environmental factors such as temperature and humidity as well as microbial activity will affect the kinetics and the extent of collagen degradation. It is assumed that degradation starts at the telopeptide ends of the triple helix (Dobberstein *et al.*, 2008). Collagen degradation will be mediated by tissue associated collagenase and to a larger degree by microbial organisms. Although collagen is normally resistant to proteolytic enzymes, at certain pH and temperature conditions the structure of collagen may change. For example, the loss of secondary structures makes proteolytic sites more accessible for digestion (Lui *et al.*, 2007).

As mentioned above, collagen cleavage commences during autolysis and cleavage results in Pro and Pro-OH release. Following digestion by collagenases, the collagen is further digested by nonspecific proteases. This occurs shortly after death and a large part of collagen breakdown occurs before the soil associated mechanisms and microbial action takes effect (Grupe, 1995). Micro-organisms gain access to skeletal material through small channels in the bone and digest the collagen into smaller fragments. This leads to leaching and increased porosity of the skeletal material (Balzer *et al.*, 1997). The determination of bone and/or tooth collagen content and integrity can provide important information regarding age estimation in unknown skeletal remains, especially teeth that have been exposed to environmental elements. Collagen may not reflect all post-mortem changes but can be used as an indicator of diagenesis in human remains (Dobberstein *et al.*, 2008). Degradation products include peptides and free amino acids and various techniques such as immunological methods, gel electrophoresis and amino acid analysis have been used to identify these molecules (Lui *et al.*, 2007). Of these compounds, hydroxyproline was

identified as an ideal marker to determine the degree of collagen preservation due to the high levels of this amino acid in collagen.

In a laboratory based aging model and in a naturally aged human and porcine teeth model, Dobberstein *et al.*, (2008) found that the collagen content decreased considerably with time. Artificially aged teeth showed a decrease in collagen yield within 20 days of heating at 90°C, but a correlation between PMI and collagen yield in the naturally aged teeth was not detectable. In the laboratory aging is a only function of high temperature and time; in the outdoors other factors such as humidity, daily changes in temperature, soil pH and bacterial activity also contribute to the rate of decomposition. The outdoor conditions may also protect collagen degradation. SDS-PAGE of collagen isolated from both artificially and naturally aged teeth showed the presence of HMW collagen with several LMW products such as peptides. Other identifiable breakdown products were free Lys-OH and/or Pro-OH (Dobbertstein *et al.*, 2008).



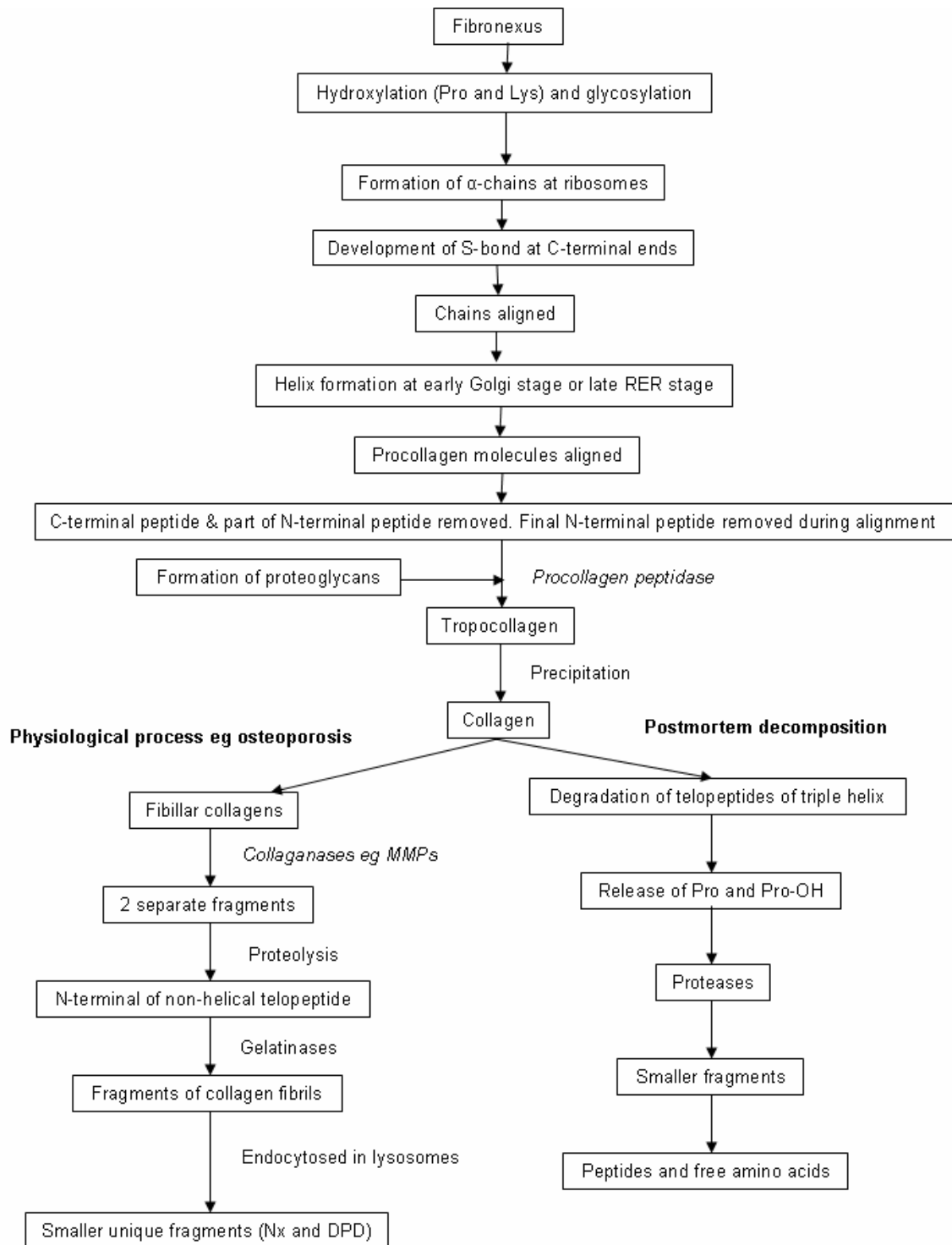


**Figure 2.7.** Summary of the biosynthesis and the process and the products that form with collagen degradation/decomposition.

### 2.2.2. Cellular components

The dental pulp contains many cell types and includes stellate fibroblasts, endothelium, erythrocytes and lymphocytes as well as neurons and supporting cells e.g. Schwann cells contained in the supporting/connective tissue, small capillaries and nerve fibres respectively

(Coetzee *et al.*, 2003, 282-4; Ross *et al.*, 2003). The proteins present in the pulp cavity are derived from the cells and supporting tissue and include structural and transport proteins as well as enzymes. A major protein that is present in the pulp cavity is haemoglobin (Hb) which is derived from the erythrocytes found in the small blood vessels. Erythrocytes contain 200 to 300 molecules of Hb making up 90% of the total protein found in erythrocytes (Schechter, 2008; Schaer and Alayash, 2009).

### **2.2.2.1. Structure, biosynthesis, biochemical and microbial degradation of Hb**

#### **2.2.2.1.1. Structure of Hb**

Protein is a linear arrangement of amino acids where the secondary and tertiary arrangement that the protein undergoes determines the degree to which a protein is resistant to proteolytic digestion. Hemoglobin (Hb) is a protein that is produced in the myeloid tissue by the process of erythropoiesis. Hb is a tetrameric protein (MW=68 000 Dalton), and consists of two  $\alpha$  and two  $\beta$  chains ( $\alpha_2\beta_2$ ). The chains are packed in a molecular form that is almost spherical. Each chain has a heme group which is located within the non-polar crevice near the surface of the molecule. The heme group is an iron containing bio-molecule while the organic portion of the heme molecule is a porphyrin which contains a tetrapyrrole structure formed by methane-bridge linkages between four pyrrole groups. Bound to the nitrogen groups via chelation bonds is Fe which is either in the ferrous ( $\text{Fe}^{2+}$ ) or ferric ( $\text{Fe}^{3+}$ ) form (Schechter, 2008; Schaer and Alayash, 2009).

#### **2.2.2.1.2. Biosynthesis of Hb**

Chromosome 11 encodes for the  $\alpha$ -globulin chain while chromosome 16 encodes for the non- $\alpha$ -globulin and  $\beta$ -chains. Biosynthesis of these chains occurs on the ribosomes of the cell. Heme synthesis takes place in the mitochondrion whereas the protoporphyrin IX ring structure is synthesized in the cytosol. The condensation of glycine and succinyl CoA to form  $\delta$ -aminolevulinic acid is the first step in the synthesis of the protoporphyrin IX ring structure. Two of these molecules condense to form porphobilinogen. In turn 4 porphobilinogen molecules condense to form a linear tetrapyrrole, and a circular uroporphyrinogen III is then formed (Stadler *et al.*, 2008; Schaer and Alayash, 2009). Subsequent reactions alter the side chains with the eventual formation of the protoporphyrin IX ring structure. The ring system returns to the mitochondrion where iron is inserted within the ring. Iron is an important transitional ion that is found in haemoglobin, myoglobin and other molecules such as the cytochromes, cytochrome oxidase, peroxidase and catalase. Of this iron 65% is found in Hb either in the ferrous ( $\text{Fe}^{2+}$ ) or ferric ( $\text{Fe}^{3+}$ ) state (Schechter, 2008; Stadler *et al.*, 2008; Schaer and Alayash, 2009).

#### **2.2.2.1.3. Biochemical degradation of Hb**

Haemolysis is the result of the macrophages phagocytosing Hb. Subsequently the  $\alpha$ -methene bridge is cleaved by monooxygenase:O<sub>2</sub> (NADPH dependent) to form biliverdin, a linear tetrapyrrole. The iron and globulin component remains attached but with time degrades further and the iron and globulin are released. The central methane bridge of biliverdin is reduced by biliverdin reductase (NADPH dependent) to form bilirubin. In the body, bilirubin complexes with albumin, is transported to the liver, is glucuronated and then is excreted via the bile. The free iron is recycled. Haemolysis may also occur during bacterial infections, parasitic infections, anaemia and in hypertonic or hypotonic solutions (Rieder, 1970; Kapert *et al.*, 1993; Schechter, 2008; Stadler *et al.*, 2008; Schaer and Alayash, 2009).

#### **2.2.2.1.4. Blood and the decomposition of Hb**

Little is known regarding the degradation of Hb during decomposition. However, the evaluation of the biochemical pathway of decomposition suggests that the protein component will degrade rapidly, similar to other proteins (refer to Figure 2.2). The heme group is chemically more stable, yet this molecule will also degrade further forming biliverdin and bilirubin with the release of iron (Ryter and Tyrnell, 2000). This degradation process is an attractive process that could be studied as a possible indicator of time after death (TAD).

The inherent stability of Hb makes it an ideal marker for the presence of blood. Blood was used as paint in bushmen rock paintings many of which are still visible today. The presence of human blood in these paintings has been confirmed using colorimetric methods such as the Hemastix® test. This test is based on the pseudoperoxidase reaction of the heme group with tetramethyl-benzidine and buffer chemicals in the test strip. The test strips are commonly used for the detection of intact red blood cells in urine but has also been successfully used for the detection of microscopic amounts of Hb in prehistoric stone tool residues as old as 30 000 BP (Williamson, 2000).

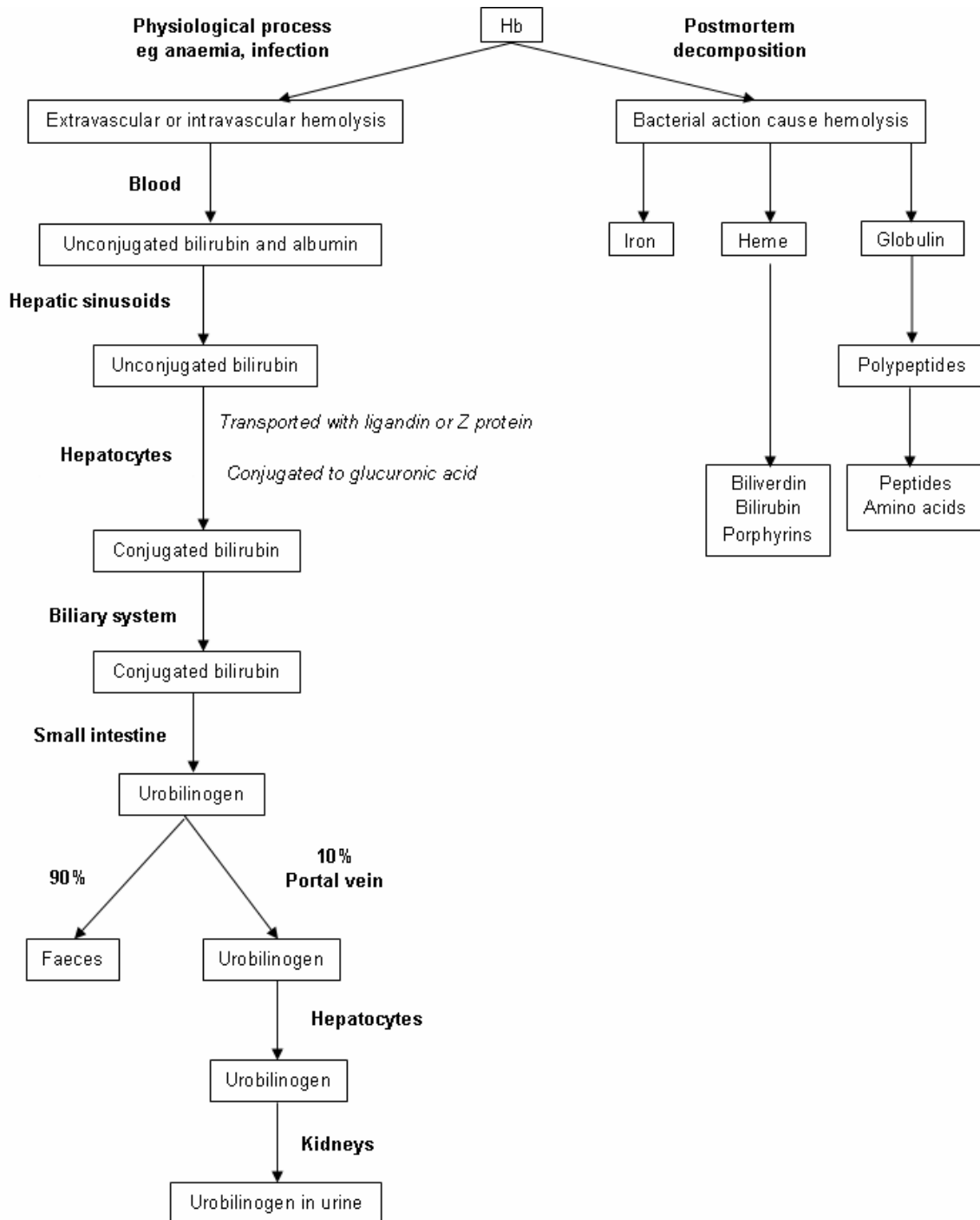


**Figure 2.8.**The physiological and post-mortem degradation of Hb.

## **2.2.2.2. Structure, biosynthesis, biochemical and microbial degradation of DNA**

### **2.2.2.2.1. Structure of DNA**

DNA is a polymer or polynucleotides that consists of monomeric nucleotides which are comprised of deoxyribose bound to a base either purine or pyrimidine and a phosphate group. Four types of nucleotides occur namely the purine bases (adenine and guanine) and the pyrimidine bases (cytosine and thymine). The phosphate groups forms the backbone of

the DNA helix consisting of complementary strands held together by weak thermodynamic forces. The helical spiral winds around a helix in a right-handed spiral. The bases of the nucleotides are found inside the helix, where adenine bases bind via two hydrogen bonds to thymine bases on the opposite strand and guanine bases bind via three hydrogen bonds to cytosine bases on the opposite strand. Each nucleotide residue is hydrated with eight to ten bound water molecules (Dickerson, 1992; Alaeddini *et al.*, 2010; Stavrianos *et al.*, 2010).

Two forms of DNA are found in all cells, except erythrocytes, and include genomic or nuclear DNA (nDNA) and mitochondrial DNA (mtDNA). nDNA encodes 100 000 genes (Presecki *et al.*, 2000); and unique genetic sequences are used in genetic sexing, nonhuman ancient DNA, maternal and paternal kinship, population continuity, population replacement and phylogenetic reconstruction (Kaestle and Horsburgh, 2002). nDNA is large and linear and is more easily degraded than mtDNA, whereas the smaller, circular mtDNA is less susceptible to exonucleases degradation. mtDNA represents 0.5% of the total DNA, occurs in the mitochondria of the cell, encodes 13 genes and is approximately 16 569 base pairs long (Presecki *et al.*, 2000; Da Silva *et al.*, 2007). The most polymorphic region is concentrated in two hypervariable regions within the non-coding D-loop region. The mutation rate of mtDNA is 5 to 10 times higher than that of nDNA (Baker *et al.*, 2001). Besides being more resistant to exonuclease degradation compared to nDNA each cell has many copies of mtDNA. The likelihood of obtaining a DNA profile from skeletal material using mtDNA is much higher (Bender *et al.*, 2000; Foran, 2006; Opel *et al.*, 2006; Da Silva *et al.*, 2007). A dry environment greatly reduces the rate of DNA degradation. The presence of water encourages the growth of bacteria and provides a substrate for hydrolytic enzymes. This explains the higher stability of DNA in skeletal tissue. A 20°C decrease in temperature can result in a ten to twenty-five fold reduction in the rate of decomposition of nucleotide bases. Environmental conditions have a greater influence DNA degradation when compared to the time elapsed since death. A neutral or slightly alkaline pH in a sample or the soil favours DNA preservation (Alaeddini *et al.*, 2010). The disadvantages of mtDNA are haploid inheritance, low discriminatory power and increased analysis time (Opel *et al.*, 2006).

#### **2.2.2.2. Biosynthesis of DNA**

In vivo DNA replication occurs in order for a cell to divide. The DNA helix is disrupted by helicase. Initiator proteins are responsible for the initiation of replication at a particular point in the DNA. The DNA strands unwind at the origin or 3' end are cut by the topoisomerases and DNA synthesis is initiated as a replication fork is formed. These strands serve as templates for DNA replication. RNA primers are created on the template strands. The

leading strand receives the RNA primers, while the lagging strand contains many RNA primers known as Okazaki fragments. The leading strand is extended in a 3' to 5' direction by DNA polymerase while RNase removes the RNA primers. Ligases fill in any gaps that may be found within the strands. A complimentary strand is formed in the 5'- 3' direction as A and T and G and C compliments, respectively. The telomerases halt DNA replication, and the DNA strands form a helical structure with a phosphate backbone and histone proteins (Goulian, 1971).

### 2.2.2.2.3. Biochemical degradation of DNA

Cellular death occurs either by apoptosis or necrosis and results in DNA fragmentation. Apoptosis is an energy dependent process which exhibits certain nuclear characteristics such as nuclear condensation, DNA degradation into oligomers of approximately 180 base pairs through the activation of endogenous endonucleases. Necrosis is an energy independent process that is induced by hypoxia or the action of membrane active toxicants and respiratory poisons. Nuclear changes include chromatin condensation and a random pattern of DNA degradation. A detailed summary of the process is presented in Figure 2.9 (Alaeddini *et al.*, 2010).

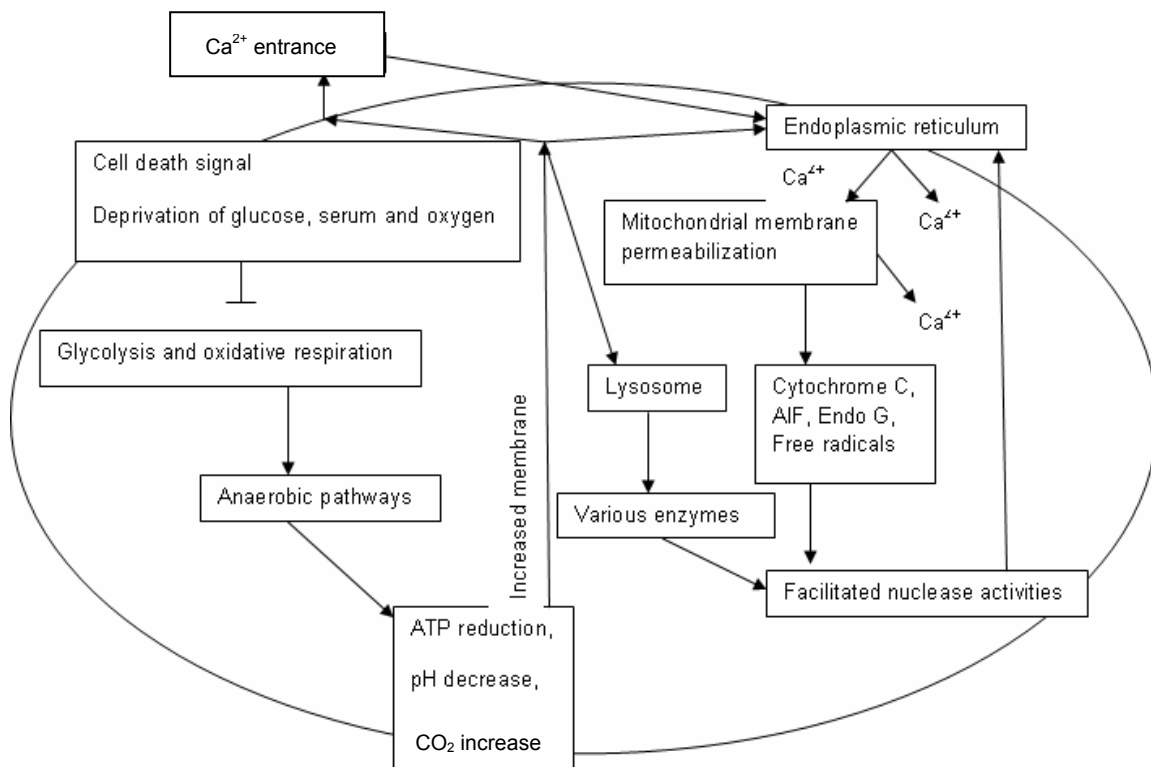


**Figure 2.9.** Biochemical pathways initiated by oxygen, serum and glucose deprivation leading to nuclease activation and cell death. AIF: apoptosis initiating factor. Adapted from Alaeddini *et al.*, (2010).

#### **2.2.2.2.4. Decomposition related changes to DNA structure**

With decomposition, endogenous nucleases initiates the process of DNA fragmentation at nuclease-sensitive sites forming high molecular weight fragments consist of 300,50 kbp. Non-enzymatic DNA degradation proceeds at a slower rate than enzymatic DNA degradation through the hydrolysis of the highly resistant phosphodiester bonds (Alaeddini *et al.*, 2010). Depurination of DNA can occur via the cleavage of the phosphate sugar backbone which forms single-strand breaks (Mitchell *et al.*, 2005). Hydrolytic reactions also degrade DNA, (Pionar, 2003; Alaeddini *et al.*, 2010); and this is due to the direct hydrolysis or destabilisation at sites of base loss where the glycosidic base sugar group is attacked (Pionar 2003; Mitchell *et al.*, 2005). Purine bases are lost faster than the pyrimidine bases. At the site where the base is lost, the aldehyde form of the deoxyribose sugar becomes vulnerable to cleavage by  $\beta$ -elimination. After such degradation, DNA fragments with terminal 3' and 5' phosphate groups are present (Mitchell *et al.*, 2005). DNA bases with secondary amine groups undergo deamination or hydrolytic loss of their amino groups. Deamination of adenine, cytosine, 5-methylcytosine, and guanine results in the formation of hypoxanthine, uracil, thymine and xanthine respectively. Cytosine residues are particularly prone to deamination which results in the formation of uracil through the transversion of the C-G base pair to the T-A base pair (O'Rourke *et al.*, 2000; Pionar, 2003; Shiroma *et al.*, 2004; Mitchell *et al.*, 2005; Alaeddini *et al.*, 2010).

Cross-links occur either between DNA and proteins or between a ring-opened sugar of the abasic sugar and an amino group on the opposite strand. These cross-links are temperature dependent and occur much slower at lower temperatures (Alaeddini *et al.*, 2010).

The 3-4' carbon bond of the deoxyribose sugar is susceptible to oxidation which leads to ring fragmentation and strand scission. However, the major site of oxidative attack is the 5-6' C=C double bonds of the pyridines and the imidazole ring in the purines (Pionar, 2003). Oxidation takes place when hydroxyl or superoxide radicals modify bases and distort the helix. These superoxide radicals and hydrogen peroxide are generated through microbial activity. During oxidative DNA damage, cytosine is converted to hydantoin, bases, cross-linkages and sugar residues are removed (Alaeddini *et al.*, 2010). mtDNA is more susceptible than nDNA. The most problematic effect is the formation of hydantoins as these molecules block extension during PCR (O'Rourke *et al.*, 2000).

Radiation, such as UV also causes a variety of lesions in DNA and these include oxidative damages, single and double strand breaks, base modifications, destruction of sugar, intra-

and interstrand cross-links and the formation of dimers (Alaeddini *et al.*, 2010). Sites at which non-enzymatic changes occur to DNA structure is presented in Figure 2.10.

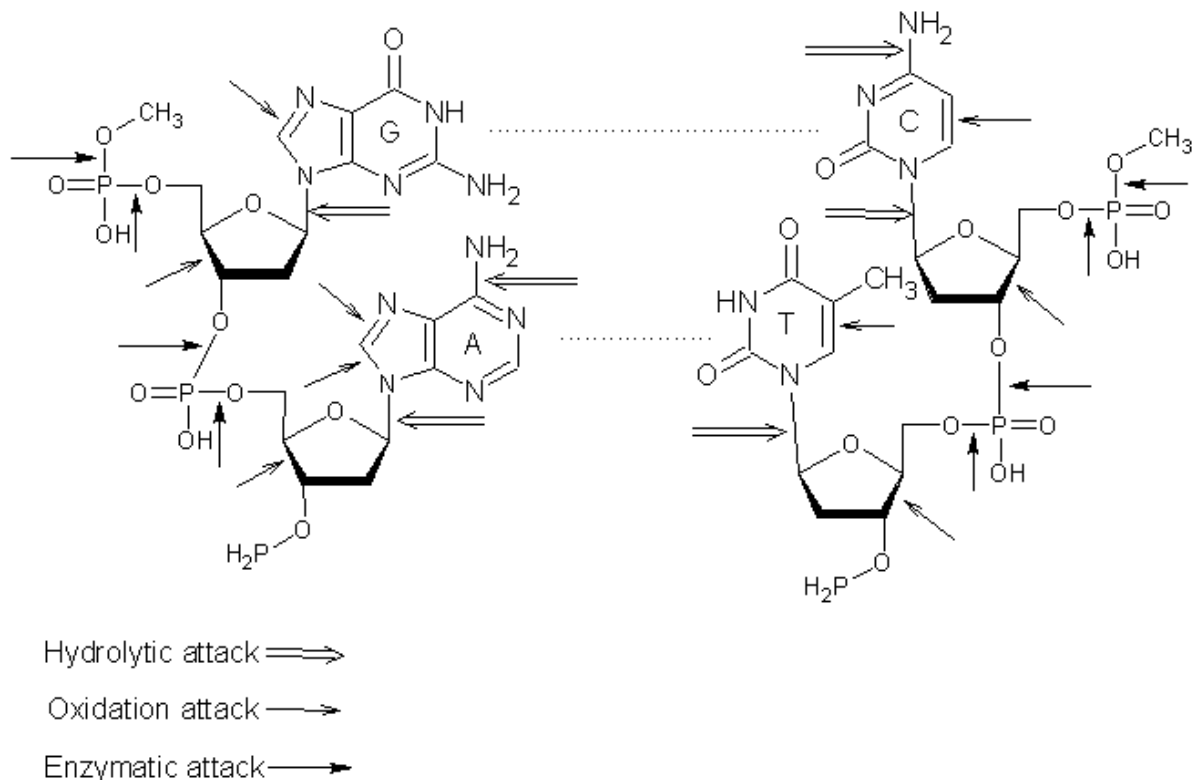


**Figure 2.10.** Oxidation, hydrolytic and enzymatic attacks associated with DNA degradation. A: adenine, G: guanine, C: cytosine, T: thymine. Adapted from Alaeddini *et al.*, (2010).

Identification of an individual is based on the polymorphic genetic information contained in nDNA and mtDNA. The first polymorphic locus was discovered by Wyman and White in 1980 and these hypervariable loci consist of tandem repeats of oligonucleotide sequences of 2-80 bp known as variable number of tandem repeats (VNTRs) or minisatellites. STR (short tandem repeats) or microsatellites are smaller regions consisting of 2-5 bp (Da Silva *et al.*, 2007). The numbers of repeats differ between individuals and are analysed by Restriction Fragment Length Polymorphism (RFLP). Although VNTRs have greater stability than previously used forensic protein and serological methods, the technique has various limitations. The sequences that are amplified are very long and therefore require non-degraded DNA samples to obtain reliable data. The technique is also time-consuming. These limitations led to the development of the polymerase chain reaction (PCR) (Carey and Mitnik, 2002; Butler, 2005).

The first application of PCR was published in 1985 (Saika *et al.*, 1985); while the first comprehensive description of the PCR protocol was described in 1988 (Saika *et al.*, 1988).



The advantage of PCR is two-fold in that small amounts of highly degraded DNA can be used for the amplification of STRs. Multiplex PCR, where more than one sequence is amplified in the same reaction, is ideal when small amounts of DNA are isolated (Rudin and Inman 2002; Butler, 2005).

#### **2.2.2.2.5. Amplification of mitochondrial DNA**

Mitochondrial DNA (mtDNA) analysis is a well-established tool used for identification in forensic case work (Pfeiffer *et al.*, 1998; Presecki *et al.*, 2000; Brandstatter *et al.*, 2004; Von Wurmb-Schwark 2004; Nelson and Melton, 2007; Alaeddini *et al.*, 2010); and archaeological collections (Hagelberg and Clegg, 1991; Gilbert *et al.*, 2003). The analysis of mtDNA is the method of choice when working with skeletal material such as bones, teeth and fingernails, where nuclear DNA testing is less successful (Bender *et al.*, 2000; Presecki *et al.*, 2000; Shiroma *et al.*, 2004; Alaeddini *et al.*, 2010). In circumstances where degraded template is expected or when faced with vestigial samples, mtDNA analysis is a good alternative to genomic DNA analysis (Bender *et al.*, 2000; Presecki *et al.*, 2000; Baker *et al.*, 2001; Bravi *et al.*, 2004; Alaeddini *et al.*, 2010).

The amount of mtDNA present in archaeological material is generally much greater than nuclear DNA. Therefore most genetic analyses are based on regions such as hypervariable region 1 (HVR1) (Bender *et al.*, 2000; Gilbert *et al.*, 2003; Bravi *et al.*, 2004; Alaeddini *et al.*, 2010); hypervariable region 2 (HV2) (Bender *et al.*, 2000; Bravi *et al.*, 2004; Nelson and Melton, 2007); and base pair fragments of genes such as cytochrome *b*, 12S rRNA (Hagelberg and Clegg, 1991); contained within the mtDNA (Gilbert *et al.*, 2003). mtDNA is more abundant in prehistoric samples as each cell contains hundreds of copies of mtDNA within the mitochondria (Hagelberg and Clegg, 1991; O'Rourke *et al.*, 2000; Presecki *et al.*, 2000; Mitchell *et al.*, 2005; Da Silva *et al.*, 2007; Alaeddini *et al.*, 2010). The likelihood of obtaining a target sequence of mtDNA is much greater and more accessible for amplification (O'Rourke *et al.*, 2000; Presecki *et al.*, 2000; Mitchell *et al.*, 2005; Da Silva *et al.*, 2007; Alaeddini *et al.*, 2010). mtDNA is also transmitted through the maternal line as a single haploid block of linked genes that can be traced several generations back through the maternal lineage (Bravi *et al.*, 2004).

mtDNA is useful for the support of other data that is available to make an identification, location and time of body recovery, personal effects and associated grave material (Nelson and Melton, 2007). Furthermore the entire human mitochondrial genome has been sequenced and is used in phylogenetic and evolutionary studies and maternal mode of

inheritance (Hagelberg and Clegg, 1991; Pfeiffer *et al.*, 1998). Advances in mtDNA analysis are occurring at a rapid rate (Baker *et al.*, 2001).

Teeth are an excellent source of mtDNA as teeth are generally resistant to degradation (Baker *et al.*, 2001; Shiroma *et al.*, 2004). mtDNA is highly abundant in the mitochondria of the odontoblastic processes within the tubules of dentine (Malaver and Yunis, 2003). It is believed that dentin constitutes the mayor source of mtDNA after long post-mortem intervals (Pfeiffer *et al.*, 1998).

The polymerase chain reaction (PCR) is used for the amplification of small amounts of DNA which are often present in forensic cases and decomposition studies (Yang *et al.*, 1998; Da Silva *et al.*, 2007). Target regions are amplified in a much shorter time (Matsunaga *et al.*, 1999). The potential of analysis of forensic samples have been enhanced by recent developments regarding length amplification of polymorphic fragments. PCR can differentiate one individual from another with a high level of reliability and with only 1ng of starting DNA (Da Silva *et al.*, 2007). Real-time quantitative PCR (qPCR) is a method that allows for the rapid and reliable quantification of mRNA transcripts or the synthesis of cDNA. The technique has a large dynamic range, is fast, easy to use and provides the simultaneous measurement of gene expression in difficult samples (Nygard *et al.*, 2007).

The cytochrome *b* (cyt *b*) gene product is one of the proteins that make up complex III of the mitochondrial oxidative phosphorylation system. The complex transfers electrons from dihydroubiquinone to cytochrome *b* across the inner mitochondrial membrane. Cyt *b* contains the two redox centers involved in electron transfer (Irwin *et al.*, 1991).

Bellis *et al.*, (2003), investigated several genetic markers including cytb as potential markers for species identification. Sequence specific primers were used for the detection of both pig and human cytb gene. Amplification was successful for both although species specific information regarding the cytb gene was not related to human vs pig. The primers used are specific for mammal DNA and therefore no amplification of bacterial sequences are possible using this primer set (Bellis *et al.*, 2002).

Amplification of the cyt *b* contained within mtDNA is widely used in the forensic sciences, identification of animal species, livestock robbery, phylogenetic studies, identification of stomach contents and identification of the biological origin of casework stains (Zehner *et al.*, 1998; Parson *et al.*, 2000; Bravi *et al.*, 2004). A number of forensic and phylogenetic studies

have used the *cyt b* nucleotide sequence as it contains species specific information (Zehner *et al.*, 1998; Parson *et al.*, 2000). RFLP is used for the splicing of amplified *cyt b* fragments for the discrimination of forensic samples in human and livestock species (Zehner *et al.*, 1998; Bravi *et al.*, 2004). Universal primers for *cyt b* are well-established and fulfil the requirement of amplifying relatively short fragment sizes (300-358bp) and sequence divergence (Bellis *et al.*, 2003; Bravi *et al.*, 2004). RFLP analysis of amplified *cyt b* fragments involves the use of *AluI*, *HaeIII* and *HinfI* restriction enzymes for the selection of specific regions within the *cyt b* fragments. These markers are then used for the discrimination between samples and for forensic analysis (Zehner *et al.*, 1998; Bravi *et al.*, 2004). This method is applicable to the forensic field where there is a demand for techniques possessing high-throughput, reproducibility and robustness (Bellis *et al.*, 2003). The application of the *cyt b* to forensic cases displays many advantages as the process is not dependent on the physical material present but biological origin can be determined by comparison of the resulting sequence with large ever growing databases of *cyt b*. The method benefits further from the advantage of mtDNA typing in conjunction with PCR and thus displays high sensitivity and stability against environmental stress when compared to other sequences (Parson *et al.*, 2000).

Three main complications can arise with the amplification of degraded DNA samples such as failure of amplification, preferential amplification and miscoding lesions.

STR multiplexes work optimally with a 1ng DNA template which is about 660 copies of nDNA. When the DNA starting amount is less than 60 copies, a high incidence of PCR failure exists. By increasing the amount of *Taq* polymerase and introducing extra PCR cycles, it can be possible to compensate for low copy number templates. Alternatively mini-STRs can be used for smaller targets and these templates can be quantified using real-time PCR (qPCR) (Alaeddini *et al.*, 2010).

Another problem that can occur is allele drop-out. In such a situation one of the alleles of a heterozygote individual is not amplified and the genotype obtained indicates that the individual is homozygote. The use of mini-STRs may reduce the occurrence of this effect (Alaeddini *et al.*, 2010).

Miscoding occurs as the result of non-enzymatic modification of nucleotides. An example of which is hydrolytic reactions that affect mostly cytosine, 5-methylcytosine, adenine and guanine. These bases are converted into uracil, thymine, hypoxanthine and xanthine

respectively. This may result in the mis-incorporation of the incorrect bases during PCR extension. By using a high-fidelity polymerase enzymes with a proofreading ability such as pfu and Taq HiFi or by duplicate analysis, this effect can be reduced (Alaeddini *et al.*, 2010).

## **CHAPTER 3: MATERIALS AND METHODS**

### **3.1. Materials**

#### **3.1.1. Teeth**

Forty five porcine teeth were collected at different time intervals from decomposing pig carcasses at the Forensic Anthropology Body Farm (FABF) located on the Miertjie le Roux experimental farm near Rayton, outside Pretoria. The pigs were part of a decomposition and burning project (EC080617-026) at the Department of Anatomy, University of Pretoria. The pigs were adults and consisted of both male and female pigs that died of natural causes. In this study the pigs were placed approximately one meter from each other in a fenced off field, at different time intervals throughout a period of one year. The pigs were left to decompose naturally in the open field. Post-mortem interval and the environmental conditions were recorded. Teeth were extracted at different time intervals of 20 days from August 2008 to 2009. Teeth were randomly selected and included molars, premolars, incisors and canines.

For the *in vitro*, laboratory based model, three porcine heads were obtained from a local abattoir. A total of fifty teeth were extracted and included all teeth types. Five teeth were used for method establishment and the remainder were used to determine the effect of heating.

#### **3.1.2. Reagents**

Phenylmethanesulfonyl fluoride (PMSF), sodium hydroxide (NaOH), sodium potassium tartrate ( $\text{NaKC}_4\text{H}_4\text{O}_6$ ), copper sulphate ( $\text{CuSO}_4$ ), potassium iodide (KI), sodium chloride (NaCl), sodium bicarbonate ( $\text{NaHCO}_3$ ), potassium ferricyanide ( $\text{K}_3\text{Fe}(\text{CN})_6$ ), potassium cyanide (KCN), Xylenol Orange, ninhydrin, L-proline, sodium carbonate ( $\text{Na}_2\text{CO}_3$ ), guanidine-HCl (GuaHCl), sodium perchlorate ( $\text{NaClO}_4$ ), sodium dodecyl sulphate (SDS) and sucrose were purchased from Merck Chemicals, Modderfontein, South Africa (SA). The following solvents were also supplied by Merck Chemicals: ethanol (EtOH), glycerol, sulphuric acid ( $\text{H}_2\text{SO}_4$ ), acetic acid ( $\text{CH}_3\text{COOH}$ ), hydrochloric acid (HCl), chloroform ( $\text{CHCl}_3$ ) and isoamylalcohol ( $(\text{CH}_3)_2\text{CHCH}_2\text{CH}_2\text{OH}$ ). Tris/HCl, was purchased from SAARCHEM, Chamdor, Krugersdorp, SA. Coomassie Brilliant Blue, Hoechst 33258 and bromophenol blue (BPB) were obtained from BioRad Laboratories, Johannesburg, SA. The GoTaq<sup>®</sup> PCR Core System II was manufactured by Promega Corporation, Madison, USA and the primers were manufactured by Integrated DNA Technologies (IDT) both were supplied by Whitehead Scientific, Cape Town, SA. The SensiMix HRM<sup>™</sup> kit manufactured by Quantace Limited,

BIOLINE was purchased from Celtis Molecular Diagnostics, Mowbray, SA. Bovine serum albumin (BSA), heamoglobin (Hb) standard and collagen type I were supplied by Sigma-Aldrich Company, Atlasville, SA. Agarose D1 LE was purchased from Whitehead Scientific, Brackenfell, Cape Town, SA.

### **3.1.3. Equipment**

Equipment used in this study included a LABCONCO freeze-drier from ALCATEL CIT. France, a Hermle Z300 Centrifuge, a Crison GLP21 pH-meter and Eppendorf pipettes manufactured by Eppendorf AG Hamburg, Germany supplied by Scientific Laboratory Equipment Company (LASEC), SA. The Lamda LS50B spectrophotometer that was used was from Perkin Elmer, Boston, MA, USA and was supplied by Separations Scientific, Honeydew, SA. The Biotek ELx800 plate reader was from Analytical and Diagnostic Products (ADP), Johannesburg, SA. A FLUOstar OPTIMA plate reader from BMG labtechnologies, Offenburg, Germany was also used. A model A1 classII (Owl Scientific, Inc, Waburn, MA, USA) coupled to a Amersham Power Supply-EPS301 was supplied by Whitehead Scientific, Cape Town, SA. A MultiGene thermocycler from Labnet and a Rotor-GeneQ 2-plexHRM thermocycler from QIAGEN, USA was also supplied by Whitehead Scientific, Cape Town SA.

Disposable plasticware include 96-well plates, 15 and 50ml tubes and pipette tips (10, 25, 100, 200 and 1000µl) from Greiner Bio-One were supplied by Laboratory Scientific, Cape Town, SA; while Eppendorf tubes were supplied by LASEC, Cape Town, SA. PCR tubes were purchased from Whitehead Scientific, Cape Town, SA.

## **3.2. Methods**

### **3.2.1. *In vitro* aging**

Forty five teeth from the pigs heads obtained from a local abattoir were extracted using utility pliers. The teeth were placed in small plastic bags, sealed and kept at  $-70^{\circ}\text{C}$  until required. For *in vitro* aging the teeth were washed in EtOH:ddH<sub>2</sub>O (2:1) and then ddH<sub>2</sub>O before being transferred to a sterile one litre glass bottle containing 800ml ddH<sub>2</sub>O. The bottle was placed at  $90^{\circ}\text{C}$  and three randomly selected teeth were removed after 0, 1, 2, 3 and 4 hours heating. Each group of teeth were placed in labelled plastic bags and stored at  $-70^{\circ}\text{C}$  until required (Von Wurmb-Schwark *et al.*, 2003; Ye *et al.*, 2004; Dobberstein *et al.*, 2008). This was performed on three different days, representing triplicate experiments.

### **3.2.2. Naturally aged teeth, field model**

The teeth were removed from the decomposing carcasses using utility pliers and placed in plastic bags. After extraction the teeth were stored at  $-70^{\circ}\text{C}$  until required for further use, whereafter each tooth was washed with a dilution of EtOH:ddH<sub>2</sub>O(2:1) and then in ddH<sub>2</sub>O before being crushed into small fragments (Von Wurmb-Schwark *et al.*, 2003).

### **3.2.3. Experimental design**

For the *in vitro*, laboratory based study and the naturally aged field model all teeth were processed in exactly the same way and were subjected to the analyses as described in the following sections.

The *in vitro* aged teeth were divided into three groups representing individual experiments and further divided into five groups that consisted of three teeth in each group. The groups of three teeth each were (i) T0, not heated, and the following were heated at  $90^{\circ}\text{C}$  (ii) T1, one hour, (iii) T2, two hours, (iv) T3, three hours and (v) T4, four hours. The process (n=15) was repeated in triplicate (n=45). The morphology of the teeth was evaluated before further processing.

The naturally aged groups consisted of five groups for each experiment. The groups of three teeth each were, (i) 20-40, post-mortem interval (PMI) of twenty to forty days (included teeth from 2008/10/28-2008/11/17 (summer) and 2008/12/27-2009/01/16 (summer)), (ii) 40-60, PMI of forty to sixty days (2008/09/18-2008/11/17 (spring and summer) and 2008/12/07-2009/01/16 (summer)), (iii) 60-80, PMI of sixty to eighty days (2008/09/18-2008/11/17 (spring and summer) and 2008/12/07-2009/01/16 (summer)), (iv) 80-100 PMI of eighty to a hundred days (2008/08/29-2008/11/17 (spring and early-summer) and 2008/10/28-2009/01/16 (summer)), and (v) 100+ PMI of more than a hundred days (included teeth from 2008/07/17-2008/11/17 (winter, spring and summer) and 2008/10/08-2009/01/16 (winter, spring and summer)), (n=15). The process was repeated in triplicate (n=45). The dates and time interval of decomposition and collection of the teeth is presented below in Figure 3.1 and Table 3.1. Morphology of the teeth were evaluated before further processing.

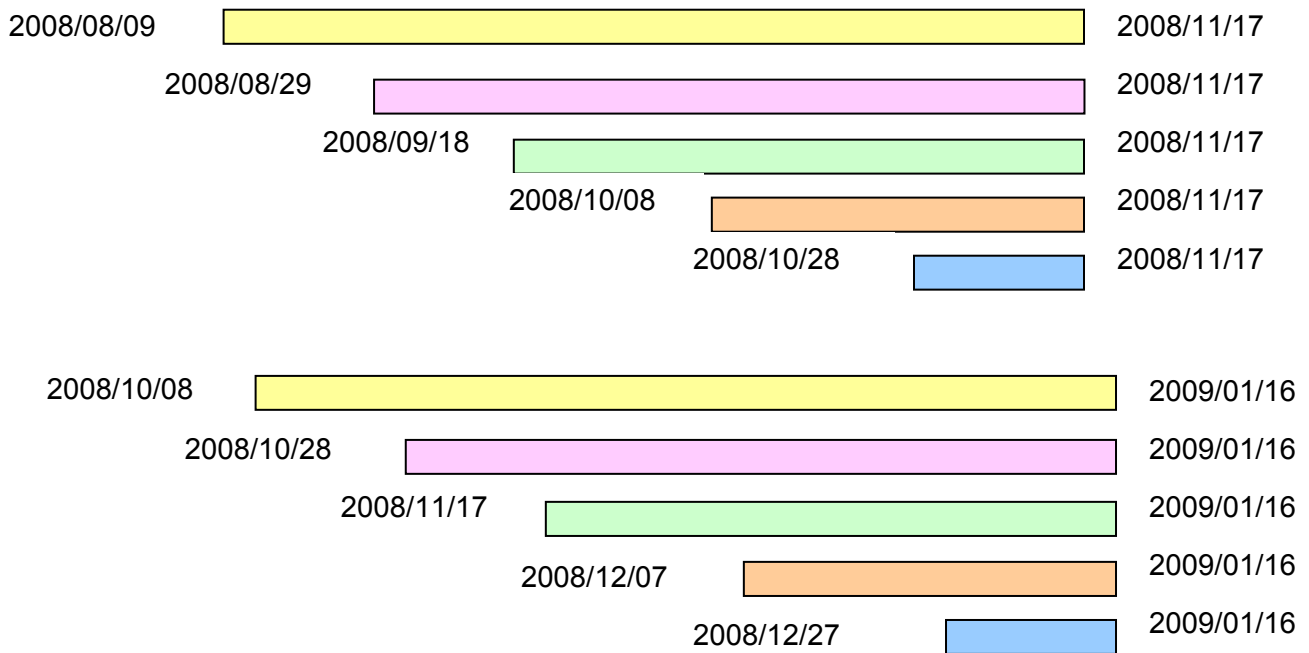



Figure 3.1. A timeline indicating the collection periods of the teeth from the field study with Blue = 20-40 days, Orange = 40-60 days , Green = 60-80 days, Pink = 80-100 days and Yellow = 100+ days.




**Table 3.1. A r** **th collected**  
**from the field teeth. The coloured blocks indicate**  
**which teeth were used for the study. P= Pig**  
**number T= tooth number and PN= Pig nigella**

<b>20-40 days</b>			
P016T1	P016T5	P013T1	P013T5
P016T2	P015T1	P013T2	P013T6
P016T3	P015T2	P013T3	P013T7
P016T4	P015T3	P013T4	P013T8
P014T1			
<b>40-60 days</b>			
P010T1	P010T5	P020T1	P009T3
P010T2	P010T6	P020T2	P009T4
P010T3	P010T7	P009T1	P009T5
P010T4		P009T2	P009T6
P009T7	P019T1	P009T11	P019T4
P009T8	P019T2	P009T12	P019T2
P009T9	P019T3	P019T1	P009T10
<b>60-80 days</b>			
P018T1	P008T1	P008T5	P008T9
P018T2	P008T2	P008T6	P017T2
P018T3	P008T3	P008T7	P017T3
P017T1	P008T4	P008T8	
<b>80-100 days</b>			
P006T1	P005T1	P004T1	P002T1
P006T2	P005T2	P004T2	P013T1
P016T1	P005T3	P004T3	P001T1
P016T2	P005T4	P004T4	
P016T3	P005T5	P004T5	P005T7
P016T4	P005T6	P004T6	P016T5
<b>100+ days</b>			
PNT1	P009T1	P019T1	P008T1
PNT2	P009T2	P019T2	P007T1
PNT3	P018T001	P019T3	P006T1
PNT4	P018T2	P019T4	P016T1
PNT5	P018T3	P019T5	P016T2
PNT6	P017T1	P019T6	P016T3
PNT7	P017T2	P019T7	P015T1
PNT8	P017T3	P019T8	P014T1
PNT9	P018T001	P019T9	PNT11
PNT10	P018T2	P019T10	

Each group of teeth (both experimental models) were roughly ground and then freeze dried for 96 hours and were then further ground into a fine powder. To each millilitre of material an equal volume of solubilising buffer solution (SBS) consisting of 0.1M Tris/HCl pH 8.00 containing 17.4mg/ml phenylmethylsulfonyl fluoride (PMSF) and 0.001% sodium dodecyl sulphate (SDS) was added. The ground material was mixed well for 48 hours at room temperature. The samples were centrifuged at 2000rpm for 5min to collect the ground material and the supernatant. The insoluble material contained in the pellet was used for the isolation of collagen. The supernatant consisting of the water soluble constituents was used for the determination of total protein, haemoglobin (Hb), pyrrole ring content, iron (Fe) Total Fe, Fe<sup>2+</sup> and Fe<sup>3+</sup>), ninhydrin positive components as well as for the isolation of DNA and subsequent amplification thereof for the detection of the genomic  $\beta$ -actin (ACTB) and the mitochondrial cytochrome b (*cytb*) gene.

A summary of all procedures used is presented in Table 3.2. and are described in the following sections:

**Table 3.2. Parameters evaluated and techniques used**

<u>Laboratory/in vitro aged teeth</u>		<u>Naturally aged/field teeth</u>	
<u>Water insoluble fraction derived from tooth matrix</u>		<u>Water insoluble matrix derived from tooth matrix</u>	
<u>Collagen</u>	<u>Quantification</u> : 230 nm and final isolated mass	<u>Collagen</u>	<u>Quantification</u> : 230 nm and final isolated mass
<u>Water soluble fraction derived from pulp cavity</u>		<u>Water soluble fraction derived from pulp cavity</u>	
<u>Total protein</u>	<u>Quantification</u> : Bradford and Biuret methods	<u>Total protein</u>	<u>Quantification</u> : Bradford and Biuret methods
<u>Haemoglobin</u>	Drabkin method	<u>Haemoglobin</u>	Drabkin method
<u>Pyrrrole groups</u>	Fluorometric	<u>Pyrrrole groups</u>	Fluorometric
<u>Fe<sup>2+</sup>/Fe<sup>3+</sup>/Total Fe</u>	Xylenol Orange	<u>Fe<sup>2+</sup>/Fe<sup>3+</sup>/Total Fe</u>	Xylenol Orange
<u>Ninhydrin (+) components</u>	Ninhydrin reaction	<u>Ninhydrin (+) components</u>	Ninhydrin reaction
<u>DNA</u>	<u>Quantification</u> : 260nm, 260nm/280nm, Hoechst assay <u>Extent of degradation</u> : Agarose gel electrophoresis <u>Structural integrity</u> : PCR amplification (Cytochrome band β-actin)	<u>DNA</u>	<u>Quantification</u> : 260nm, 260nm/280nm, Hoechst assay <u>Extent of degradation</u> : Agarose gel electrophoresis <u>Structural integrity</u> : PCR amplification (Cytochrome and β-actin)



### **3.2.3.1. Collagen concentration**

#### **3.2.3.1.1. Isolation of collagen from the insoluble tooth fraction**

The insoluble pellet was demineralised in 0.5M hydrochloric acid (HCl) at 4<sup>0</sup>C until all the solid tooth material was dissolved, usually for several days. The remaining material was rinsed with ddH<sub>2</sub>O, the pH was adjusted to 3.00 with 0.1M Na<sub>2</sub>CO<sub>3</sub> and then gelatinized at pH 3 for 48 hours at 75<sup>0</sup>C using 6M guanidine hydroxychloride (GuaHCl). The volume of GuaHCl added was according to the original mass of each sample. (Kakuichi and Kobayash, 1971; Mandell and Sodek, 1982). The concentration of the collagen content of each sample was determined by measuring the absorbance at 230nm, using skin collagen type 1 as standard (1mg/ml). In addition the concentration of collagen was also determined by the Bradford method as described in section 3.2.4.1.1. The samples were then filtered using PD-10 desalting columns and again the concentration of collagen was determined as described above. Each column was equilibrated using a total volume of 25ml ddH<sub>2</sub>O. A 500µl sample volume was loaded onto each column and the flow-through was discarded. The collagen was eluted with 3.5ml ddH<sub>2</sub>O in 500µl fractions. The fractions were combined, freeze-dried for 36 hours and then weighed (Peterszegi *et al.*, 2008). The total collagen content was expressed as mg/g dried mass of teeth (DMT).

### **3.2.3.2. Analysis of water soluble constituents**

#### **3.2.3.2.1. Determination of total protein content**

Total protein content was determined using the Bradford and the Biuret methods. For the Bradford method, Coomassie Brilliant Blue (CBB) reagent was diluted (1:4) with ddH<sub>2</sub>O. A standard curve was prepared using 0-100µg/ml bovine serum albumin (BSA) prepared from a 10mg/ml stock BSA solution in the lysis buffer. Final volume of each sample used for the preparation of the standard curve was 10µl and to make this final volume lysis buffer was used. To a volume of 10µl of sample, 100µl of the diluted CBB was added. The samples were mixed well and the absorbance measured at 630nm (Laemmli, 1970; Kruger, 2002; Georgiou *et al.*, 2008; Melander and Tommerass, 2008); using a Biotek ELx800 plate reader. Data was expressed as mg/g DMT.

The Biuret reagent was prepared by dissolving 4.0g NaOH in 400ml ddH<sub>2</sub>O. To this 4.5g NaKC<sub>4</sub>H<sub>4</sub>O<sub>6</sub> was added and after mixing well, 1.5g CuSO<sub>4</sub> and 4.5g KI were added and the solution made up to a final volume of 500ml with ddH<sub>2</sub>O. A standard curve was prepared using 0-100µg/ml BSA in SDS buffer was used as described above. To 20µl sample, 80µl NaCl and 120µl Biuret reagent was added. The samples were mixed and incubated at room temperature for 15 minutes after which the absorbance was measured at 540nm using a

Biotek ELx800 plate reader (Gornall *et al.*, 1948; Zhou and Regenstein, 2006). Data was expressed as mg/g DTM.

#### **3.2.3.2.2. Determination of total haemoglobin (Hb) content**

The major constituent protein present in the pulp cavity is haemoglobin (Hb). To specifically determine the concentration of Hb the Drabkin method was used. The Drabkin reagent was prepared using 0.1g sodium bicarbonate ( $\text{NaHCO}_3$ ), 0.02g potassium ferricyanide ( $\text{K}_3\text{Fe}(\text{CN})_6$ ) and 5mg potassium cyanide (KCN) made up to 100ml with ddH<sub>2</sub>O. A Hb concentration series of 0-0.9µg/ml Hb in lysis buffer was used. To 10µl sample 100µl Drabkin reagent was added (Depositor *et al.*, 1972) and then the colour of cyanmethemoglobin that formed was measured at 540nm and expressed as mg/g DTM.

#### **3.2.3.2.3. Determination of pyrrole ring content**

The pyrrole ring, is an important part of the ring structure of many biological molecules such as protoporphyrins and Hb. The latter is an important constituent protein of erythrocytes which are one of the most common cell types found in the pulp cavity. Pyrrole groups have specific fluorescence properties and the concentrations thereof can be measured at an excitation wavelength of 404nm and emission wavelength of 624nm (Biesaga *et al.*, 2000). The fluorescence properties of 10µl volume of each sample in 100µl H<sub>2</sub>O was determined. A standard curve of 0-250µg/ml was generated using 1mg/ml protoporphyrin standard in lysis buffer. Data was expressed as mg/g DTM.

#### **3.2.3.2.4. Determination of total iron content**

Iron (Fe) is a transitional metal that is found in the ferrous ( $\text{Fe}^{2+}$ ) state in Hb and is contained within the haem group of Hb. With protein degradation it can be expected that the protein (globin) would degrade and the more stable porphyrin ring and iron will remain (Biesaga *et al.*, 2000); and  $\text{Fe}^{2+}$  will then become oxidized in the presence of oxygen to  $\text{Fe}^{3+}$ .

The concentration of  $\text{Fe}^{3+}$  can be determined using Xylenol Orange which binds to  $\text{Fe}^{3+}$  in an acidic environment resulting in the formation of a blue purple complex with an absorbance maximum at 570nm (Banerjee *et al.*, 2004; Erel, 2005). The oxidation of  $\text{Fe}^{2+}$  by H<sub>2</sub>O<sub>2</sub> to  $\text{Fe}^{3+}$  enables the measurement of total iron (TFe). The  $\text{Fe}^{2+}$  concentration was then calculated as follows:  $[\text{Fe}^{2+}] = [\text{TFe}] - [\text{Fe}^{3+}]$ .

The ratio of  $\text{Fe}^{3+}$  to  $\text{Fe}^{2+}$  was also determined. A concentration series of 0-500µM of  $\text{FeCl}_2$  and  $\text{FeCl}_3$  was used for the preparation of a standard curves. FOX reagent was prepared and

consisted of 150µM Xylenol Orange (XO), 140mM NaCl, 25mM sulfuric acid and 1.35mM glycerol (Erel, 2005). The Fe<sup>3+</sup> concentration of each sample was determined by adding 150µl FOX reagent to 10µl sample after which the plate was incubated at 37<sup>0</sup>C for 30min. Total Fe content was determined by adding 10µl H<sub>2</sub>O<sub>2</sub> (1:100) to 25µl samples followed by 150µl FOX reagent. The plate was incubated for 30min at 37<sup>0</sup>C and the absorbance of all samples was measured at 570nm. Data was expressed as µM/g DTM.

#### **3.2.3.2.5. Determination of ninhydrin reactive nitrogen**

With tissue degradation, protein becomes fragmented through proteolytic digestion or physical degradation resulting in the formation of peptides and free amino acids. The breakdown of other bio-molecules such as nucleotides results in the formation of smaller molecules with secondary amine groups. As the actual composition of these compounds is unknown, these breakdown products will be referred to as NRN due to a positive reaction with ninhydrin (Block and Bolling, 1951; Schweet, 1953; Erickson *et al.*, 1993; Wess and Orgel, 2000).

Ninhydrin reagent was prepared by dissolving 0.5g ninhydrin in 50ml dH<sub>2</sub>O and adding 2% acetic acid (CH<sub>3</sub>COOH). A standard curve was generated using a concentration series of 0-23mM L-proline. To 10µl sample 100µl ninhydrin was added, the plate incubated at 37<sup>0</sup>C overnight and the reaction measured at 405nm (Block and Bolling, 1951; Schweet, 1953; Erickson *et al.*, 1993; Wess and Orgel, 2000).

#### **3.2.3.2.6. Determination of DNA concentration, structure and integrity**

##### **3.2.3.2.6.1. DNA isolation**

As tissue and bone ages DNA also undergoes fragmentation and degradation. It is crucial to know the extent of degradation as this will determine whether PCR amplification will be successful. To achieve this, the amount of DNA present and the structural integrity thereof must be determined before being used for PCR amplification.

To isolate DNA 100µl of a 2.5M sodium perchlorate (NaClO<sub>4</sub>) solution was added to 500µl supernatant and the sample mixed well. Equal volumes of CHCl<sub>3</sub>:isoamylalcohol (24:1) was added and the samples mixed for a further 15 to 20 minutes. The samples were centrifuged at 1800rpm at 4<sup>0</sup>C for 10 minutes. The upper layers were transferred to a clean 15ml tubes and two volumes of ice cold ethanol added to the samples. The DNA samples were kept overnight at -20<sup>0</sup>C and the following morning the samples were collected by centrifugation at 2000rpm. All ethanol was removed by blotting and the samples were resuspended in 100µl

Tris/EDTA (TE) buffer consisting of 10mM of 1mM Tris/HCl, pH 7.5 and 1mM of 500mM EDTA, pH 8.0 (Potsch *et al.*, 1992; Evison, 1997; Bender *et al.*, 2000; Baker *et al.*, 2001; Von Wurmb-Schwark *et al.*, 2003; Ye *et al.*, 2004; Opel *et al.*, 2006; Rohland and Hofreiter, 2007; Dobberstein *et al.*, 2008).

#### **3.2.3.2.6.2. Analysis DNA quantity and quality**

After isolation, DNA concentration was quantified by using absorbance spectrometry and fluorometry. The quality/purity of the DNA was determined spectrophotometrically at 260nm and 280nm. The extent to which the DNA had undergone fragmentation was determined by agarose gel electrophoresis (AGE) (Rohland and Hofreiter, 2007).

To determine the absorbance at 260nm 50µl aliquots of the DNA samples were diluted with 2ml TE buffer. Absorbance was measured at 260nm and 280nm against 1xTE buffer. DNA concentration for each sample was determined from the 260nm reading where  $1A = 50\mu\text{g/ml}$ . To determine the purity of each sample, the 260nm/280nm ratio was calculated (Kaiser *et al.*, 2008).

The concentration of DNA was also determined using Hoechst dye 33258 which binds the minor groove of double stranded DNA. To each sample 10µl Hoechst 33258 of a 0.11M solution was added to either a 10µl or 20µl volume sample respectively. After 10 minutes fluorescence was measured at an excitation wavelength of 350nm and an emission wavelength of 460nm (Potsch *et al.*, 1992; Bester *et al.*, 1994). A DNA standard curve of 0-20µg/ml was used.

#### **3.2.3.2.6.2. Agarose gel electrophoresis (AGE)**

To determine the quality, i.e. the presence of and whether DNA fragmentation has occurred, DNA electrophoresis was performed. A 0.8% agarose gel was prepared in 1xTris-acetate/EDTA (TAE) buffer containing 0.01% ethidium bromide (EtBr). A 50x TAE buffer consisted of 0.089M Tris, 0.079M acetic acid and 0.5M EDTA at pH 8.3 which was diluted to 50times before use. The DNA samples were diluted 1:1 with loading buffer (60% sucrose in 1xTAE buffer containing 0.001% bromophenol blue (BPB)) and loaded onto the gel (Von Wurmb-Schwark *et al.*, 2003). A 30µl sample of the field samples and 20µl sample of the *in vitro* aged samples were loaded. Electrophoresis was carried out at 90V for 1h. The gel was visualised using ultraviolet radiation and photographed using the Firereader UVTech Documentation System (Evison, 1997; Baker *et al.*, 2001; Von Wurmb-Schwark *et al.*, 2003; Dobberstein *et al.*, 2008).

### **3.2.3.2.6.3. Detection of the $\beta$ -actin and cytochrome *b* gene**

A major advantage of PCR amplification is that it can be used for minute quantities or degraded DNA samples (Primorac, 2004). Bellis and researchers (2003) investigated potential markers within chromosomal, mitochondrial and ribosomal DNA for forensic animal species identification. Two of these genes, the genomic,  $\beta$ -actin (ACTB) and the mitochondrial, cytochrome *b* (*cytb*) genes were evaluated. The  $\beta$ -actin (ACTB) gene could be used to discriminate between human and porcine origin due to size differences of 289bp and 248bp for *S. Scrofa* and human, respectively (Bellis *et al.*, 2003). Although the *cytb* gene is highly homologous between vertebrate species, it is a region of the mitochondrial genome that is easy to amplify (356bp) and is very resistant against environmental factors (Parson *et al.*, 2000; Bellis *et al.*, 2003). For these reasons these two genes were used in this study. Two methods were used namely PCR in combination with AGE and real-time PCR.

For PCR the total reaction volume of 20 $\mu$ l was used and contained 25mM MgCl<sub>2</sub>, 400 $\mu$ M nucleotide mix (dNTP), 5 units/ $\mu$ l GoTaq<sup>®</sup> DNA polymerase, Green GoTaq<sup>®</sup> Flexi Buffer and 15 $\mu$ M of each primer. Reaction conditions consisted of an initial denaturation step at 95<sup>o</sup>C for 2min., followed by 30 cycles of denaturation at 95<sup>o</sup>C for 1min., annealing at 57<sup>o</sup>C for 1min. and extension at 72<sup>o</sup>C for 1min. Final extension was carried out at 72<sup>o</sup>C for 5minutes. To ensure the effectiveness of all reagents and the absence of contamination of all the reagents, positive control plasmid DNA was subjected to all the PCR conditions. For the control plasmid, the primers were excluded. A negative template control (ntc) was also included where no DNA was added to the reaction mixture in order to ensure the absence of contaminants of the primers (Bellis *et al.*, 2003).

Real-time PCR was performed using the Rotor-Gene Q thermocycler. For real-time PCR of both *cytb* and ACTB all reactions were carried out in a total final volume of 20 $\mu$ l using 5ng DNA as template. The reaction mixture consisted of 6.25 $\mu$ l reaction mixture (SensiMix HRM<sup>™</sup>) purchased from BioLine 0.5 $\mu$ l EvaGreen<sup>™</sup>, 5 $\mu$ l of each primer and 3.75 $\mu$ l ddH<sub>2</sub>O. Amplification was conducted in a Rotor-GeneQ thermocycler with an initial denaturation at 94<sup>o</sup>C for 5 min. followed 30 cycles of 94<sup>o</sup>C for 30s, 57<sup>o</sup>C for 30s and 72<sup>o</sup>C for 1min and a final extension step at 72<sup>o</sup>C for 7 min. (Bellis *et al.*, 2003). A negative template control (ntc) was also included where no DNA was added to the reaction mixture in order to ensure the absence of contaminants of the primers. An ntc was included for each experiment to ensure the effectiveness of the reagents and the avoidance of contamination.



The DNA isolated from fresh teeth,  $T_0$  for the *in vitro* model was used for the optimization of all PCR procedures. The advantage of real time PCR was that this technique was rapid, a small amount of DNA was required and the amount of product that formed could be quantified (Primorac, 2004). Initial method development was undertaken using conventional PCR, all methodologies were adapted for real time PCR and this is the data that is presented in the following chapter.

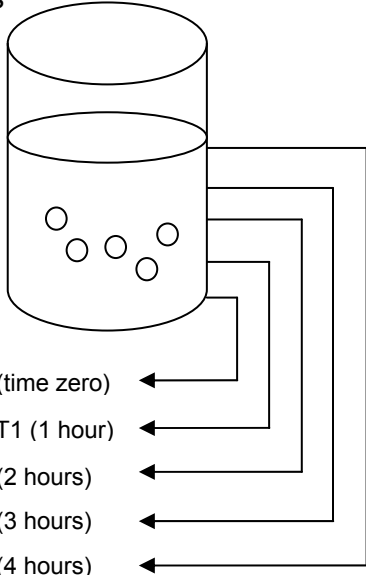
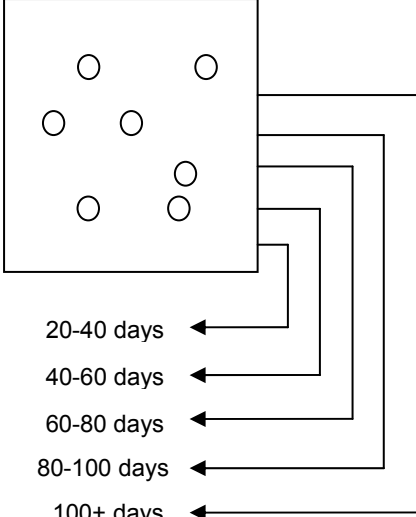
**Table 3.3. Primer sequences from Bellis and associates (Bellis, *et al.*, 2003)**

<b>ACTB</b>	Forward 5'-CGGAACCGCTCATTGCC-3'	$T_m=57.1^{\circ}\text{C}$
	Reverse 5'-TAGATGGGCACAGTGTGGGT-3'	$T_m=58.5^{\circ}\text{C}$
<b>Cytb5</b>	Forward 5'-CCCCTCAGAATGATATTTGTC-3'	$T_m=56.3^{\circ}\text{C}$
	Reverse 5'-CCATCCAACATCTCAGCATGA-3'	$T_m=57.5^{\circ}\text{C}$

### **3.2.3.2.6.5. Agarose gel electrophoresis of PCR products**

For the identification of the PCR amplification of the PCR products and the confirmation of the size of the PCR product following real time PCR equal volumes of loading buffer (50% glycerol containing 0.001% bromophenol blue (BPB)) was added and the PCR amplification products were separated by AGE. For AGE a 2% agarose gel was made by diluting 0.5g agarose in 25ml TAE buffer containing 0.01% EtBr. The DNA samples were diluted 1:1 with loading buffer (Von Wurmb-Schwark *et al.*, 2003). 10 $\mu\text{l}$  and 5 $\mu\text{l}$  volumes respectively of the field and *in vitro* aged PCR amplification products were loaded onto the gel. Electrophoresis was performed at 90V for 1h. The gel was visualised using ultraviolet radiation and photographed (Evison, 1997; Baker *et al.*, 2001; Von Wurmb-Schwark *et al.*, 2003; Dobberstein *et al.*, 2008).

### 3.3. Data management

<i>In vitro</i>	Field
<p>5 pigs</p>  <p>T0 (time zero) ← T1 (1 hour) ← T2 (2 hours) ← T3 (3 hours) ← T4 (4 hours) ←</p> <p>Collected samples irrespective of animal are pooled as time interval stored at -70°C</p> <p style="text-align: center;">↓</p> <p>Thawed randomly divided in 3 groups and each group consisted 3 randomly selected teeth</p> <p>Each data point is the average of three independent experiments, average for 9 teeth.</p> <p>Each assay was done in quadruple, average of 12 assays per data point</p>	<p>20 pigs</p>  <p>20-40 days ← 40-60 days ← 60-80 days ← 80-100 days ← 100+ days ←</p> <p>Collected samples irrespective of animal are pooled as time interval stored at -70°C</p> <p style="text-align: center;">↓</p> <p>Thawed randomly divided in 3 groups and each group consisted of 3 randomly selected teeth</p> <p>Each data point is the average of three independent experiments, average for 9 teeth.</p> <p>Each assay was done in quadruple, average of 12 assays per data point</p>

### 3.4. Statistical analysis

The *in vitro* based laboratory method and field study was based on the teeth from a genetic homogenous pig population. This study sets out to assess trend over time with respect to the concentration of certain bio-molecules, i.e. total protein, collagen, haemoglobin, iron, porphyrins, ninhydrin positive components and DNA.

All data represents an average of three experiments and each measurement was done at least in quadruple, thereby generating 12 data points. The results are expressed as mean ±

standard error of mean (SEM) of three experiments where each experiment point is the average of 3 assays. Data was statistically evaluated using analysis of variance (ANOVA), using samples as independent variables and the values determined as dependent variables. Fisher's least significant difference (LSD) test was used for comparison of means using statistica software Version 9.0 (StatSoft, Tulsa, OK). Correlation analysis was also run with the same statistical package, and Microsoft Excel 2007.

### **3.5. Ethical considerations**

Permission to use the porcine teeth of the decomposing pigs at the Miertjie le Roux farm has been obtained. (Protocol EC080617-026). The Animal Ethics Committee (AUCC) of the University of Pretoria's Biomedical Research Council (UPBRC) was approached regarding ethical concerns concerning the pigs head obtained from the abattoir. The Animal Use and Care Committee (AUCC) responded that no ethical clearance was required.

## **CHAPTER 4: RESULTS AND DISCUSSION**

The purpose of this study was to use porcine teeth to identify molecules that demonstrated a time related change in concentration and structure with heating. Porcine teeth were used in this model as they are comparable to human teeth in size, variation, composition and morphology (Douglas, 1971).

### **4.1 *In vitro* model**

The *in vitro* model is a laboratory based method in which bones or teeth are heated for specific time intervals and usually at high temperatures. The purpose of using a high temperature is to accelerate the decomposition process. Also changes can be studied without the effect of bacterial and microbial activity. This enables scientists to develop methodologies to measure the concentration and to study the structural integrity of bio-molecules that could be used to identify an individual, such as DNA, or provide an indication of time after death (TAD) (Dobberstein *et al.*, 2008).

Several researchers have studied the effect of heating and aging on the bio-molecules found in teeth (Von Wurmb-Schwark *et al.*, 2003; Dobberstein *et al.*, 2008). Dobberstein *et al.*, (2008), studied the effect of heating at 90<sup>0</sup>C for a period of 20 days in human and porcine teeth. Von Wurmb-Schark *et al.*, (2003), studied the effect of heating for 0-96 hrs (2 hour intervals) using human femoral bones. Temperature has been identified as one of the most important factors that determine the rate of decomposition. By using an elevated temperature, the decomposition process can be accelerated and for this reason at temperature of 90<sup>0</sup>C was used in this study. This temperature ensures rapid degradation of bio-molecules without denaturation, which occurs at 100<sup>0</sup>C and higher. Most studies based on this model use a temperature of 90<sup>0</sup>C. Based on the findings of Dobberstein *et al.*, (2008); in which DNA rapidly degraded within the first 16 hours (most rapid decline the first 6 hours), where Von Wurmb-Schark *et al.*, (2003); found complete DNA degradation after 12 hours and based on a pilot study in our laboratory using porcine ribs in which degradation was found to be complete in the first 8 hours (Myburgh *et al.*, 2008); it was decided in this study to heat the samples for a maximum of 4 hrs with 1 hour intervals.

Using porcine teeth, heated for 0-4 hours, the concentration of several constituent bio-molecules was determined and these included collagen, total protein, haemoglobin (Hb), pyrroles, iron, ninhydrin reactive nitrogen (NRN) and DNA. In this study the concentrations of

collagen, protein and DNA as well as the usability thereof for PCR amplification was determined.

The effects of decomposition on the concentration and structure of Hb was studied. Hb is a major constituent of erythrocytes. Contained within Hb is the highly stable heme group containing Fe. Therefore with degradation the protein associated with Hb will be the first to degrade, this will be followed by the more stable tetrapyrrole ring structures with free Fe remaining. With further decomposition, the tooth matrix becomes more porous and the free Fe will eventually leach away (Schicker and Miller, 2006; Schaer and Alayash, 2009). Therefore the degradation of Hb would serve as a time related indicator of decomposition.

The concentration of ninhydrin reactive nitrogen (NRN) was also determined. Researchers mostly focus on the determination of NRN influx in grave-soil where decomposition has taken place (Van Bell *et al.*, 2009; Lovestead and Bruno, 2011; Moreno *et al.*, 2011). Van Bell *et al.*, (2009), measured the influx of NRN in grave-soil during above ground and below ground decomposition of porcine carcasses. The researchers found that most NRN's were released during the early stages of decomposition and that the NRN's showed a steady decline as decomposition progressed (Van Belle *et al.*, 2009). Similarly Lovestead and Bruno, (2011), found that NRN concentrations declined as decomposition progressed in rat carcasses. Moreno *et al.*, (2011), used ninhydrin to determine the microbial composition of grave-soil. The researchers found that the concentrations of microbes in the soil increased as decomposition proceeded. It was found that the concentration of NRN in the soil increased as decomposition progressed and that nitrogen fixing bacteria also had an effect on the concentrations of NRN. As decomposition progressed the nitrogen fixing bacteria consumed nitrogen during their nitrogen fixing cycles. Eventually the nitrogen becomes depleted and the concentration of NRN decreases in the late stages of decomposition (Moreno *et al.*, 2011). NRN levels increase in grave soil with TAD, therefore it can be assumed that possibly there would be a decrease in NRN within the carcass and in this case the isolated environment of the tooth cavity. This is the first study in which the concentration of NRN was determined within the pulp cavity of teeth.

### **Morphology and mass of the teeth**

For the *in vitro* model, 45 extracted teeth were used. The teeth were divided into three groups, 15 teeth each and this represented three independent experiments. All 15 teeth were placed in a beaker and were heated in ddH<sub>2</sub>O at 90°C, over a period of 4 hours every hour (groups T0, T1, T2, T3 and T4) three teeth were randomly removed. This was repeated

three times. The teeth were blotted dry the morphology evaluated, weighed, fragmented and then freeze-dried.

Heating at 90<sup>0</sup>C caused teeth to display a yellowish discolouration and increase in brittleness as seen in a similar study conducted by Dobberstein et al., (2008). When compared to the field teeth, the *in vitro* teeth displayed a smooth, shiny surface. Even after heating for 4 hours, teeth still displayed a glossy appearance. The teeth were intact with no fracture lines, cracking, weathering or corrosion of the tooth surfaces. All roots remained intact and no microtunneling caused by bacterial activity was visible.

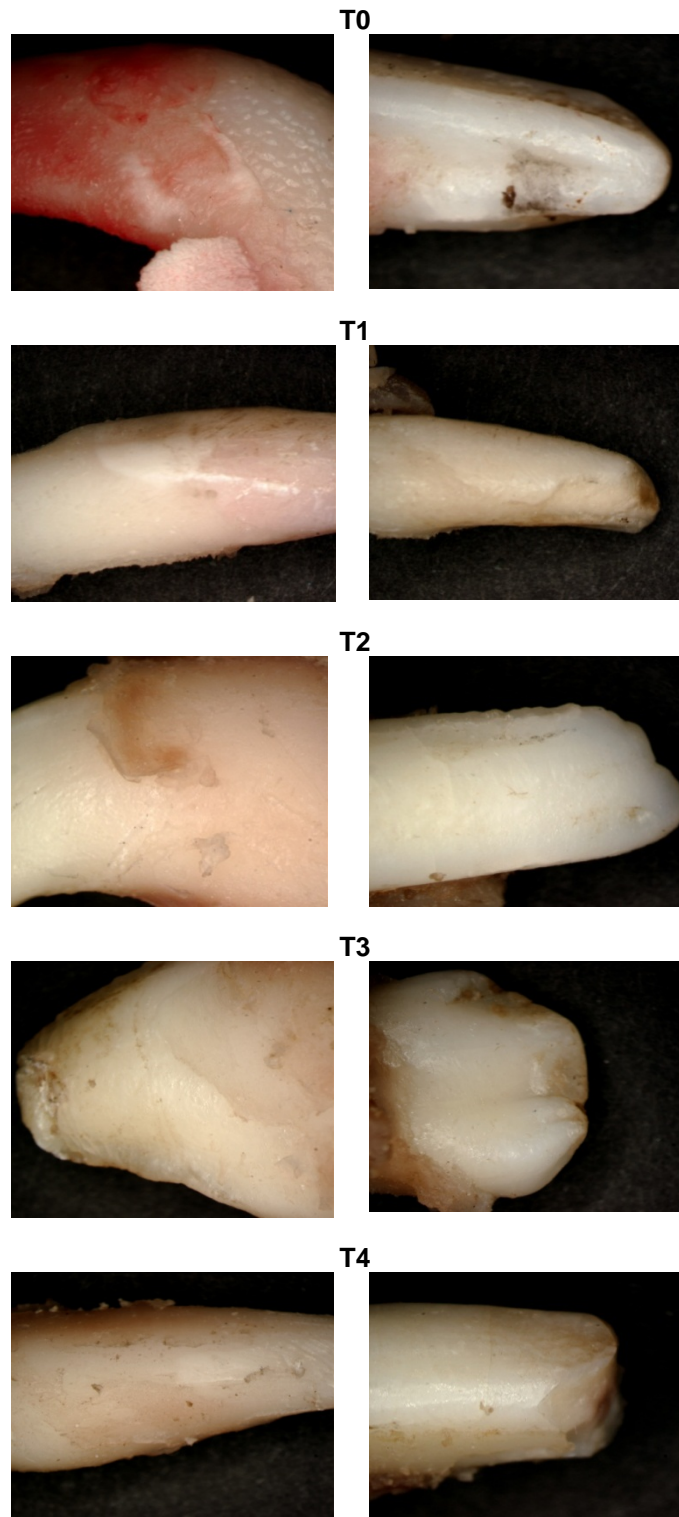


**Fig 4.1.1.** Typical morphology of porcine teeth heated for 0, 1, 2, 3 and 4 hours.

The mass of each group (T0-T4) (Figure 4.1a.) varied from 4.47-8.32g with a median of 5.81g. After freeze-drying for 96 hrs (Figure 4.1b) the mass of the teeth decreased and was 2.79-5.51g with a median mass of 3.91g. No statistically significant differences in mass between groups were found before ( $p=0.2907$ ) and after freeze-drying ( $p=0.2416$ ).

**Table 4.1.1. Mass of all teeth, *in vitro* study before and after freeze-drying.**

	<u>Range (g)</u>	<u>Mean (g)</u>	<u>SEM (g)</u>	<u>%SEM</u>	<u>Median (g)</u>
<b>Before</b>	4.47-8.32	6.00	1.04	16.66	5.81
<b>After</b>	2.79-5.51	4.00	0.72	18.0	3.91

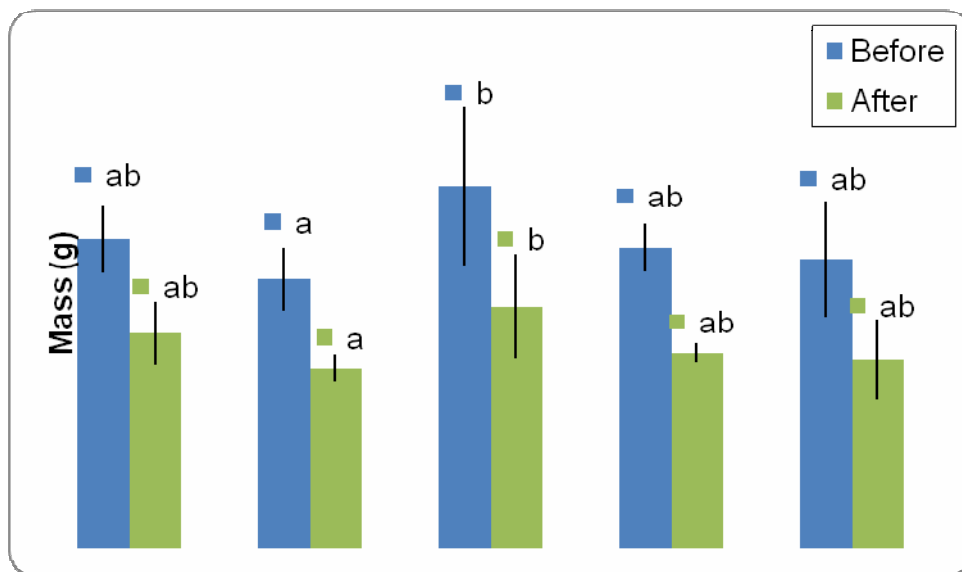


**Fig 4.1.2.** Mass of teeth after heating for 0-4 hours, before and after freeze-drying. Each data point is a mean  $\pm$ SEM of three separate experiments, total number of teeth (n)=45. Average of three independent experiments. Samples with the same letters are statistically similar.

This decrease in mass was due to the loss of water during freeze-drying and was calculated as percentage of starting mass and is presented in Table 4.1.2. This decrease was 29.98-39.19% of the original mass. Furthermore a correlation of 0.974 between before vs after freeze-drying indicates that there is no significant difference between groups due to moisture loss during processing. In all experiments, the data was expressed as g/g dry mass to eliminate the variations in the mass of the teeth between the two experimental groups, laboratory based *in vitro* study and the field study. The assumption is made that the amount protein/DNA in teeth is directly proportional to its dry mass.



**Table 4.1.2. Percentage loss in mass of all teeth, *in vitro* study with freeze-drying.**

<u>Range (%)</u>	<u>Mean (%)</u>	<u>SEM(%)</u>	<u>%SEM</u>	<u>Median (%)</u>
29.98-39.19	33.21	3.63	10.93	33.02

#### **4.1.1. Water insoluble fraction**

##### **4.1.1.1. Collagen content of the teeth**

After drying, the ground tooth material was suspended in buffer containing SDS and PMSF. Two fractions were collected after centrifugation (i) the supernatant containing the water soluble molecules and (ii) the insoluble bone material. The water soluble fraction was used in Section B. The fraction containing the bone material was demineralised and the collagen was solubilised using GuaHCl. GuaHCl causes a change in the circular dichroism of collagen similar to that induced by a high salt concentration that results in the formation of an  $\alpha$ -structure and subsequently an increase in solubility. (Cortijo *et al.*, 1973; Fuertes *et al.*, 2004).

In this soluble crude fraction, the protein content was determined using the Bradford method with collagen 0-100mg/ml as standard. The protein content varied from 0.25-0.434g/g with a mean value of 0.33g/g. Differences between samples were significant with  $p=0.0026$ . At T1 the concentration of collagen decreased from 0.434 g/g at T0 to 0.268 g/g at T1. The concentration of collagen then increased linearly to 0.354g/g ( $R^2=0.9217$ ). The crude collagen extract contains both collagen and other minor proteins present in the tooth matrix.

The Bradford method is based on the dye Coomassie blue binding residues (Melander and Tommerass, 2008). Therefore with degradation, there is a loss of collagen helical structure and also collagen degradation as observed by Dobberstein *et al.*, (2008). During this process the amino acid residues become more exposed and result in increased accessibility of the binding sites due to these amino acids resulting in an increase in absorbance.

Komsa-Penkova *et al.*, (1996), reported that concentration of collagen can be determined from the absorbance at 230nm. The collagen concentration determined using this method was 1.33-3.98 g/g with a mean of 2.71 g/g. As concentrations are measured per g mass of the teeth a concentration of greater than 1 g/g cannot be obtained. Therefore this indicates that GuaHCl causes interference at this wavelength. The structure of GuaHCl contains a double bond and nitrogen groups that has a strong absorbance wavelength at 230nm (Fish *et al.*, 1969; Fuertes *et al.*, 2004). The GuaHCl was subsequently removed, using a desalting column and this resulted in the measurement of lower collagen concentrations of 0.67-

1.41g/g with a mean of 1.00 g/g. The fractions were then freeze-dried and the final concentrations of collagen were 0.34-0.64g/g collagen indicating that there was still GuaHCl as contaminant in the samples.

**Table 4.1.3. Collagen content, *in vitro* model**

<b>Method</b>	<b>Range (g/g)</b>	<b>Mean (g/g)</b>	<b>SEM (g/g)</b>	<b>%SEM</b>	<b>Median (g/g)</b>
<b>CB</b>	0.25-0.43	0.33	0.06	19.35	0.33
<b>Abs 230nm</b>	1.33-3.98	2.71	1.00	38.71	2.58
<b>Abs 230nm after desalting</b>	0.67-1.41	1.00	0.18	17.41	1.07
<b>Final mass, isolated collagen (g/g)</b>	0.34-0.64	0.46	0.20	45.34	0.43

Differences between the concentrations of collagen (g/g) determined using the Bradford method for protein ( $p=0.0026$ ) and the absorbance at 230nm before ( $p=0.0063$ ) and after desalting ( $p=0.00$ ) was significant between groups. However these differences were not related to time heated. No significant differences were found in the final mass of all groups ( $p=0.292$ ) but an increase in collagen yield was observed. A contributing factor to these differences between groups is that each group contained different types of teeth. For example, the groups had only one type or a mixture of tooth types. Molars for example had a thicker layer of dentine and enamel than incisors (Ten Cate, 2004). Dobberstein *et al.*, (2008), reported a decrease in collagen yield from 16% to 1%. However these experiments were done over 18 days with 6 day intervals (Dobberstein *et al.*, 2008). The shorter time period used in this study shows no changes in collagen content from 1hr to 4hrs heating. The average yield of collagen was found to be 46% dry mass and 30.6% wet mass/original, which was the of the same order as reported byGotherstrometal.,(2002).

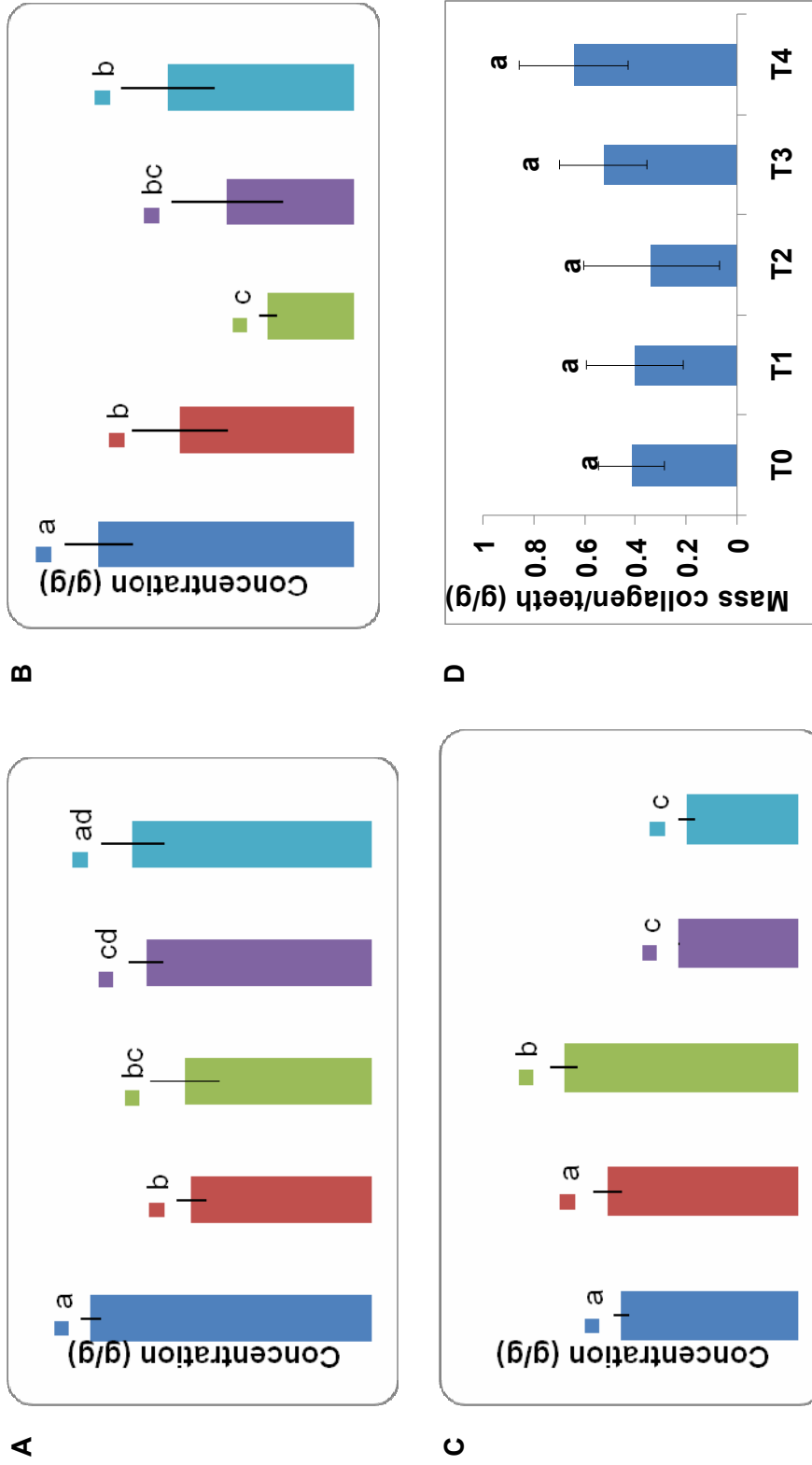


**Fig 4.1.3.** Collagen concentration *in vitro* model, after heating for 0-4 hours, demineralisation and solubilisation (A) determined by the Bradford method and (B) 230nm absorbance, (C) after desalting, absorbance 230nm absorbance and (D) then freeze-drying. Each data point is a mean  $\pm$ SEM of three separate experiments, total population size n=45. Samples with the same letters are statistically similar.

#### **4.1.2. Water soluble fraction**

##### **4.1.2.1. Protein, haemoglobin, pyrrole, iron and NRN present in the pulp cavity.**

###### **4.1.2.1.1. Protein**

Teeth consist of two protein components (i) the water soluble proteins usually present in the pulp and (ii) the water insoluble matrix proteins associated with the dentine and enamel (Klein *et al.*, 1982; Ten Cate *et al.*, 1994). The water soluble proteins were extracted with buffer containing the ionic detergent SDS and PMSF. SDS was added to increase protein solubility, while PMSF was used to prevent proteolytic protein degradation (Cirkovas and Sereikatte, 2011). The protein concentration was determined using the Bradford and Biuret methods with BSA as a standard. The Bradford method is based on the principle that Coomassie brilliant Blue (CBB) dye binds to arginine, tyrosine, tryptophan and phenylalanine residues. The binding of CBB is largely variable between different proteins and is a function of amino acid composition. The use of BSA as a standard leads to the underestimation of protein content in a sample (Kruger, 2002); as BSA does not accurately represent all the proteins present in an unknown sample (Melander and Tommerass, 2008). The dye binds equally well to both high molecular weight (HMW) and low molecular weight (LMW) proteins regardless of the degree of degradation but this dye does not bind to free amino acids and peptides. Detergents such as SDS can cause interference. SDS has two modes of interference. If the SDS concentration is below critical micelle concentration (CMC), SDS binds to the dye and inhibits the protein binding sites. When the SDS concentration is above CMC, the detergent associates with the green form of the dye and causes an equilibrium shift that produces more of the blue form (Melander and Tommerass, 2008). To prevent this effect, the SDS concentration used for the solubilisation was kept low and SDS at the same concentration was included in the preparation of the standard curves. A standard curve of 0-100µl BSA (0.005mg/ml) was used ( $R^2=0.98$ ) and the data was expressed as mg/g dried mass (Table 4.3 and Figure 4.3 and 4.4).

**Table 4.1.4. Protein content, *in vitro* study**

<b><u>Total Protein</u></b>	<b><u>Range (mg/g)</u></b>	<b><u>Mean (mg/g)</u></b>	<b><u>SEM (mg/g)</u></b>	<b><u>%SEM</u></b>	<b><u>Median (mg/g)</u></b>
<b>Bradford</b>	240.93-470.68	349.72	67.99	19.44	341.88
<b>Biuret</b>	176.94-481.34	374.48	80.20	21.41	364.63

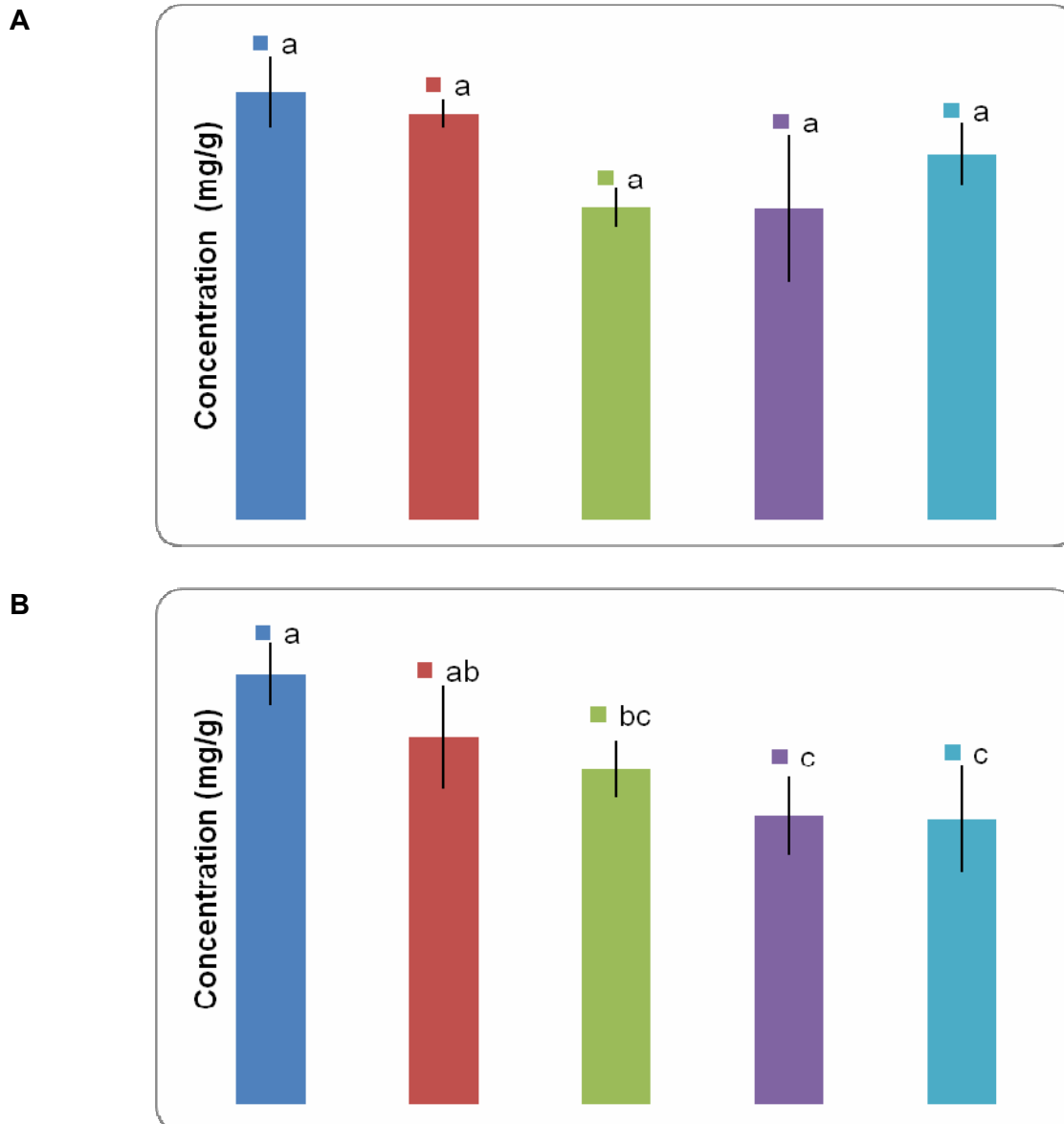


**Fig 4.1.4.** Average protein content of the pulp cavity of the teeth, *in vitro study*, after heating for 0-4 hours determined using the (A) Bradford and (B) Biuret assay. Each data point is a mean  $\pm$ SEM of three separate experiments, n=45. Samples with the same letters are statistically similar.

For the Bradford method, the protein concentration varied from 176.94-481.34 mg/g with a median of 364.63mg/g and a standard deviation of 80.20mg/g with no significant difference in protein content between groups ( $p=0.2385$ ). The Biuret method was also used to determine the protein content of the water soluble extract from the pulp cavity. The Biuret method is less sensitive than the Bradford assay but more linear because its colour depends on a direct complex between peptide bonds of the protein sample and  $\text{Cu}^{2+}$  ions. However a slight protein-to-protein variation in the assay results among different proteins with respect to three amino acid residues namely cysteine, tyrosine and tryptophan. The reaction is also

influenced by substances that reduce copper. Reagents that chelate copper can interfere with the accuracy of protein quantification. The Biuret reagent measures different proteins with similar equivalency per peptide bond; however proline residues appear to diminish the reactivity (Hortin and Meilinger, 2005). With degradation, protein becomes fragmented and/or the amino acid residues undergo chemical structural changes. Biuret reagent only reacts with peptide bonds (Hortin and Meilinger, 2005); therefore with degradation there will be a direct correlation between the rate of degradation and the amount of peptide bonds. However in the Bradford method, there is an additional factor, beside fragmentation, namely the amino acid residues that undergo chemical modification. As a result binding of CBB will be variable either increased or decreased (Melander and Tommerass, 2008). Using the Biuret method an exponential decrease ( $y=7.67x^2-68.54x+440.78$ ,  $R^2= 0.988$ ) in protein content from 481.34 to 176.94 to mg/g was measured. Differences were significant with  $p = 0.0091$  and these were between T0 and T2, T3 and T4 but not T0 and T1. Although less sensitive, based on the mechanism of reaction, less possible interference of detergents, as well as the associated decrease with increased time of heating at  $90^{\circ}\text{C}$ , the Biuret method is possibly the better method for the determination of protein concentration.

#### **4.1.2.1.2. Haemoglobin**

Erythrocytes are the predominant cell type found in the pulp cavity of which haemoglobin (Hb) is the major constituent protein. Hb is a tetrameric protein with two alpha and beta chains associated with a heme group that is an iron containing bio-molecule. The organic portion of the heme group contains a tetrapyrrole group while the iron is either in the ferrous ( $\text{Fe}^{2+}$ , able to bind  $\text{O}_2$ ) or ferric state ( $\text{Fe}^{3+}$ , not able to bind  $\text{O}_2$ ) (Schechter, 2008). The Drabkin's method is used for the determination of Hb concentration. Hb is oxidised to methaemoglobin ( $\text{Fe}^{2+}$  is oxidized to  $\text{Fe}^{3+}$ ) by potassium ferricyanide, the iron then reacts with cyanide ions of potassium cyanide to form cyanmet haemoglobin, a coloured product (Depositar *et al.*, 1972; Kapert *et al.*, 1993). Besides being an important constituent of erythrocytes found in the pulp cavity, Hb has also been found to be a highly stable macromolecule that is resistant to environmental factors and the Hb molecule has been detected in bushman rock paintings as old as 2000 years (Williamson, 2000). A standard curve of 0-100 $\mu\text{l}$  using human Hb as standard, concentration 0-1.9  $\mu\text{g}/\text{ml}$ , ( $R^2=0.985$ ) was used to determine the Hb contained in the pulp cavity and the data was expressed as mg/g dried mass (Table 4.1.5 and Figure 4.1.4). The Hb concentration varied from 99.06-269.38mg/g with a median of 14.69mg/g and a standard deviation of 33.00mg/g.

**Table 4.1.5. Hb content, *in vitro* model**

<u>Range (mg/g)</u>	<u>Mean (mg/g)</u>	<u>SEM (mg/g)</u>	<u>%SEM</u>	<u>Median (mg/g)</u>
99.06-269.38	133.98	33.00	24.64	134.69

No time related change in Hb concentration was found ( $p=0.0748$ ) (Figure 4.3).

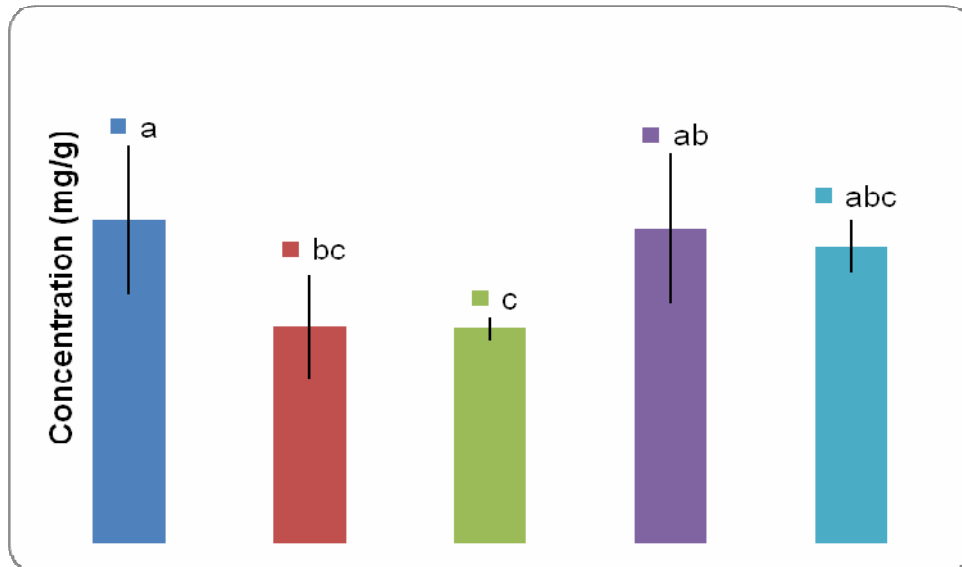


**Fig 4.1.5.** Hb content (mg/g) of the pulp cavity of the teeth used in the *in vitro* model determined using the Drabkin method. Each data point is a mean  $\pm$ SEM of three separate experiments,  $n=45$ . Samples with the same letters are statistically similar.

For the Bradford and Buret methods the percentage of Hb to total protein was  $36.28\% \pm 4.71\%$  and  $39.34\% \pm 6.22\%$ , respectively. As 90% of the erythrocyte content is Hb (Schechter, 2008 then 40% of the protein present in the pulp cavity is derived from erythrocytes. Therefore the investigation regarding the evaluation of predominantly erythrocyte derived bio-molecules is important as these molecules are usually present in high concentrations, are resistant to degradation especially during early phases of decomposition and may only undergo changes with time at a later stage.

#### **4.1.2.1.3. Pyrrole concentration**

The pyrrole ring structure is an important part of the heme group of Hb and other porphyrin molecules such as Hb, macrocycles (porphyrins, expanded porphyrins, calixpyrroles), pheromones, plant hormones, porphobilinogen, antibiotics neotropsin and the DNA minor groove binding distamycin (Biesaga *et al.*, 2000; Bellina and Rossi, 2006). A characteristic of tetrapyrrole containing molecules is the intense red fluorescence that is emitted following

excitation with light at 400 nm and as consequence concentrations as low as  $10^{-8}$  mol/l can be detected at 345nm (Shepard and Daily, 2005).

**Table 4.1.6. Pyrrole content, *in vitro* model.**

<u>Range (mg/g)</u>	<u>Mean (mg/g)</u>	<u>SD (mg/g)</u>	<u>%SD</u>	<u>Median (mg/g)</u>
1.57-5.98	3.69	1.24	33.62	3.77

Using 1mg/ml protoporphyrin a standard curve in lysis buffer ( $R^2=0.936$ ) ( $y=831.5x + 18.25$ ) was used and the data was expressed as mg/g. The concentration varied from 1.57-5.98mg/g with a median of 3.77mg/g and a standard deviation of 1.24mg/g (Table 4.1.6 and Figure 4.1.5).

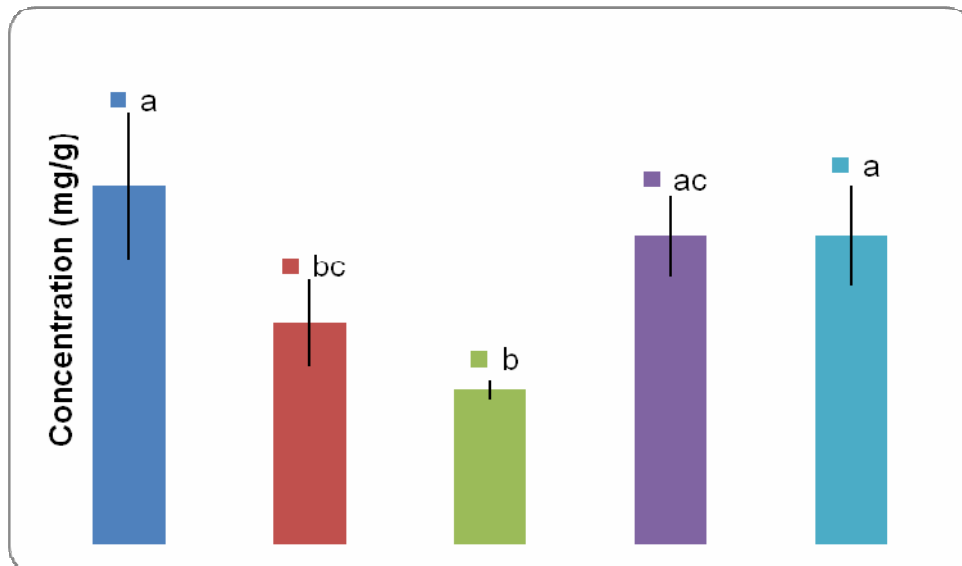


**Fig 4.1.6.** Pyrrole concentration (mg/g), model the pulp cavity of the teeth used in the *in vitro* model determined with fluorescence (Ex  $404_{nm}$  and Em  $624_{nm}$ ). Each data point is a mean  $\pm$ SEM of three separate experiments, n=45. Samples with the same letters are statistically similar.

The pyrrole concentration did not differ significantly between the groups but did show a strong correlation of 0.946 with Hb.

#### **4.1.2.1.4. Iron content**

Associated with the heme group is an iron molecule either as  $Fe^{2+}$  or  $Fe^{3+}$ .  $Fe^{3+}$  is the predominant type and is converted by enzyme systems to  $Fe^{2+}$  which is necessary for oxygen binding  $Fe^{3+}$  binds Xylenol Orange forming a blue product. To determine total iron  $Fe^{2+}$  is reduced to  $Fe^{3+}$ . Free iron is a small molecule and can diffuse from tissue resulting in reduced concentrations (Hermes-Lima *et al.*, 1995; Gay and Gebicki, 2000; Erel, 2005).



**Table 4.1.7. Total iron, Fe<sup>3+</sup> and Fe<sup>2+</sup> concentrations, *in vitro* model**

	<u>Range</u>	<u>Mean (mg/g)</u>	<u>SEM (mg/g)</u>	<u>%SEM</u>	<u>Median (mg/g)</u>
<b>Total iron</b>	6.48-9.35	7.28	0.410	5.62	6.75
<b>Fe<sup>3+</sup></b>	4.33-8.63	6.11	0.549	8.99	5.90
<b>Fe<sup>2+</sup></b>	0.77-3.30	1.70	0.337	19.81	1.25

A standard curve of 0-500µM ( $y=0.305x + 0.004$ ,  $R^2=0.994$ ) was used to determine iron concentrations. The concentration of total Fe decreased exponentially ( $y=0.307x^2 - 1.98x + 9.26$ ,  $R^2=0.988$ ) from 9.81-5.33 mg/g from T0 to T4 but these differences were not significant ( $p=0.0143$ ) (Figure 4.1.6). In contrast a significant ( $p=0.0002$ ) linear decrease ( $y=-1.01x + 8.14$ ,  $R^2=0.743$ ) in Fe<sup>3+</sup> was observed. Fe<sup>3+</sup> concentration at T2, T3 and T4 differed significantly from Fe<sup>3+</sup> concentrations at T0 and T1. A decrease in Fe<sup>3+</sup> is associated with an exponential increase in Fe<sup>2+</sup> ( $y= 0.7374e^{0.352x}$ ,  $R^2=0.965$ ), but this difference was not significant ( $p=0.78$ ). Levels at T2-T4 were higher than levels measured levels at T0 and T1.

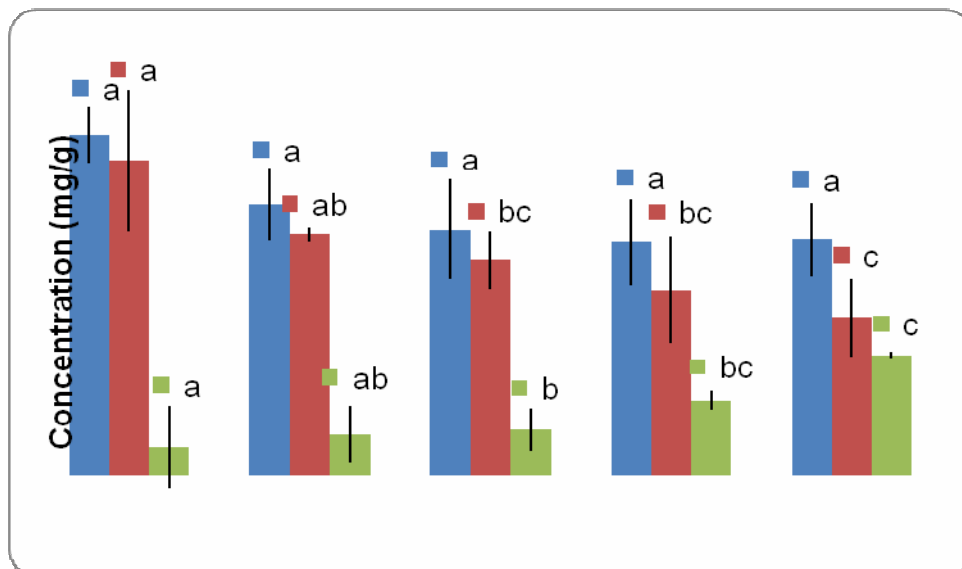


**Fig 4.1.7.** Total iron, Fe<sup>3+</sup> and Fe<sup>2+</sup> concentration of the pulp cavity of the teeth used in the *in vitro* model determined using Xylenol Orange. Each data point is a mean  $\pm$ SEM of three separate experiments, n=45. Samples with the same letters are statistically similar.

With increasing time the ratio of Fe<sup>2+</sup>:Fe<sup>3+</sup> changes from 12:1 to 2:1 (Table 4.1.8). In other words, decreasing concentrations of Fe<sup>3+</sup> is associated with increasing levels of Fe<sup>2+</sup>. Fe<sup>2+</sup> has a reduction potential ( $E_0$ ) of +1.229V in acidic solutions (Wiberg *et al.*, 2001). This means that Fe<sup>2+</sup> has a positive tendency to acquire electrons in an acidic environment.

**Table 4.1.8. The ratio of Fe<sup>3+</sup>:Fe<sup>2+</sup> of all teeth in the *in vitro* model**

	<u>T0</u>	<u>T1</u>	<u>T2</u>	<u>T3</u>	<u>T4</u>
Fe <sup>3+</sup> :Fe <sup>2+</sup>	12:1	8:1	7:1	4:1	2:1

**4.1.2.1.1.5. Ninhydrin reactive nitrogen**

Ninhydrin Reactive Nitrogen (NRN) is derived from nitrogen that is an important element present in proteins, peptides, amino acids, amines and ammonia (Lovestead and Bruno, 2011). During decomposition these NRN's are released from the body and leach into the surrounding soil and is therefore used to detect graves. As decomposition progresses, the concentration of NRN in the soil increases. Likewise degradation of protein in the pulp cavity will also result in the formation of NRN and smaller NRN's such as ammonia will leach through the porous bone matrix into the soil and consequently the NRN's inside the pulp cavity will decrease with time (Hopkinset *al.*, 2000; Von Belleet *al.*, 2009; Lovestead and Bruno, 2011).

Most amino acids are primary and secondary amines that react with ninhydrin to form a purple product known as Ruhemann's purple. No reaction occurs with tertiary amines while with  $\alpha$ -imino acids such as proline, pyrroles, pyrrolidine or pyrrolidone a yellow product forms (Troll and Cannan, 1953). Water extracts derived from the protein contained in the pulp cavity produced a yellow product and for this reason L-proline was used for the preparation of a standard curve. A standard curve of 0-0.2mg/ml with  $y=0.566x+0.0032$  and  $R^2=0.985$  was used to determine all NRN concentrations. A linear decrease ( $y= -4.3789x + 25.74$ ,  $R^2 = 0.989$ , Figure 4.6) was observed in the NRN from T0-T4. The concentration of the NRN decreased from 29.62 mg/g to 7.49 mg/g after 4 hours of heating. Differences were highly significant ( $p=0.00002$ ). Like Fe<sup>3+</sup>, a significant difference compared to T0 was found after 2 hours.

**Table 4.1.9. Ninhydrin positive components, *in vitro* model.**

<u>Range (mg/g)</u>	<u>Mean (mg/g)</u>	<u>SEM (mg/g)</u>	<u>%SD</u>	<u>Median (mg/g)</u>
7.49-24.92	16.95	2.32	13.68	17.81

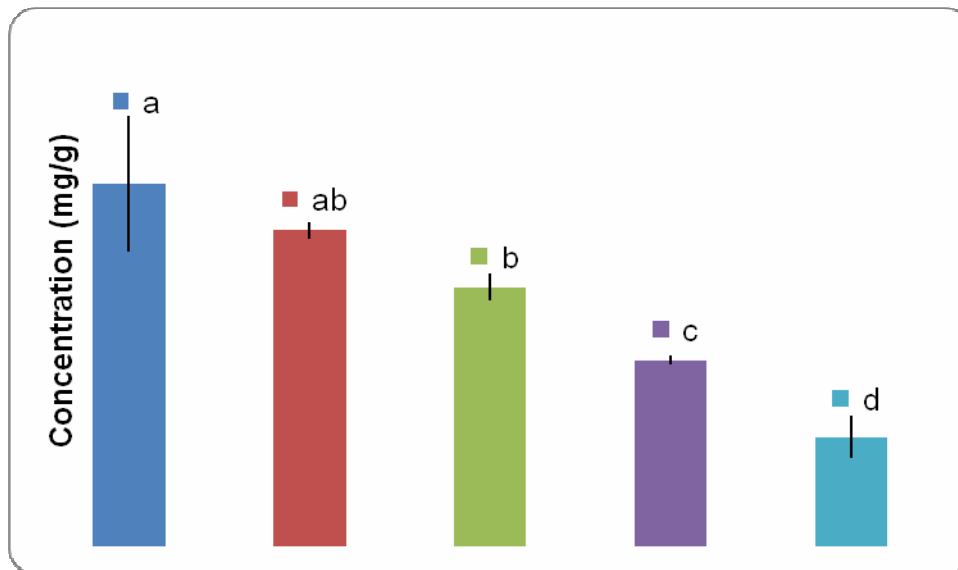


**Fig 4.1.8.** NRN present in the pulp cavity after heating for 0-4 hours. Each data point is a mean  $\pm$ SEM of three separate experiments, n=45. Samples with the same letters are statistically similar.

The NRN's contained within the pulp cavity forms a yellow product which indicates high concentrations of  $\alpha$ -imino acids such as proline, pyrroles, pyrroline or pyrrolidine (Troll and Cannan, 1953). Levels of free cellular proline are low (Wu, 1997); and therefore an alternative source for a positive reaction should be considered.

Hb is the major erythrocyte protein present in the pulp cavity and consists of four pyrrole rings with methane-bridge linkages contained in a ring structure that binds iron via coordination linkages to form the heme group. Associated via tertiary and quaternary interactions and with the heme group are four polypeptide strands ( $\alpha$ - and  $\beta$ -globulin, as  $\alpha_2\beta_2$ ) (Stadler *et al.*, 2008). The use of SDS an ionic detergent for extraction will result in the loss of secondary, tertiary and quaternary structure and this will result in the heme group becoming separated from the  $\alpha$ - and  $\beta$ - strands. Further thermal degradation will result in the release of the iron molecule from the heme group (Ryter and Tyrnell, 2000). The methane linkages can break which can result in the formation of a linear bilirubin which can also bind ninhydrin (Ryter and Tyrnell, 2000; Friedman, 2004; Mulsow *et al.*, 2009). Further thermal decomposition will result in the formation of hydrogen cyanide and propyne (Ryter and Tyrnell, 2000), which will not bind ninhydrin and as a consequence there will be a decrease in NRN. Mulsow *et al.*, (2009), reported that increases in temperature results in protein denaturation and this is associated with loss of tertiary and secondary structure with increased ninhydrin binding (Friedman, 2004). This however is related to the unravelling of the protein strands making previously inaccessible residues available for ninhydrin binding (Mulsow *et al.*, 2009). In these water soluble fractions the use of SDS ensures the loss of

secondary structure and the effect described by Mulscow *et al.* (2009). Therefore the decrease is directly related to degradation.

Another possibly major cellular component is RNA and DNA (Coetzee *et al.*, 2003). Nucleotides namely adenine, guanine and cytosine contain primary amines while secondary amines (NRN's) are found in the ring structure of purines and pyrimidines (Tudek, 2003). Deamination of these residues will result in the amounts of detectable NRN (Mulsow *et al.*, 2009), as this may be related to the decrease in DNA seen in the following section.

#### **4.1.2.1.6. DNA content**

Erythrocytes do not contain DNA and DNA that can be isolated from the pulp cavity is derived for other cell components such as lymphocytes, fibroblasts and endothelial cells. Some DNA can be recovered from the dentin or cementum but none within the enamel (Stavrianos *et al.*, 2010). Stavrianos *et al.*, (2010), reported that the maximum amount of DNA can be isolated from crushing the entire specimen as was done in this study. The DNA was isolated using the chloroform:isoamyl alcohol method and the concentration of the DNA was determined from the 260 nm absorbance reading (Figure 4.1.8A) (Von Wurmb-Schwark *et al.*, 2003); and from the increase in blue fluorescence observed due to Hoe binding the minor groove of DNA at AT rich regions (Figure 4.1.8B) (Bester *et al.*, 1994; Haq *et al.*, 1997; Kakkar 2002; Rengarajan *et al.*, 2002). Hoe binds to the N-groups of adenine and cytosine by means of H-bonds (Haq *et al.*, 1997). A standard curve of 0-20µg/ml with  $y=1477x+310.44$ ,  $R^2=0.979$ , was used to determine all DNA concretions. With heating of the teeth the concentration of DNA determined from the 260 nm absorbance measurements decreased exponentially ( $y = 3.208x^2 - 20.229x + 56.43$ ,  $R^2 = 0.933$ ). At T0 the DNA concentration was 71.30mg/g and decreased to 23.50 mg/g at T4. Differences between the groups were significant with  $p=0.0002$ .

**Table 4.1.10. DNAcontent, *in vitro* study**

<u>Total DNA</u>	<u>Range (mg/g)</u>	<u>Mean (mg/g)</u>	<u>SEM (mg/g)</u>	<u>%SEM</u>	<u>Median (mg/g)</u>
<b>Abs 260nm</b>	24.6-58.5	34.9	13.61	39.02	29.80
<b>Hoe</b>	34.67-80.00	48.63	18.7	38.45	44.98

Likewise for Hoechst binding, the DNA concentration with heating an exponential decrease ( $y = 4.151x^2 - 26.89x + 77.53$ ,  $R^2 = 0.927$ ) from 80.77 mg/g to 34.67 mg/g was observed (significant  $p=0.0000007$ ). A level of correlation ( $p=0.993$ ) was found between both methods. The concentration measured by Hoe binding was 30% greater than that which was

calculated from the 260 nm readings, but both methods showed a 42.05% and a 42.96% decrease in DNA concentration.

For both methods used, the quantification of DNA content decreased significantly within the first hour of heating. No significant differences were found between T1-T4.

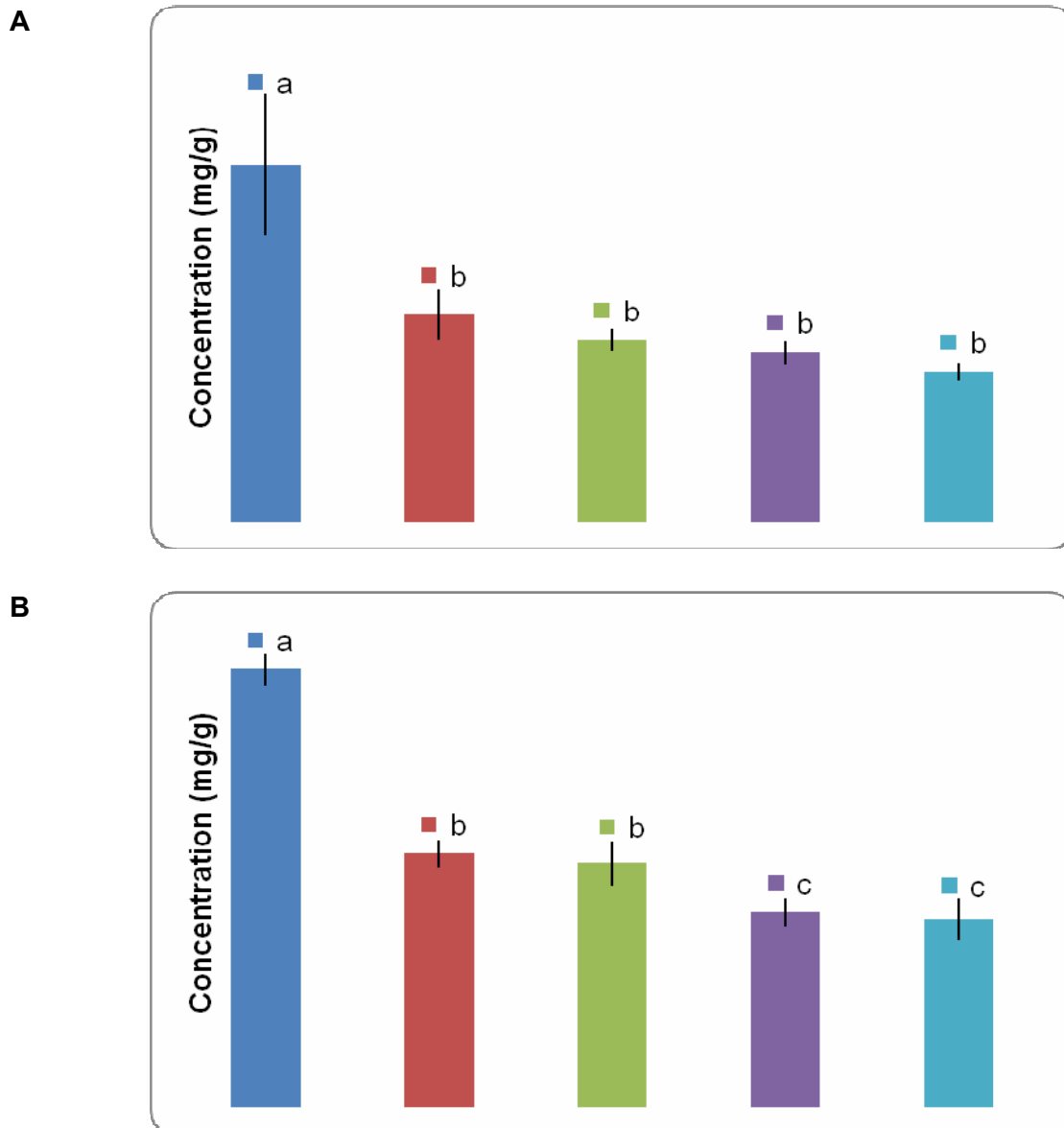


**Fig 4.1.9.** DNA concentration of the pulp cavity of the teeth heated 0-4 hours determined (A) from the 260 nm absorbance readings and (B) fluorescence following Hoechst binding. Each data point is a mean  $\pm$ SEM of three separate experiments, n=45. Samples with the same letters are statistically similar.

The purity of the DNA was determined from the 260nm/280nm ratio (Yeates *et al.*, 1998). The ratio was 1.27-1.54 with a mean of 1.45 (%SD = 6.11). No significant differences ( $p=0.0124$ ) were found between groups.

In a similar study, Dobberstein *et al.*, (2008), found the DNA concentration for *in vitro* aged teeth to be 300ng per 500mg of tooth powder, while AGE showed a detection threshold of 5ng HMW DNA. Von Wurmb-Schwark *et al.*, (2003), found that 100mg of bone powder yielded 6mg/g DNA. The amount of DNA fell with time from 250pg/ $\mu$ l to 50pg/ $\mu$ l extract (Von Wurmb-Schwark 2003). A further study conducted by Rubio *et al.*, (2009), concerning the short and long term effects of storage on DNA in teeth, found that with an one-way ANOVA the DNA concentrations between teeth stored from 0-10 years showed significant differences. When comparing the groups with each other, it was found that T0 differed significantly from all other groups. But, none of the other groups showed significant differences when compared to each other. The researchers also found that the amount of DNA isolated from the anterior teeth (incisors and canines) did not differ significantly from the amount of DNA isolated from the posterior teeth (premolars and molars) (mean = 26.38ng/5 $\mu$ l vs 25.95ng/5 $\mu$ l) (Rubio *et al.*, 2009).

In this study for 1g of tooth powder 24.6-58.5 mg (A260nm determination) and 34.67-80.00 mg DNA (Hoechst determination) was isolated. The amount of DNA isolated is much higher than that reported by other researchers. This may be related to the methods used to isolate the DNA. Several authors used commercial kits in their studies, whereas in this study DNA was isolated using a method specifically optimized for this application. The kits used were the Invisorb Forensic kit specifically designed for the extraction of DNA from blood, bone, teeth and hair. Although these kits allow the rapid isolation of DNA, the amount of DNA isolated may not be optimal. The most important step in the isolation of DNA is the rupture of cells and the release of cellular content including DNA. In this study the extensive washing of the tooth powder for 48hrs in the presence of SDS ensure the extraction of DNA from all cells. Further optimization specifically for this application ensures optimal extraction.

A A260/A280 ratio of 1.8-2.00 is ideal for successful PCR (Yeates *et al.*, 1998). The integrity of the isolated DNA samples was determined by agarose gel electrophoresis (Von Wurmb-Schwark *et al.*, 2003). The same volume of DNA was loaded into each well. The band intensity of T0-T3 was similar but the intensity of the band at T4 was less than that for T0-T3 and did not quiet reflect the findings shown in Figure 4.1.8 A and B. Compared to the control, T0 very little fragmentation had occurred.

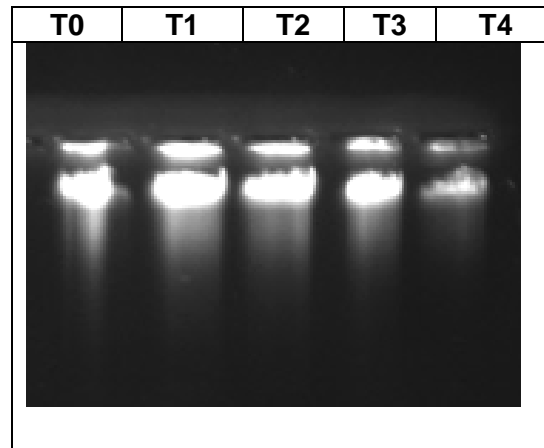


**Fig 4.1.10** Agarose gel electrophoresis (AGE) of the isolated DNA from samples heated for 0-4 hours. (10 $\mu$ l), Lane 1=236 $\mu$ g, lane 2=115  $\mu$ g, lane 3=188  $\mu$ g and lane4=95  $\mu$ g and lane 5=135  $\mu$ g calculated from Hoe determination respectively.

#### **4.1.2.1.6.1. PCR amplification**

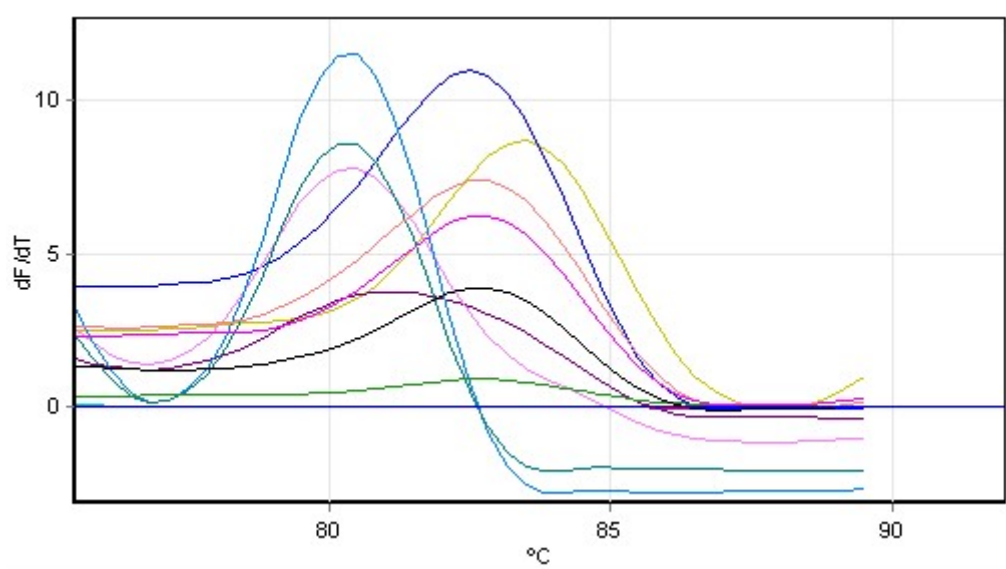
Isolated DNA contains both genomic and mitochondrial DNA. (Von Wurmb-Schwark *et al.*, 2003). The amplification of the genomic beta actin (ACTB) gene and the *cytb5* was undertaken. The method of Bellis *et al.*, (2003), for the amplification of ACTB was chosen as amplification results in products of different sizes for human (289bp) and porcine (248bp) DNA. This is important as it will indicate if porcine DNA has been contaminated with human DNA following PCR and gel electrophoresis of the samples (Bellis *et al.*, 2003). Two techniques were used namely standard PCR with AGE and real-time PCR. For both methods, the amplification of ACTB was not obtained even though a range of annealing temperatures, template and primer concentrations as well as different MgCl<sub>2</sub> concentrations was used. This was not a function of DNA fragmentation as successful amplification was also not obtained for T0, the control porcine DNA. An additional literature search found that only one other study was ever undertaken using these primer sequences (Bellis *et al.*, 2003; Maharat *et al.*, 2005). In this study, amplification resulted in the formation of many unspecific products. Other factors that can result in failed PCR amplification of the desired region include:

- allele dropout,
- preferential amplification when there is differential denaturation or annealing temperature between the PCR products,
- presence of exo- or endogenous PCR inhibitors which often present in ancient DNA,
- miscoding lesions where erroneous bases are mis-incorporated during the extension phase of PCR

- jumping PCR where no amplifiable template DNA molecules that span the complete fragment defined by the primer sets exist (Alaeddini *et al.*, 2010).

In contrast the amplification of the *cytb5* region was found to be relatively easy. The method was found to be robust and reproducible and it was possible to amplify DNA from all material, even the 100+ samples from the field study. A relative indication of concentration could be obtained from the dF/DT, from this data the greatest amount of product was found in T4, T3, T2, T0 and then T1. This does not correlate with the amount of DNA isolated where the most DNA was isolated from T1. It is known that high concentrations of template DNA can lead to inhibition of PCR amplification (Alaeddini *et al.*, 2010). With increased heating times (T0-T4) there is a shift in the melting temperature ( $T_m$ ) from 82.5 for T0 to 80.3 for T4 indicating possible modification of DNA bases with secondary amino groups such as adenine, cytosine, 5-methylcytosine and guanine residues. The deamination of adenine, cytosine, 5-methylcytosine and guanine result in the formation of hypoxanthine, uracil, thymine and xanthine respectively. The cytosine residues are especially prone to deamination when the DNA is exposed to high temperatures (Alaeddini 2010). Deamination of these residues may also lead to a decrease in the NRN. According to Ussery, (2001), the  $T_m$  of DNA is dependent on the length of the DNA sequence, base composition, topological condition and composition of the buffer. Following amplification the presence of the 356bp product was confirmed by AGE and corresponded to the same size of human sequence using DNA isolated from blood (positive control) as shown in Figure 4.1.10.





No.	Colour	Name	Peak 1	Peak 2
1	Red	ntc	79.5	84.0
2	Yellow	human	83.5	
3	Blue	T0	82.5	
4	Purple	T1	81.2	
5	Pink	T2	80.5	
6	Light Blue	T3	80.3	
7	Teal	T4	80.3	

**Fig 4.1.11.** RT-PCR amplification of 1) no template control, 2) human DNA (positive control 1, 3) porcine DNA (positive control 2), T0 and samples 4) T1, 5) T2, 6) T3 and 7) T4.

**100bp ladder    Human    T0    T1    T2    T3    T4**

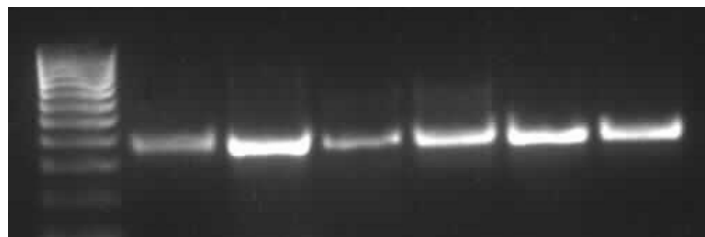


**Fig 4.1.12.** Agarose gel electrophoresis, of PCR products derived from PCR amplification of DNA isolated from teeth that were heated for 0-4 hours. Lane 1: 100bp ladder, lane 2: human DNA, used as control, lane 3-7 contains T0, T1, T2, T3 and T4 respectively.

### 4.1.3. Identification of bio-molecules as indicators of heating time

**Table 4.1.11 Summary: Line equations, R<sup>2</sup> and p-values of all the parameters measured**

<u>Parameter</u>	<u>Type line/curve</u>	<u>Regression</u>	<u>R<sup>2</sup></u>	<u>p-values</u>	<u>Indicator*</u>
Mass before	Linear	y=-0.02x+6.038	0.0016	0.2907	X
Mass after	Linear	y=0.0047x+4.0797	0.0001	0.2416	X
Collagen	Polynomial	Y=0.0014x <sup>2</sup> - 0.007 = 0.0219	<b>0.823</b>	0.29	X
TP-Bradford	Polynomial	y = <b>17.963</b> x <sup>2</sup> - 94.392x + 455.49	<b>0.807</b>	0.2385	X
TP-Biuret	Polynomial	y= <b>7.67</b> x <sup>2</sup> -68.54x+440.78	<b>0.988</b>	<b>0.0091</b>	√
Hb	Polynomial	y = <b>25.399</b> x <sup>2</sup> - 77.577x + 158.6	<b>1.00</b>	0.0748	X
Tetrapyrrole	Polynomial	y = 0.4882x <sup>2</sup> - 1.9704x + 4.7345	0.665	<b>0.0027</b>	X
TFe		y=0.307x <sup>2</sup> -1.98x+9.26	<b>0.988</b>	0.0378	X
Fe <sup>3+</sup>	Linear	y= <b>-1.01</b> x + 8.14	0.743	0.0143	X
Fe <sup>2+</sup>	Exponential	y= 0.7374e <sup>0.352x</sup>	<b>0.965</b>	0.0143	X
NRN	Linear	y= <b>-4.3789</b> x + 25.74	<b>0.989</b>	<b>0.00002</b>	√
DNA 260 nm	Polynomial	y = <b>3.208</b> x <sup>2</sup> - 20.229x + 56.43	<b>0.933</b>	<b>0.0002</b>	√
DNA Hoe	Polynomial	y = <b>4.151</b> x <sup>2</sup> - 26.89x + 77.53	<b>0.927</b>	<b>0.0000007</b>	√

\* X not a good measure of time heated, √ good indicator of time heated.

All data is summarised in Table 4.1.11. For the identification of bio-molecules that changed significantly in concentration with heating time two parameters must be considered (i) measurement between groups must show significant differences (low p<0.01) and there should be either a decrease or increase in concentrations (equation has a high gradient (m value >1 or < -1)) which can be linear, exponential and polynomial with a high degree of curve fit (R<sup>2</sup>>0.8.00). The molecules that fulfil these requirements are the total protein (Biuret method), NRN and DNA that both decrease with increased heating time.

### 4.2. Field study

Most methods only describe postmortem changes in the field. Henssge and Madea, (2007), proposed that a combination of different methods for a common result of time since death should be investigated. A laboratory based model such as that described above assists in the identification of bio-molecules that can change with heating time.

Therefore field studies can incorporate additional variables to assess the effect of other factors besides temperature and time on the degradation of bio-molecules such as DNA, NRN, proteins, lipids and carbohydrates (Swann *et al.*, 2010). Environmental effects are region specific and are related to height above sea level, day-night temperatures, humidity,

soil composition, levels of UV radiation, microbial cosmos types and location and accessibility of the body. During decomposition biology, geology and culture play a role as well. Researchers believe that temperature and moisture are the dominant parameters that administer decomposition of cadavers in soil. Microbial activity is related to both of these variables (Carter *et al.*, 2007).

Literature on chemical methods for estimating time since death is increasing. Most of these methods have never gained any practical relevance as they are not precise, reliable and give intermediate results. Furthermore, control studies on independent but similar materials such as a laboratory based model have not been carried out to prove the accuracy of a method before applying it to unknown samples. The use of field studies on cases with known postmortem intervals is necessary to confirm the practical applicability, reliability, reproducibility and accuracy of these methods.

In the South African context a field model was established within the highveld region close to Pretoria. Characteristic of this region is extreme temperatures with hot, wet summers with thunderstorms and cold, dry winters (Reference, high-veld temperatures, give C ranges). The advantage of this field model is that all factors such as temperature, humidity and rainfall were documented. This differs from studies using ancient, archaeological and forensic material as the origin, environmental exposure and storage conditions are unknown. Furthermore the field study provides a large number of samples from porcine carcasses obtained from a known source (Myburgh, 2010).

In the field model used in this study pig carcasses were placed in a field to decompose and teeth were collected at intervals of 20-40, 40-60, 60-80 and 100+ days. Although the study occurred over 2 years the teeth collected per time interval were exposed to similar conditions and predominantly in the summer months. Typical of these time intervals were 20-40 days summer, 40-60 days summer, 60-80 days summer, 80-100 days summer and 100+ days summer.

Decomposition rarely progresses linearly but rather follows a curvilinear fashion. In the later stages of decomposition the process becomes variable and a fixed pattern is not followed. With the field teeth used in this study, it was seen that decomposition progressed faster in the summer than in winter and followed a linear pattern in the early decomposition stages. In some cases complete skeletonization of the remains was reached in only a few days. In contrast, the winter period showed a plateau phase where hardly any decomposition took

place and skeletonization appeared much later (after 100 days) (Myburgh, 2010). The teeth used in this study were collected in the summer and winter of 2008 and 2009 and had the same number of post-mortem days (See appendix A.). This may contribute to variable results as factors such as humidity promotes the rapid nuclease mediated degradation of DNA. (Rubio *et al.*, 2009).

The physical state of the teeth varied. The roots were broken on some teeth, on others the tooth was cracked and the dentine was exposed with brown discolouration (described in Table 2.1). The presence of broken roots and cracks may result in the loss of material from the pulp cavity and subsequent measurement of lower protein and DNA levels. This may also account for large variations within each group, such that large standard errors of mean are present when measuring and comparing tooth content.



0-20 days



20-40 days



40-60 days



60-80 days



80-100 days









100+ days

Fig 4.2.1. Decomposition of pig carcasses representing time intervals 20-40, 40-60, 60-80, 80-100 and 100+ days.

The collected teeth were placed into plastic bags, transported to the laboratory and stored at  $-70^{\circ}\text{C}$  until all teeth had been collected. Excess soil was removed from the teeth; the teeth were rinsed in distilled water and air-dried. The morphology of the teeth was evaluated and a large variation was obtained between groups and these such as cracking, open roots and weathering as summarised in Figure 2.2.2.



<u>Effect</u>	<u>Group</u>	<u>Description</u>	<u>Example</u>
<b>Cracking</b>	<b>60-80</b>	Cracked tooth, either a post-mortem event or antemortem due to advanced age of the pig.	
<b>Open roots</b>	<b>60-80</b>	Post-mortem effect. The root is open and bacteria and pathogens can enter the pulp cavity.	
<b>Open pulp cavity</b>	<b>100+</b>	The tooth has completely broken in half and the pulp cavity is exposed to environmental conditions and bacteria.	
<b>Weathering</b>	<b>80-100</b>	The tooth shows signs of taphonomic degradation.	
<b>White plaque</b>	<b>40-60</b>	Evidence of white plaques on surface.	
<b>Brown colour</b>	<b>40-60</b>	The specimen exhibits a dark brown colour.	



**Corrosion**                    **60-80**                    The tooth enamel has eroded so that parts of the dentin can be seen. The surface has a scooped out appearance much like that made by carnivore chewing. The surface may show thin microtunneling and density destruction. This is heavily affected by soil acidity and environmental conditions and moss, fungi and bacterial action.



**Stained**                        **100+**                    The tooth show purplish stains as a result of porphyrin containing bacteria.



**Discolouration**            **20-40**                    The surface has a purple discolouration due to porphyrin-containing bacteria



**Broken**                        **40-60**                    The tooth is broken. This may be either a antemortem or post-mortem event.



**Smooth surface, with no evidence of corrosion or weathering**                    **20-40**                    No or little taphonomic changes is seen with no or little colour or surface changes.



**Figure 4.2.2.** Typical tooth morphology found in field samples. Tooth descriptions according to Fernandez, Jalvo *et al.*, (2010).



The teeth were divided into groups according to decomposition time and further processed as described for the laboratory *invitro* model. The teeth from each group were then divided into three groups and each group had an equal distribution of the same type of teeth. The average mass of each group of teeth was determined after which the teeth were fragmented and freeze-dried and further ground into fine powder. The mass of the teeth prior to freeze-drying and after freeze-drying is presented in Table 4.2.1 and Figure 4.2.3. No significant differences in mass between groups were found ( $p=0.722$  and  $0.697$ ).

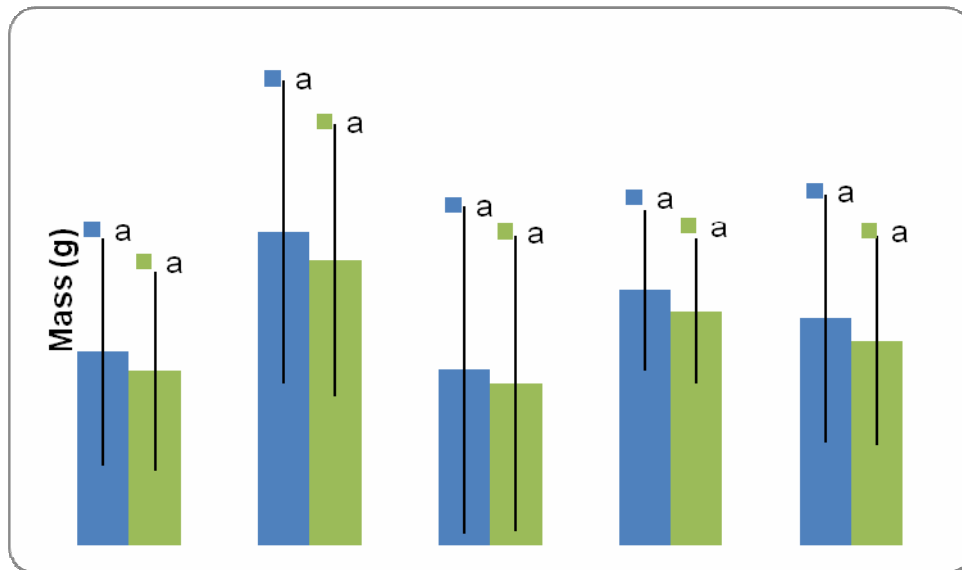


**Fig 4.2.3.** Mass of teeth collected in field study, (a) before and (b) after freeze-drying. Each data point is a mean  $\pm$ SEM of three separate experiments,  $n=45$ . Samples with the same letters are statistically similar.

**Table 4.2.1. Mass of all teeth collected from field study before and after freeze-drying**

	<u>Range (g)</u>	<u>Mean (g)</u>	<u>SEM (g) (%SEM)</u>	<u>Median (g)</u>
<b>Before</b>	1.21-2.15	1.60	0.37 (23%)	1.68
<b>After</b>	1.2-1.96	1.46	0.34 (23%)	1.53

This decrease in mass was due to the loss of water during freeze-drying and was calculated as percentage of starting mass and is presented in Table 4.2. This decrease was 7.99-9.77% of the original mass. For all mass determinations, no significant differences ( $p= 0.809$ ) were observed between the groups. Differences in moisture content between groups were not statistically different. In the *in vitro*, laboratory study a 30% difference in mass was observed before and after freeze-drying and this was not a function of the time heated. This seems to indicate that the greatest loss of moisture occurred during the first 20 days. To confirm this it would have been of value to have collected a tooth sample from each pig prior to placing them in the field.

**Table 4.2.2. Loss in mass of all teeth used in the field study with freeze-drying. (n=45)**

<u>Range (%)</u>	<u>Mean (%)</u>	<u>SEM</u>	<u>%SEM</u>	<u>Median (%)</u>
7.99-9.77	8.84	0.85	9.6	8.40

#### **4.2.1. Water insoluble fraction**

##### **4.2.1.1. Collagen content**

After a 100 days post-mortem, the available collagen in the teeth was isolated and the concentration of collagen was determined using the Bradford method (A), from the absorbance at 230nm before (B) and after desalting (C) and then the final mass (D) was determined after freeze-drying, Figure 4.2.5A-D. Data was expressed as g/g of freeze-dried mass. Using the standard method for protein determination, the concentration of total protein (the majority being collagen), was found to be 0.22-0.25 g/g. Calculated collagen concentration based on the 230nm absorbance readings was 1.79-2.66g/g which is an overestimation as was seen for the *in vitro* laboratory experiments as GuaHCl causes interference. Following removal the calculated collagen was 0.25-0.62g/g and following freeze-drying was 0.41-1.74g/g. The collagen concentration did not differ significantly between the groups and no time related decrease was found. A large standard error of mean was obtained for all groups indicating the high degree of variability in the collagen content between samples. This is most likely related to the structural integrity of the teeth.

**Table 4.2.3. Collagen content, field model**

<u>Method</u>	<u>Range (g/g)</u>	<u>Mean (g/g)</u>	<u>SEM (g/g)</u>	<u>%SEM</u>	<u>Median (g/g)</u>
<b>CB</b>	0.215-0.25	0.22	0.007	3.18	0.22
<b>Abs 230nm</b>	1.79-2.66	2.17	0.034	9.89	2.03
<b>Abs 230nm after desalting</b>	0.254-0.618	0.463	0.091	7.46	0.45
<b>Mass after freeze-drying</b>	0.70-1.19	0.93	0.12	12.7	0.99

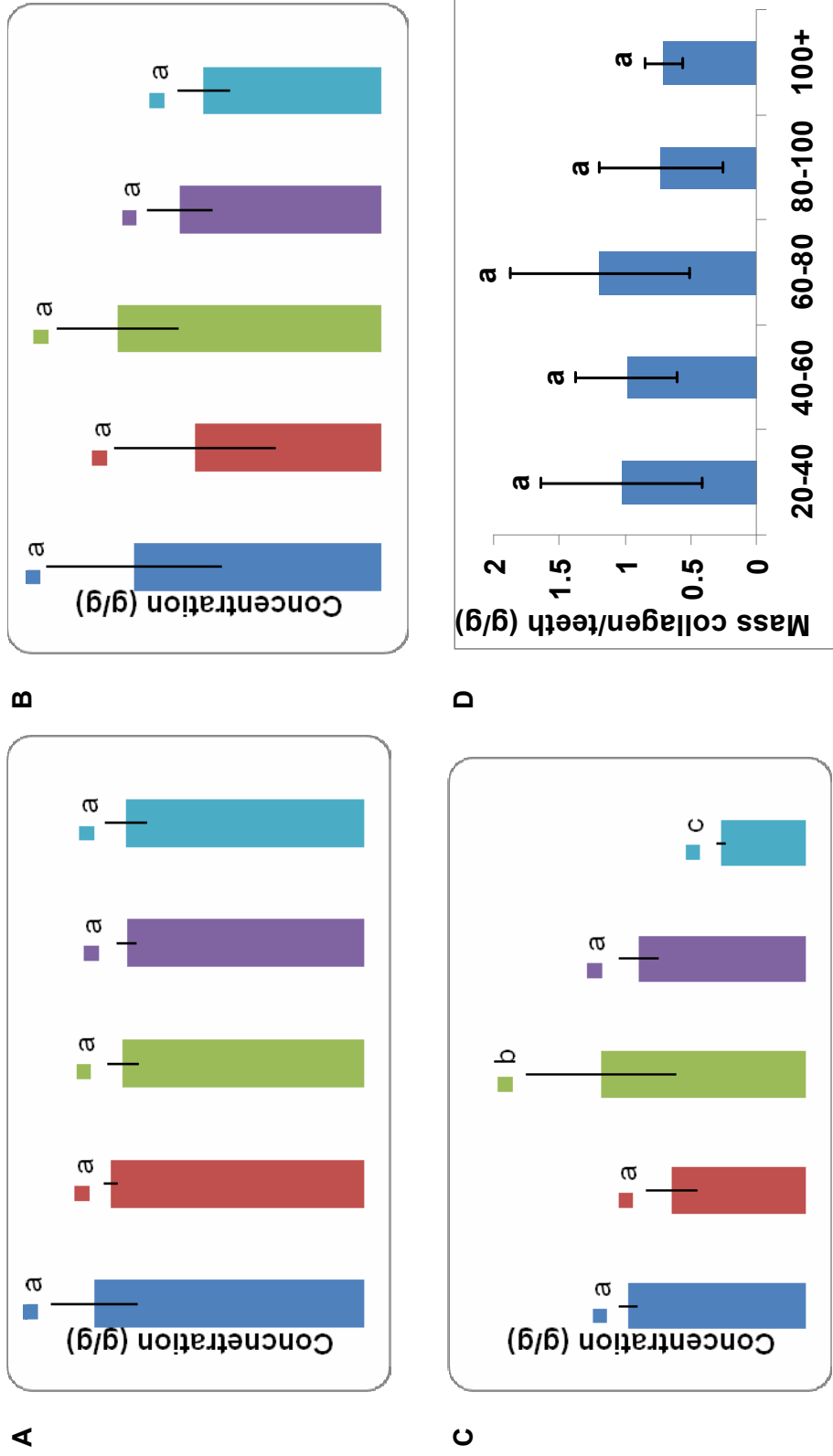


**Fig 4.2.4.** Collagen concentration field model, after heating for 0-4 hours, demineralisation and solubilisation (A) determined by the Bradford method and (B) Absorbance at 230nm, (C) after desalting 230nm absorbance and (D) then freeze-drying. Each data point is a mean  $\pm$ SEM of three separate experiments, n=45. Samples with the same letters are statistically similar.

## **4.2.2. Water soluble fraction**

### **4.2.2.1. Protein, haemoglobin, pyrrole, iron and NRN present in the pulp cavity.**

#### **4.2.2.1.1. Protein content**

The protein content of the water extract of the pulp cavity was determined using the Bradford and Biuret methods. Data was expressed as mg/g dried mass and is presented in Table 4.2.4 and Figure 4.3.5.

**Table 4.2.4. Protein concentration, field study**

<b><u>Total Protein</u></b>	<b><u>Range (mg/g)</u></b>	<b><u>Mean (mg/g)</u></b>	<b><u>SEM (mg/g)</u></b>	<b><u>%SEM</u></b>	<b><u>Median (mg/g)</u></b>
<b>Bradford</b>	536.13-961.37	793.82	159.56	90.14	803.1
<b>Buuret</b>	573-1129.99	734.37	234.9	32.00	692.9

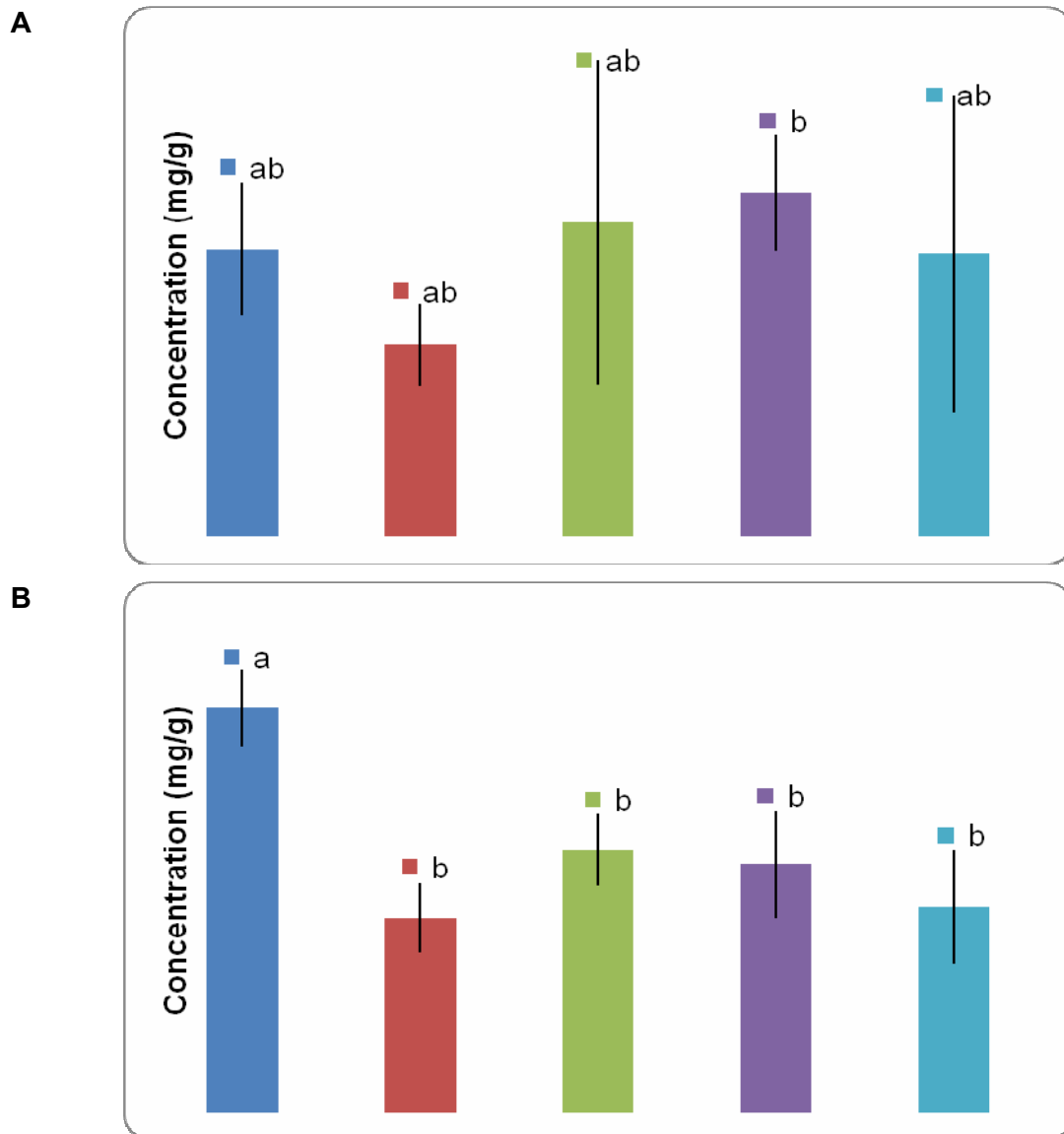


**Fig 4.2.5.** Protein content of the pulp cavity of the teeth collected in the field study determined using the (a) Bradford and (b) Biuret assay. Each data point is a mean  $\pm$  SEM of three separate experiments,  $n=45$ . Samples with the same letters are statistically similar.

For the Bradford method, the protein concentration varied from 536.13-961.37mg/g with a median of 803.1 mg/g and a standard deviation of 159.56 mg/g with no significant difference in protein content between groups ( $p=0.549$ ). For the Biuret method, concentrations varied from 573-1130 mg/g and for groups 40-60, 60-80, 80-100 and 100+ the concentrations were significantly less than 20-40. Differences were significant with  $p=0.00133$ . Although the range of protein concentration measured using either the Bradford or the Biuret methods was the same, only with the Biuret method was there a decrease in protein concentration associated with a small standard error of means. The latter is a further indication that the Biuret method is a more accurate method for the determination of the soluble protein content

of decomposing teeth and that protein concentration decreases with time. The protein was found to be at least twice that of the laboratory based study. With decomposition, there is an increase in microbial biomass and an associated increase in total protein. Masses greater than 1g/g is possibly an indication of increased bacterial activity.

Moreno *et al.*, (2011), measured the abundance of nitrogen fixing bacteria found in the underlying soil where cadavers had been placed. When there is an abundance of nitrogenous material, the metabolism of the bacteria changes and there is an increase in nitrogen fixation. This effect occurs after 4 weeks. Once nutritional substrates become depleted, the rate of bacteria replication decreases and by the time that complete skeletonization occurs bacterial activity has ceased. This would result in a decrease in the total protein measured (Moreno *et al.*, 2011). Intervals 20-40 days correspond to 3-6 weeks where optimal bacterial activity occurs. In later weeks, these levels are reduced as found in Figure 4.2.5. Two types of bacteria are present during decomposition namely enteric and non-enteric bacteria. Exogenous bacteria gain access to teeth via the dental tubules (Love and Jenkinson, 2002). Bacterial aggregates and remnants of bacterial cell membranes can absorb to bone and teeth and this has been observed using scanning electron microscopy (SEM) (Collins *et al.*, 2002).

#### **4.2.2.1.2. Heamoglobin content of the teeth**

As for the *in vitro* model, Hb levels were determined and were found to vary from 99.06-269.38mg/g with a median of 14.69mg/g and a standard deviation of 33.00mg/g. The Hb concentration did not differ significantly between the groups ( $p=0.324$ ), although a logarithmic increase was found  $y=26.43\ln x + 112.28$ ,  $R^2=0.905$ . The percentage of Hb to total protein was  $18.0\% \pm 4.9\%$  for the  $20.45\% \pm 6.8\%$ , Bradford and Biuret methods respectively.

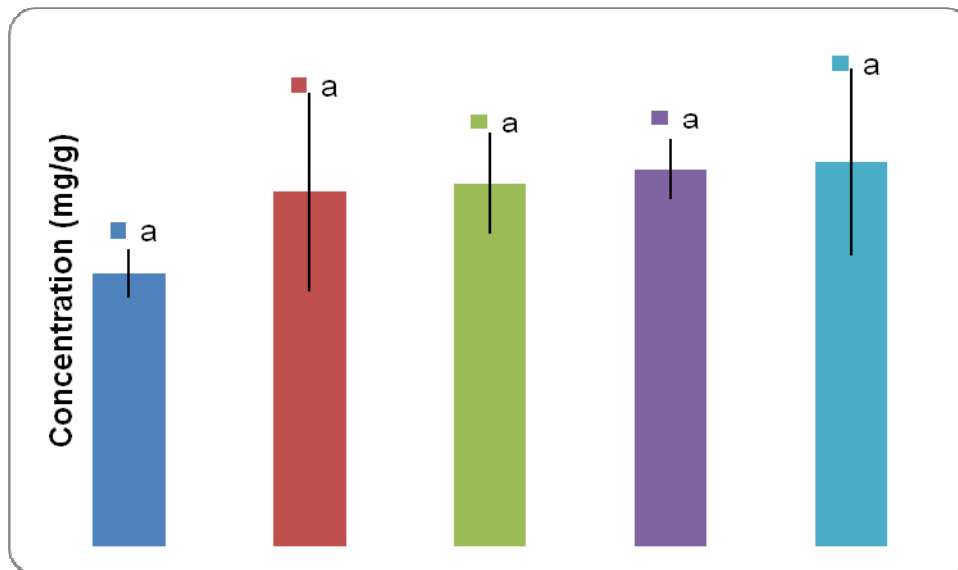


**Fig 4.2.6.** Hb content (mg/g) of the pulp cavity of the teeth collected in the field study determined using the Drabkin method. Each data point is a mean  $\pm$ SEM of three separate experiments, n=45. Samples with the same letters are statistically similar.

**Table 4.2.5. Hb content, field study**

<u>Range (mg/g)</u>	<u>Mean (mg/g)</u>	<u>SEM (mg/g)</u>	<u>%SEM</u>	<u>Median (mg/g)</u>
107.09-150.9	137.58	17.65	12.83	142.60

The concentrations of Hb found in the field study were similar to that found in the laboratory based model. This means with decomposition the concentration of Hb remains constant and like other studies has been found to be resistant to degradation (Williamson 2000).

#### **4.2.2.1.3. Pyrrole content**

Pyrrole groups are important structural components of Hb, porphyrins and other heme containing proteins. The pyrrole content of each time interval was determined, expressed as mg/g (Figure 4.2.7) and varied from 9.21-18.34 mg/g with a median of 10.54mg/g and a standard error of mean of 4.62mg/g (Table 4.2.6). An increase in pyrrole concentration was found especially for group 100+ compared to groups 20-40, 40-60 and 60-80, was significant ( $p=0.013$ ) and this was a polynomial increase with  $y=1.27x^2- 2.747x + 8.79$ , ( $R^2=0.89$ ). Pyrrole content for all groups was similar except for 100+ days which statistically differed from all other groups.

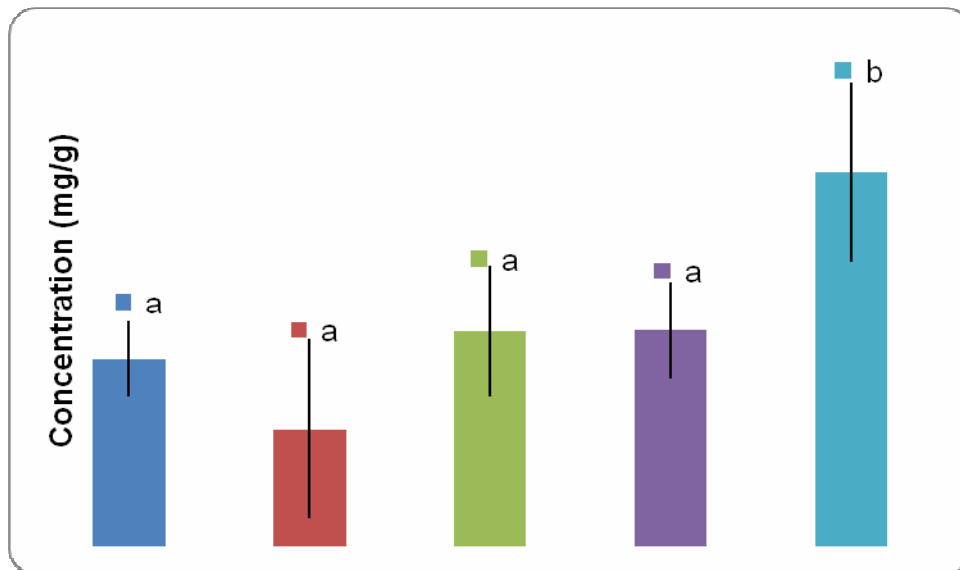


**Fig 4.2.7.** Pyrrole concentration of the pulp cavity of the teeth collected in the field study determined with fluorescence ( $Ex_{404nm}$  and  $Em_{624nm}$ ). Each data point is a mean  $\pm$ SEM of three separate experiments,  $n=45$ . Samples with the same letters are statistically similar.

**Table 4.2.6. Pyrrole content, field study**

<u>Range (mg/g)</u>	<u>Mean (mg/g)</u>	<u>SEM (mg/g)</u>	<u>%SEM</u>	<u>Median (mg/g)</u>
9.21-18.34	10.89	4.62	42.4%	10.54

#### **4.2.2.1.4. Iron content**

Total iron,  $Fe^{3+}$ ,  $Fe^{2+}$  (Figure 4.2.8) and the ratio of  $Fe^{3+}:Fe^{2+}$  (Table 4.2.8) was determined using the FOX assay. With time of exposure, no statistically significant differences were found between groups for  $Fe^{3+}$  and  $Fe^{2+}$ ,  $p=0.14$  and  $0.58$  respectively. The total iron showed a statistically significant difference between groups,  $p=0.01$ . No differences between iron content from 20-40 and 100+ which indicates that no or very little leaching of the iron occurred. The possibility is that the lower concentrations found in T40-60 may be due to the fact that some of the teeth had open root canals.



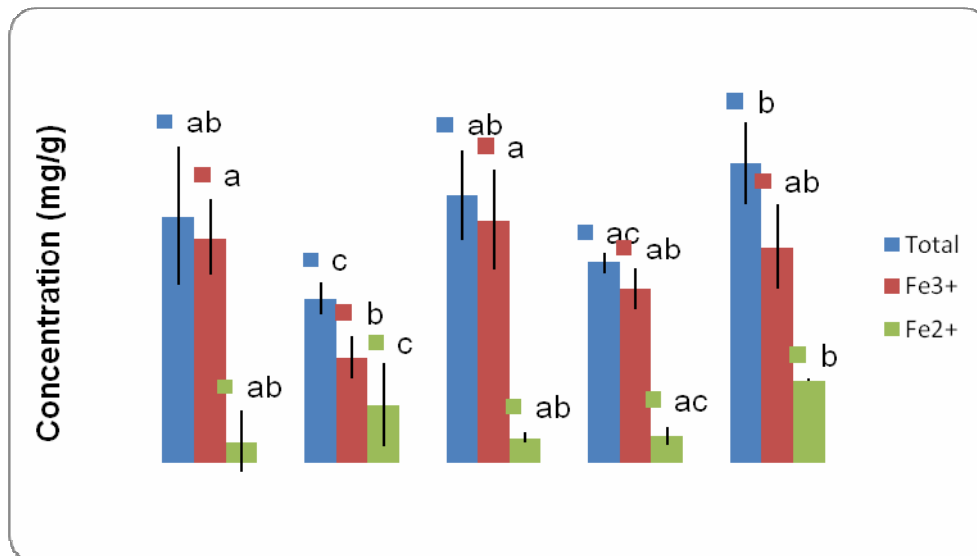


**Fig 4.2.8.** Total iron, Fe<sup>3+</sup> and Fe<sup>2+</sup> concentration of the pulp cavity of the teeth collected in the field study determined using Xylenol Orange. Each data point is a mean ±SEM of three separate experiments, n=45. Samples with the same letters are statistically similar.

**Table 4.2.7. Total iron, Fe<sup>3+</sup> and Fe<sup>2+</sup> content, field study.**

<u>Parameter</u>	<u>Range (mg/g)</u>	<u>Mean (mg/g)</u>	<u>SEM (mg/g)</u>	<u>%SEM</u>	<u>Median (mg/g)</u>
Total Fe	16.32-29.77	23.42	5.35	22.84	24.50
Fe <sup>3+</sup>	10.54-24.15	19.17	5.44	28.42	21.51
Fe <sup>2+</sup>	2.11-8.25	4.25	2.68	62.9	2.65

With increasing time the ratio of Fe<sup>2+</sup>:Fe<sup>3+</sup> changed variably, from 11:1 for 20-40 to 2:1 for 40-60 and then 3:1 for 100+. Changes in ratio may mean that Fe<sup>3+</sup> had decreased, and this is often in the form of free iron. The total iron concentration was about 2.5x greater than that found in the laboratory model. It has been described that many bacteria accumulate iron through high-affinity chelating agents such as siderophores and therefore increased bacterial activity may be associated with an increased iron accumulation.

**Table 4.2.8. The ratio of Fe<sup>3+</sup>:Fe<sup>2+</sup>, field study.**

	<u>20-40</u>	<u>40-60</u>	<u>60-80</u>	<u>80-100</u>	<u>100+</u>
Fe <sup>3+</sup> : Fe <sup>2+</sup>	11:1	2:1	10:1	7:1	3:1

#### **4.2.2.1.5. Ninhydrin reactive nitrogen**

The concentration of ninhydrin reactive nitrogen (NRN) was determined and is presented in Figure 4.2.9 and Table 4.2.9. Highest levels were found in group 40-60 and for groups 40-60 through to 100+ a linear decrease ( $y = -5.41x + 62.78$ ,  $R^2=0.987$ ) was observed. Group 100+ was significantly less than group 40-60. Levels of NRN are higher than those found for the laboratory based *in vitro* model. In the laboratory based model, the temperature and time

heated will cause the denaturation of protein and any inherent microorganisms to be eliminated. The measured NRN is only a function of chemical degradation. With decomposition, autolysis results in protein degradation and subsequent microbial activity is responsible for further protein decomposition (Dent *et al.*, 2003; Carter and Tibbett, 2008). This will result in increased levels of NRN compared to the laboratory based study (Hopkins *et al.*, 2000; Van Belle *et al.*, 2009; Lovestead and Bruno, 2011; Moreno *et al.*, 2011). Once the microbial nutrients are depleted a decrease in NRN occurred and this effect is seen in 80-100 and 100+. As seen for protein and iron, the total NRN also increased and this may be related to an increase in endogenous bacterial activity. This was also noted with total protein counts. As decomposition progresses and with an associated decrease in bacterial activity, there is also a decrease in NRN.

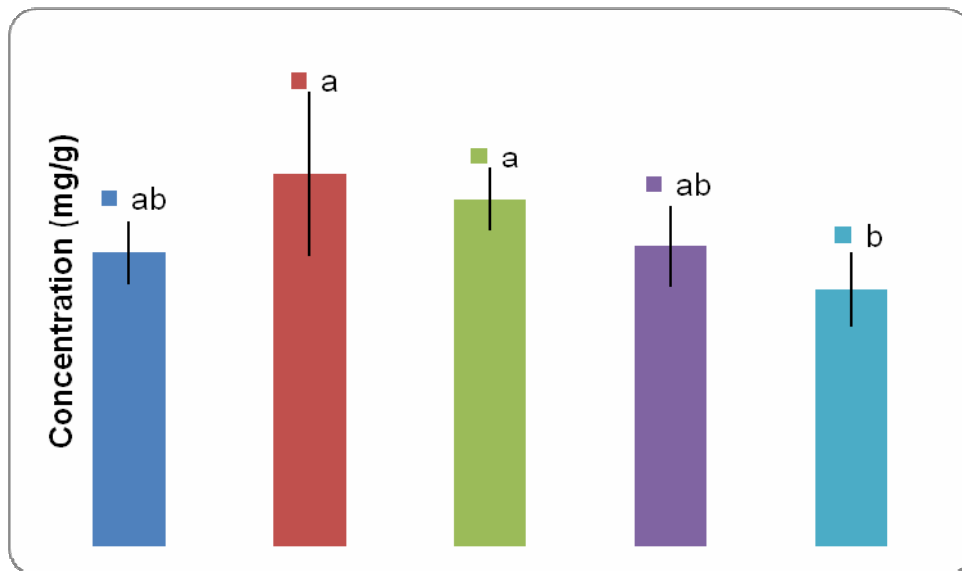


**Fig 4.2.9.** NRN present in the pulp cavity of teeth collected in the field study. Each data point is a mean  $\pm$ SEM of three separate experiments, n=45. Samples with the same letters are statistically similar.

**Table 4.2.9. Ninhydrin positive components, field study.**

<u>Range (mg/g)</u>	<u>Mean (mg/g)</u>	<u>SEM (mg/g)</u>	<u>%SEM</u>	<u>Median (mg/g)</u>
35.30-51.20	43.16	6.27	14.54	41.22

#### **4.2.2.1.6. DNA content**

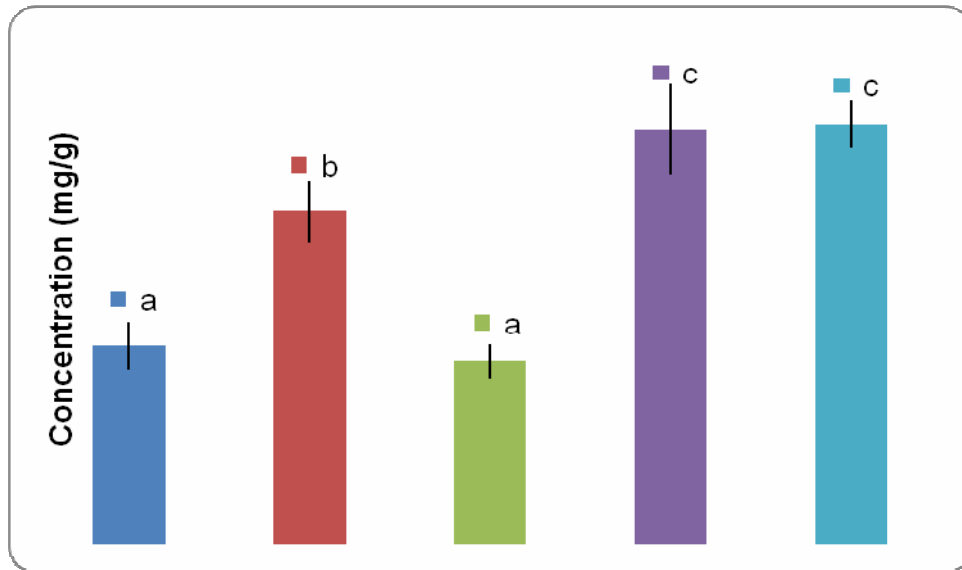
The DNA content of each group of samples was determined from the 260 nm reading and the capacity of the DNA to bind Hoechst (Hoe). Concentrations calculated from the 260nm readings were the lowest for groups 20-40 and 60-80, differences between groups were significant  $p=0.00017$ . DNA concentration determined at 260nm for 20-40 days was statistically similar to 60-80 days but was less than that of groups 40-60, 80-100 and 100+

days. DNA concentrations determined with Hoe were higher than that determined from the 260nm readings, differences between groups was significant ( $p=0.000045$ ) and a linear decrease was observed for groups 20-40 through to 100+ ( $y=-8.368x + 94.44$ ,  $R^2 = 0.88$ ). In this study the amount of DNA isolated was 28.8-66.00 mg/g (A260nm determination) and 50.82-84.59 mg/g (Hoechst determination). The amount of DNA obtained is similar to that of the laboratory based study, but it is not known if this is tissue or bacterial derived.

Dobberstein *et al.*, (2008), found a strong inter-individual relationship between the amount of DNA isolated from naturally aged teeth. In a study concerning the effect of soil storage on DNA concentration in teeth, Pfeiffer *et al.*, (1999), found that the amount of DNA isolated from controlled teeth varied from 1.00-30.00 ng/ $\mu$ l DNA, after 6 weeks the amount of DNA varied from 0-0.750ng/ $\mu$ l, after 18 weeks the amount of DNA varied from 0.004-1.00ng/ $\mu$ l and after two years the amount of DNA isolated from 0.00-1.00ng/ $\mu$ l (Pfeiffer *et al.*, 1999).

Of the two methods used for the determination of DNA concentration, the Hoechst method was more accurate due to its highest specificity for the AT rich region located within the minor groove (Bester *et al.*, 1994; Haq *et al.*, 1997; Kakkar 2002; Rengarajan *et al.*, 2002). The concentration of DNA isolated was similar to that of the laboratory based, *in vitro* study. Two sources of DNA would be genomic/mitochondrial and bacterial. PCR amplification using porcine specific primers would confirm the presence of porcine DNA.

A



B

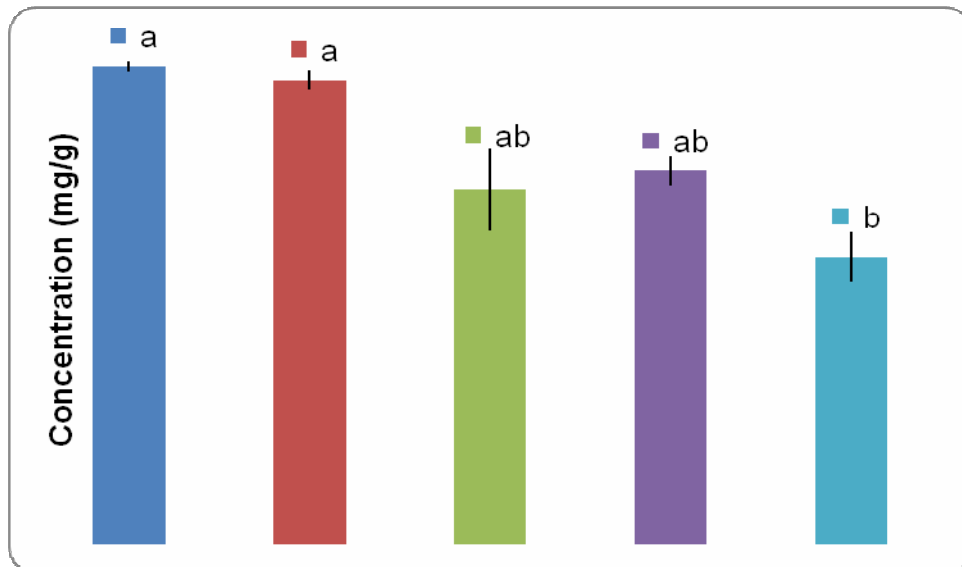


**Fig 4.2.10.** DNA concentration of the pulp cavity of the teeth collected in the field study determined (A) from the 260 nm absorbance readings and (B) fluorescence following Hoechst binding. Each data point is a mean  $\pm$ SEM of three separate experiments, n=45. Samples with the same letters are statistically similar.

**Table 4.2.10. DNA content, field study.**

	<u>Range (mg/g)</u>	<u>Mean (mg/g)</u>	<u>SEM (mg/g)</u>	<u>%SEM</u>	<u>Median (mg/g)</u>
<b>Abs 260 nm</b>	28.8-66.00	48.67	17.92	36.82	52.24
<b>Hoe</b>	50.82-84.59	69.33	14.09	20.32	66.12

The purity of the DNA was determined from the 260nm/280nm ratio and was 1.46-2.00 with a mean of 1.64 (%SD = 13.36) which fulfils the requirements for successful PCR and for all samples. No significant differences ( $p=0.0124$ ) was found between groups. The integrity of the isolated DNA samples was determined by agarose gel electrophoresis. The same volume of DNA was loaded into each well. Band intensity reflects the concentrations presented in Figure 4.2.10B. Differences in band intensity compared to Figure 4.1.9 is due to the amount of DNA loaded which is ten times less than that used for the *in vitro* samples.

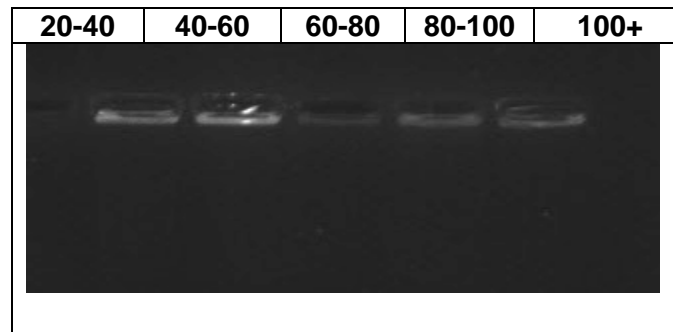
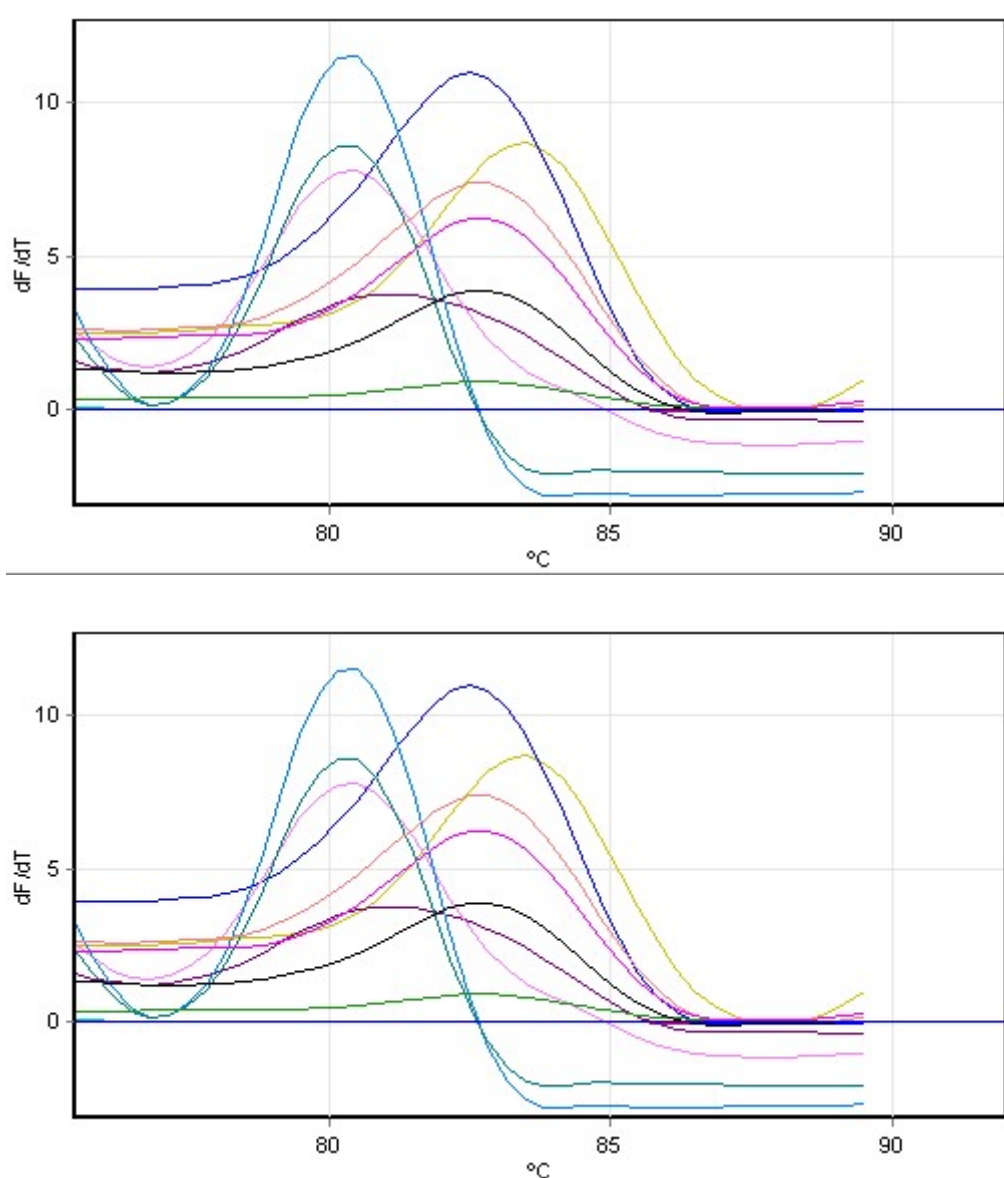


**Fig 4.2.11.** Agarose gel electrophoresis (AGE) of the isolated DNA from samples collected in the field study. (20 $\mu$ l), Lane 1 =20.3 $\mu$ g, lane 2= 32.2  $\mu$ g, lane 3= 14.01  $\mu$ g and lane 4=21.29  $\mu$ g and lane 5=14.32  $\mu$ g calculated from Hoe determination.

#### **4.2.2.1.6.1. PCR amplification**

As with the *in vitro* laboratory based model, amplification of the ACTB gene was not successful. However for all samples the mitochondrial *cytb5* gene could be amplified and the product formed had a  $T_m$  point of 82.7. Subsequent agarose gel electrophoresis confirmed the presence of a PCR product of 356 bp.



No.	Colour	Name	Genotype	Peak 1	Peak 2
1	Red	ntc		79.5	84.0
2	Yellow	human		83.5	
3	Blue	porcine		82.5	
8	Light Red	20-40		82.7	
9	Green	40-60		82.7	
10	Magenta	60-80		82.7	
11	Black	80-100		82.7	
12	Cyan	100		82.3	85.7

**Fig 4.2.12.** RT-PCR amplification of 1) no template control, 2) human DNA (positive control 1, 3) porcine DNA (positive control 2) and samples 8) 20-40, 9) 40-60, 10) 60-80, 11) 80-100 and 12) 100+ field samples.

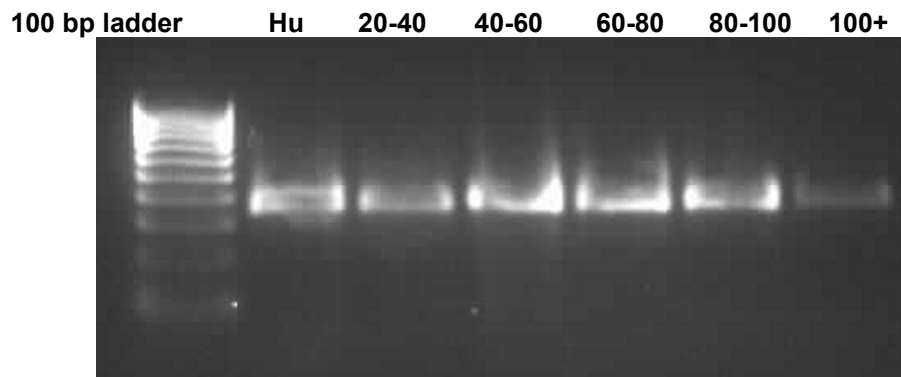


**Fig 4.2.13.** Agarose gel electrophoresis, of PCR products derived from amplification of DNA isolated from teeth that collected at 0-20, 20-40, 40-60, 60-80 and 100+ days. Lane 1: 100bp ladder, lane 2: Hu=human DNA, used as control, lane 3-7 contains 20-40, 40-60, 60-80, 80-100, 100+ respectively.

To summarise with increasing decomposition time, a decrease in protein concentration (Buret method), NRN and DNA (Hoe method) was observed while in contrast an increase in Hb and pyrrole concentrations was found.

#### **4.2.3. Identification of bio-molecules as indicators of heating time**

As was undertaken for the *in vitro* study, all data generated from the field study is contained in Table 4.2.11. The identification of a bio-molecule as an important indicator molecules is that (i) measurement between experiments must show significant differences between samples (low  $p < 0.01$ ), either a decrease or increase in concentrations (equation has a high gradient ( $m$  value  $> 1$  or  $< -1$ ) between samples (low  $p$  value), a high degree of curve fit ( $R^2 > 0.8.00$ ). Of these three possible molecules were identified and were pyrrole content, NRN and DNA concentration determined following Hoechst binding. Of these the NRN and DNA concentration are possibly the best indicators changes related to time as both decrease with time, have a negative gradient.

**Table 4.2.11. Summary of line equations, R<sup>2</sup> and p-values of all the parameters measured**

<u>Parameter</u>	<u>Type line/curve</u>	<u>Regression</u>	<u>R<sup>2</sup></u>	<u>p-values</u>	<u>Indicator</u>
Mass before	Linear	$y = 0.0057x + 1.5837$	0.0006	0.72	X
Mass after	Linear	$y = 0.0067x + 1.4393$	0.001	0.69	X
Collagen	Linear	$Y = -0.0042x = 0.0501$	0.436	0.60	X
TP-Bradford	Linear	$y = 39.8x + 674.4$	0.116	0.55	X
TP-Buiret	Polynomial	$y = 50.42x^2 - 398.83x + 1376.3$	0.516	0.00	X
Hb	Exponential	$y = 26.43\ln(x) + 112.28$	<b>0.905</b>	0.32	X
Pyrrole	Polynomial	$y = 1.27x^2 - 2.75x + 8.80$	<b>0.891</b>	<b>0.01</b>	√
TFe	Linear	$y = 1.412x + 19.12$	0.174	0.01	X
Fe <sup>3+</sup>	Linear	$y = 0.50x + 17.7$	0.0207	0.14	X
Fe <sup>2+</sup>	Polynomial	$y = 0.53x^2 - 2.26x + 5.21$	0.429	0.58	X
NRN	Linear	$y = -5.41x + 62.78$	<b>0.987</b>	<b>0.09</b>	√
DNA 260 nm	Linear	$y = 8.25x + 23.9$	0.53	<b>0.00</b>	X
DNA Hoe	Linear	$y = -8.36x + 94.44$	<b>0.88</b>	<b>0.00</b>	√

\* X not a good measure of time since death, √ good indicator of time since death.

### **4.3 Comparison between *in vitro* and field models**

Although both models are unrelated where the laboratory based *in vitro* model represents the effect of a single parameter while the field model represents the effect of many parameters such as rainfall, humidity, soil composition, microbial activity and humidity, Dobberstein *et al.*, (2008), recognized heat/temperature as the major contributing factor to decomposition and therefore both models can be compared. Two parameters that showed a significant decrease with time was the NRN and DNA determined with Hoechst binding. For both sufficient amounts of DNA of such a quality that successful PCR amplification of the *cytb* gene was possible.



## **CHAPTER 5: CONCLUDING DISCUSSION**

### **Limitations of the study and future research**

A major limitation of the *in vitro* laboratory based study is that only two parameters contribute to the degradation observed and these are high temperature and time heated. A high temperature is used to compress time, however this kills bacteria and the effect of bacterial activity on decomposition cannot be studied. This can be overcome by creating a model that is a combination of the *in vitro* laboratory based model and the field model. Teeth can be placed in transparent ventilated chambers that contain soil similar to that in the field study. These chambers can be placed in incubators with controlled temperature, light and humidity based on regional weather information.

During decomposition, such as occurred with the field model, the type of tooth i.e. incisor, molar and canine, would differ in the rate of decomposition and this is a function of environmental factors (temperature, rainfall, humidity) and the structure of the teeth (collagen and mineral content). Ideally each group of teeth that is evaluated should contain teeth of the same type.

Prior to placing the pigs in the field a tooth/teeth should be extracted i.e. each pig becomes its own control. Therefore changes compared to control are measured. This will eliminate the effects of age, nutritional status and disease.

A study over a period of 100 days usually includes two seasons that vary regarding changes in day and night temperatures, rainfall, vegetation, insect and scavenging activity. Time intervals are only a vague measurement and these and other factors must be in some way included. A suggestion is that pigs at 100 days summer should be compared to pigs 100 days winter. With each pig serving as its own control, comparisons can then be made.

In both models the concentration of several biomolecules was determined and these included collagen, protein, Hb, pyrroles, Fe, ninhydrin positive components and DNA. For the *in vitro* based model a decrease in protein, DNA and ninhydrin positive components was found. In the field a less well defined decrease was found for protein, DNA and ninhydrin and pyrroles.

Amplification of genomic DNA was difficult and this could be a function of the sequence that was amplified. Further studies should involve the identification of other genomic regions such as the *TP53* tumor suppressor gene that could be amplified. Furthermore sequencing of this DNA would provide information regarding the chemical alteration of bases such as the

methylation of cytosine to 5-methylcytosine and the deamination of bases that is a function of temperature and proteolytic activity. Furthermore due the large structure of DNA, the rate at which it undergoes fragmentation or the degree with which the genomic DNA can be amplified could be a sensitive indicator of time since death.

The structure of the molecules that causes a ninhydrin positive reaction in the teeth used in this study is unknown. Using high performance liquid chromatography (HPLC) the structure of these molecules can be elucidated possibly to identify a specific marker molecule in the water soluble fraction of teeth that changes in concentration with time.

Collagen is an inert and highly stable molecule that did not show any significant differences between groups in both models. Several researchers have shown that there are changes to the structure of collagen with decomposition. The isolation of collagen and subsequent gel electrophoresis to identify these changes is time consuming. Collagen degradation results in the formation of smaller fragments and molecules such matrix metalloproteinases (MMPs). These molecules will either leach from the matrix or may accumulate within the pulp cavity. Methods for the measurement of the levels of these molecules have been established and can be used to indicate whether there are changes in the concentration of these molecules occur during decomposition.

In conclusion, this study has provided an indication of the changes in the concentration, integrity and structure of important bio-molecules found in teeth. Further research should focus on improving the experimental design of the model and the identification of specific molecular markers of decomposition.

## CHAPTER 6: REFERENCES

- Abraham E, Cox M, Quincey D. 2008. Post-mortem iris colour change in the eyes of *Sus scrofa*. *Journal of Forensic Sciences* 53(3):626-31.
- Alaeddini R, Walsh SJ, Abbas A. 2010. Forensic implications of genetic analyses from degraded DNA – A review. *Forensic Science International: Genetics* 4:148-57.
- Anderson GS, Hobischak NR. 2004. Decomposition of carrion in the marine environment in British Columbia, Canada. *International Journal of Legal Medicine* 118:206-9.
- Baker LE, McCormick WF, Matteson KJ. 2001. A silica-based mitochondrial DNA extraction method applied to forensic hair shafts and teeth. *Journal of Forensic Sciences* 46(1):126-30.
- Balzer A, Gleixner G, Grupe G, Schmidt H –L, Schramm S, Turban-Just S. 1997. *In vitro* decomposition of bone collagen by soil bacteria: The implications for stable isotope analysis in archaeometry. *Archaeometry* 39(2):415-29.
- Banerjee D, Jacob J, Kunjamma G, Madhusoodanan UK, Ghosh S. 2004. Measurement of urinary hydrogen peroxide by FOX-1 method in conjunction with catalase in diabetes mellitus—sensitive and specific approach. *Clinica Chimica Acta* 350:233-6.
- Bass B, Jefferson J. 2003. *Death's Acre: Inside the legendary body farm*. New York: Time Warner:51-65.
- Bass WM, Jefferson J. 2007. *Beyond the body farm*. New York: William Marrow:120-237.
- Bellina F, Rossi R. 2006. Synthesis and biological activity of pyrrole, pyrroline and pyrrolidine derivatives with two aryl groups on adjacent positions. *Tetrahedron* 62(31):7213-56.
- Bellis C, Ashton KJ, Freney L, Blair B, Griffiths LR. 2003. A molecular genetic approach for forensic animal species identification. *Forensic Science International* 134:99-108.
- Bender K, Schneider PM, Rittner C. 2000. Application of mtDNA sequence analysis in forensic casework for the identification of human remains. *Forensic Science International* 113:103-7.

Bester MJ, Potgieter HC, Vermaak WJH. 1994. Cholate and pH reduce interference by sodium dodecyl sulfate in the determination of DNA with Hoechst. *Analytical Biochemistry* 223:299-305.

Biesaga M, Pyrzynska K, Trojanowicz M. 2000. Porphyrins in analytical chemistry: A review. *Talanta* 51:209-24.

Block RJ, Bolling D. 1951. The amino acid composition of proteins and foods. *Journal of the American Pharmaceutical Association* 40(6):303.

Brandstatter A, Peterson CT, Irwin JA, Mpoke S, Koech DK, Parson W, Parsons TJ. 2004. Mitochondrial DNA control region sequences from Nairobi (Kenya): inferring phylogenetic parameters for the establishment of a forensic database. *International Journal of Legal Medicine* 118:294-306.

Bravi CM, Lirón JP, Mirol PM, Ripoli MV, Peral-García P, Giovambattista G. 2004. A simple method for domestic animal identification in Argentina using PCR-RFLP analysis of cytochrome *b* gene. *Legal Medicine* 6:246-51.

Butler JM. 2005. Forensic DNA typing: Biology, technology and genetics of STR markers. 2<sup>nd</sup> ed. London: Elsevier Academic Press:1-49.

Byers SN. 2008. Estimating time since death. In: Introduction to Forensic Anthropology. 3<sup>rd</sup> ed. BostonMA:Allynand Bacon:110-11.

Campbell MK, Farrell SO. 2006. The three-dimensional structure of proteins. In: Biochemistry. 5<sup>th</sup> ed. Thomson Brooks/Cole:90-1.

Campobasso C, Di Vella G, Introna F. 2001. Factors affecting decomposition and Diptera colonization. *Forensic Science International* 120:18-27.

Carey L, Mitnik L. 2002. Trends in DNA forensic analysis. *Electrophoresis* 23:1386-1397.

Carter DO, Tibbett M. 2008. Cadaver decomposition and soil processes. In: M Tibbett and DO Carter, eds. Soil analysis in forensic Taphonomy. USA:Boca Rayton: CRC Press:29-51.

Carter DO, Yellowlees D, Tibbit M. 2007. Cadaver decomposition in terrestrial ecosystems. *Naturwissenschaften* 94:12-24.

Cirkovas A, Sereikatte J. 2011. Increase in the solubility of recombinant milk growth hormone at low cultivation temperature of E.coli. *Biotechnology and Biotechnological equipment* 24(4):2169-71.

Coetzee HL, Loots GP, Meiring JH. 2003. Connective tissue. In: *Human Histology*. Pretoria:Van Schaik:74-75.

Coetzee HL, Loots GP, Meiring JH. 2003. Digestive system. In: *Human Histology*. Pretoria:Van Schaik:282-4.

Collins MJ, Nielsen-Marsh CM, Hiller J, Smith CI, Roberts JP. 2002. The survival of organic matter in bone: A review. *Archaeometry* 44(3):383-94.

Cortijo M, Panijpan B, Gratzner B. 1973. Guanidine hydrochloride and the circular dichroism of random coil polypeptides. *International Journal of Peptide and Protein Research* 5(4):179-86.

Cross P, Simmons T, Cunliffe R, Chatfield L. 2009. Establishing a taphonomic research facility in the United Kingdom. *Forensic Science Policy and Management* 1(4):187-91.

Da Silva RHA, De Oliveira RN. 2008. Forensic anthropology and molecular biology: independent or complimentary sciences in forensic dentistry? An overview. *Brazilian Journal of Oral Science* 7(25):1575-9.

Da Silva RHA, Sales-Peres A, De Oliveira RN, De Oliveira FT, Sales-Peres SHC. 2007. Use of DNA technology in forensic dentistry. *Journal of Applied Oral Science* 15(3):156-61.

Dent BB, Forbes SL, Stuart BH. 2004. Review of human decomposition processes in soil. *Environmental Geology* 45:576-85.

Depositor EL, Shipley RK, Sanrore DT, inventors. 1972. Method for determining hemoglobin. US Patent 3663175.

Dickerson RE. 1992. DNA structure from A to Z. *Methods in Enzymology* 211:67-111.

- Dobberstein RC, Huppertz J, Von Wurmb-Schwark N, Ritz-Timme S. 2008. Degradation of biomolecules in artificially and naturally aged teeth: Implications for age estimation based on aspartic acid racemization and DNA analysis. *Forensic Science International* 179:181-191.
- Douglas WR. 1971. Of pigs and men and research. *Origins of life and evolutions of biospheres* 3(3):226-34.
- Erel O. 2005. A new colorimetric method for measuring total oxidant status. *Clinical Biochemistry* 38:1103-1.
- Erickson SJ, Probst RW, Timins ME. 1993. The “Magic Angle” effect: Background physics and clinical relevance. *Radiology* 188:23-5.
- Evison MP, Smillie DM, Chamberlain AT. 1997. Extraction of single-copy nuclear DNA from forensic specimens with a variety of postmortem histories. *Journal of Forensic Sciences* 42(6):1032-8.
- Fish WW, Mann KG, Tanford C. 1969. The estimation of polypeptide chain molecular weights by gel filtration in 6M guanidine hydrochloride. *Journal of Biological Chemistry* 244(15):4859-94.
- Foran DR. 2006. Relative degradation of nuclear and mitochondrial DNA: An experimental approach. *Journal of Forensic Sciences* 51(4):766-770.
- Friedman M. 2004. Applications of the ninhydrin reaction for analysis of amino acids, peptides, and proteins to agricultural and biomedical sciences. *Journal of Agricultural and Food Chemistry* 52:385-406.
- Fuertes MA, Pérez JM, Alonso C. 2004. Small amounts of urea and guanidine hydrochloride can be detected by a far-UV spectrophotometric method in dialyzed protein solutions. *Journal of Biochemical and Biophysics Methods* 59:209-16.
- García AA, Munoz I, Pestoni C, Lareu MV, Rodriguez-Calvo MS, Carracedo A. 1996. Effect of environmental factors on PCR-DNA analysis from dental pulp. *Journal of Legal Medicine* 109:125-9.

Garnero P, Delmas PD. 2003. An immunoassay for type 1 collagen  $\alpha 1$  heliocidal peptide 620-633, a new marker of bone resorption in osteoporosis. *Bone* 32(1):20-6.

Gay C, Gebicki JM. 2000. A critical evaluation of the effect of sorbitol on the ferric-xyleneol orange hydroxyperoxide assay. *Analytical Biochemistry* 284:217-20.

Georgiou CD, Grintzalis K, Zervoudakis G, Papapostoloul. 2008. Mechanism of Coomassie brilliant blue G-250 binding to proteins: a hydrophobic assay for nanogram quantities of proteins. *Analytical and Bioanalytical Chemistry* 391(1):391-403.

Gilbert MTP, Willerslev E, Hansen AJ, Barnes I, Rudbeck L, Lynnerup N, Cooper A. 2003. Distribution patterns of postmortem damage in human mitochondrial DNA. *American Journal of Human Genetics* 72:32-47.

Gornall AG, Bardawill CJ, David MM. 1948. Determination of serum proteins by means of the biuret reaction. *Journal of Biological Chemistry* 751-66.

Götherström A, Collins MJ, Angerbjörn A, Lidén K. 2002. Bone preservation and DNA amplification. *Archaeometry* 44:395-404.

Goulian M. 1971. Biosynthesis of DNA. *Annual Review of Biochemistry* 40:855-98.

Grupe G. 1995. Preservation of collagen in bone from dry, sandy soil. *Journal Archaeological Sciences* 22:193-9.

Hagelberg E, Clegg JB. 1991. Isolation and characterization of DNA from archaeological bone. *Proceedings: Biological Sciences* 244(1309):45-50.

Haglund WD, Sorg MH. 1999. Chemical and ultrastructure aspects of decomposition 1999. In: WD Haglund, MH Sorg, eds. *Forensic Taphonomy*. CRC Press: Boca Raton: 139-50.

Haq I, Ladbury JE, Chowdhry BZ, Jenkins TC, Chaires JB. 1997. Specific binding of Hoechst 33258 to the d(CGCAAATTTGCG)<sub>2</sub> Duplex: Calorimetric and spectroscopic studies. *Journal of Molecular Biology* 271:244-57.

Henssge C, Madea B. 2007. Estimation of the time since death. *Forensic Science International* 165:182-4.

Hermes-Lima M, Willmore WG, Storey KB. 1995. Quantification of lipid peroxidation in tissue extracts based on Fe(III)xylanol orange formation. *Free Radical Biology and Medicine* 19(3):271-80.

Higham TFG, Petchey FJ. 2000. On the reliability of archaeological rat bone for radiocarbon dating in New Zealand. *Journal of the Royal Society of New Zealand* 30(4):399-409.

Hopkins DW, Wiltshire PEJ, Turner BD. 2000. Microbial characteristics of soils from graves: an investigation at the interface of soil microbiology and forensic science. *Applied Soil Ecology* 14:283-8.

Hortin GL, Meilinger B. 2005. Cross-reactivity of amino acids and other compounds in the biuret reaction: Interference with urinary peptide measurements. *Clinical Chemistry* 51(8):1411-9.

Irwin DM, Kocher TD, Wilson AC. 1991. Evolution of the cytochrome b gene of mammals. *Journal Molecular Evolution* 32:128-44.

Janaway RC, Percival SL, Wilson AS. 2009. Decomposition of human remains. *Microbiology and Aging* 1:313-34.

John JC, Facucho-Oliveira J, Jiang Y, Kelly R, Salah R. 2010. Mitochondrial DNA transmission, replication and inheritance: a journey from the gamete through the embryo and into offspring and embryonic cells. *Human Reproduction Update* 16(5):488-509.

Kaiser C, Bachmeier B, Conrad C, Nerlich A, Bratzke H, Eisenmenger W, Peschel O. 2008. Molecular study of time dependent changes in DNA stability in soil buried skeletal residues. *Forensic Science International* 177:32-6.

Kakkar R, Garg R, Suruchi. 2002. Theoretical study of tautomeric structures and fluorescence spectra of Hoechst 33258. *Theochem* 579:109-13.

Kakuichi K, Kobayashi Y. 1971. Sedimentation analysis of soluble collagen and its subunits of chicken leg tendon. *Journal Biochemistry* 69(1):42-52.



- Kapert PE, Gonzales A, Gomes CL, MacDonald VW, Hess JR, Winslow RM. 1993. Acute changes in systemic blood pressure and urine output of conscious rats following exchange transfusion with diaspirin-crosslinked hemoglobin solution. *Transfusion* 33(9):701-8.
- Kararli TT. 1995. Comparison of the gastrointestinal anatomy, physiology, and biochemistry of humans and commonly used laboratory animals. *Biopharmaceutics and Drug Disposition* 16:351-80.
- Klein JP, Schölter M, Frank RM. 1982. Soluble and insoluble proteins of normal human mature enamel. *Archives of Oral Biology* 27(2):133-9.
- Komsa-Penkova R, Spirova R, Bechev B. 1996. Modifications of Lowry's method for collagen concentration measurement. *Journal of Biochemical and Biophysical Methods* 32:33-43.
- Kruger NJ. 2002. The Bradford method for protein quantitation. In: JM Walker, ed. *The protein protocols handbook*. Totowa :Springer:15-20.
- Laemmli UK. 1970. Cleavage of structural proteins during the assembly of the head of bacteriophage T4. *Nature* 227:680-5.
- Love RM, Jenkinson HF. 2002. Invasion of dental tubules by oral bacteria. *Critical Reviews in Oral Biology and Medicine* 13(2):171-84.
- Lovestead TM, Bruno TJ. 2011. Detecting gravesoil with headspace analysis with adsorption on short porous layer open tubular (PLOT) columns. *Forensic Science International* 204:156-61.
- Lui A-J, Chen Y, Jia Y-L, Lui Y-Z, Wang W-H, Zhang G-R. 2007. Separation of  $\beta$ 22 dimer from bovine bone collagen. *Process Biochemistry* 42:542-6.
- Maharat C, Intaraphad U, Jantarasamee P. 2005. Development of pork DNA detection in meat products by PCR technique. *Songklanakarin Journal of Science and Technology* 27(5):995-1002.
- Malaver PC, Yunis JJ. 2003. Different dental tissues as source of DNA for human identification in forensic cases. *Croatian Medical Journal* 44(3):306-9.

Mandell MS, Sodek J. 1982. Metabolism of collagen types I, III, and V in the estradiol-stimulated uterus. *Journal of Biological Chemistry* 257(9):5268-73.

Matsunaga T, Chikuni K, Tanabe R, Muroya S, Shibata K, Yamada J, Shinmura Y. 1999. A quick and simple method for the identification of meat species and meat products by PCR assay. *Meat Science* 51:143-8.

Melander C, Tommerass K. 2008. The influence of sodium hyaluronate molecular weight on protein content according to Lowry and Coomassie blue assays. *Carbohydrate Polymers* 74:745-8.

Mitchell D, Willerslev E, Hansen A. 2005. Damage and repair of ancient DNA. *Mutation Research* 571:265-76.

Moreno LI, Mills D, Fetsher J, John-Williams K, Meadows-Jantz L, McCord B. 2011. The application of amplicon length heterogeneity PCR (LH-PCR) for monitoring the dynamics of soil microbial communities associated with cadaver decomposition. *Journal of Microbiological Methods* 84:388-93.

Mulsow BB, Jacob M, Henle T. 2009. Studies on the impact of glycation on the denaturation of whey proteins. *Europe Food Research Technology* 228(4):643-9.

Myburgh J, Bester MJ, L'Abbe EN. 2008. The use of in vitro bone aging model for the evaluation of DNA isolation methods. Poster presentation. 38<sup>th</sup> Annual Conference of the Anatomical Society of Southern Africa.

Myburgh J. 2010. Estimating the postmortem interval using accumulated degree days in a South African setting. Dissertation (MSc.). University of Pretoria.

Nelson K, Melton T. 2007. Forensic mitochondrial DNA analysis of 116 casework skeletal samples. *Journal of Forensic Sciences* 52(3):557-61.

Nygaard A, Jorgensen CB, Cirera S, Fredholm M. 2007. Selection of candidate reference genes for gene expression studies in pig tissues using SYBR green qPCR. *BMC Molecular Biology* 8:67.

O'Rourke DH, Hayes MG, Carlyle SW. 2000. Ancient DNA studies in Physical Anthropology. *Annual Reviews of Anthropology* 29:217-42.

Opel KL, Chung DT, Drabek J, Tatarek NE, Jantz LM, McCord BR. 2006. The application of miniplex primer sets in the analysis of degraded DNA from human skeletal remains. *Journal of Forensic Sciences* 51(2):351-6.

Parson W, Pegoraro K, Niederstätter H, Föger M, Steinlechner M. 2000. Species identification by means of the cytochrome *b* gene. *Journal of Legal Medicine* 114:23-8.

Payne JA. 1965. A summer carrion study of the baby pig *Sus Scrofa Linnaeus*. *Ecology* 46:592-602.

Perez-Tamayo. 1978. Pathology of collagen degradation. *American Journal of Pathology* 92(2):507-66.

Perotti MA, Goff ML, Baker AS, Turner BD, Braig HR. 2009. Forensic acarology: An introduction. *Experimental and Applied Acarology* 49:3-13.

Péterszegi G, Andrès E, Molinari J, Ravelojaona V, Robert L. 2008. Effect of cellular aging on collagen biosynthesis. Methodological considerations and pharmacological applications. *Archives of Gerontology and Geriatrics* 47:356-67.

Pfeiffer H, Hühne J, Seitz B, Brinkmann B. 1999. Influence of soil storage and exposure period on DNA recovery on DNA recovery from teeth. *International Journal of Legal Medicine* 112:142-4.

Pfeiffer H, Steighner R, Fisher R, Mörnstad H, Yoon C-L, Holland MM. 1998. Mitochondrial DNA extraction and typing from isolated dentin-experimental evaluation in a Korean population. *International Journal of Legal Medicine* 111:309-13.

Pinheiro J. 2006. Decay process of a cadaver. In: A Schmidt, E Cumha, J Pinheiro, eds. *Forensic anthropology and medicine*. Totowa:Humana Press:85-116.

Poinar HN. 2003. The top 10 list: criteria of authenticity for DNA from ancient and forensic samples. *International Congress Series* 1239:575-9.

Pötsch L, Meyer U, Rothschild S, Schneider PM, Rittner C. 1992. Application of DNA techniques for identification using human dental pulp as a source of DNA. *International Journal of Legal Medicine* 105:139-43.

Presecki Z, Brkic H, Primorac D, Drmicl. 2000. Methods of preparing the tooth for DNA isolation. *Acta Stomatology Croatia* 4(1):21-4.

Primorac D. 2004. The role of DNA technology in identification of skeletal remains discovered in mass graves. *Forensic Science International* 1468:S163-S164.

Reeves NM, 2009. Taphonomic effects of vulture scavenging. *Journal of Forensic Sciences* 54(3):523-8.

Rengarajan K, Cristol SM, Mehta M, Nickerson JM. 2002. Quantifying DNA concentrations using fluorometry: A comparison of fluorophores. *Molecular Vision* 8:416-21.

Rieder RF. 1970. Hemoglobin solubility: Observations on the denaturation of normal and abnormal hemoglobins by oxidant dyes, heat and alkali. *The Journal of Clinical Investigation* 49:2369-76.

Rohland N, Hofreiter M. 2007. Comparison and optimization of ancient DNA extraction. *Biotechniques* 42(3):343-52.

Ross MH, Kaye GI, Pawlina W. 2003. Digestive System I: Oral cavity and associated structures. In: *Histology: A text and atlas*. 4<sup>th</sup> ed. Baltimore: Lippincott Williams and Wilkins:440-52.

Rubio L, Martinez LJ, Martinez E, De Las Heras SM. 2009. Study of short- and long-term storage of teeth and its influence on DNA. *Journal of Forensic Sciences* 54(6):1411-3.

Rudin N, Inman K. 2002. *An introduction to forensic DNA analysis*. 2<sup>nd</sup> ed. Boca Raton: CRC Press:21-63.

Ryter SW, Tyrnell RM. 2000. The heme synthesis and degradation pathways: role in oxidant sensitivity: Heme oxygenase has both pro- and antioxidant properties. *Free Radical Biology and Medicine* 28(8):289-309.

Saika RK, Gelfand DH, Stoffel S, Scharf SJ, Miguchi R, Horn GT. 1988. Primer-directed enzymatic amplification of DNA with thermostable DNA polymerase. *Science* 239:487-91.

Saika RK, Scharf S, Fallona F, Mullis KB, Horn GT, Erlich HA. 1985. Enzymatic amplification of  $\beta$ -globin genomic sequences and restriction site analysis for diagnosis of sickle cell anemia. *Science* 230:1350-54.

Sambrook J, Fritsch EF, Maniatis T. 1989. *Molecular cloning: A Laboratory Manual*. New York: ColdSpringHarbor Laboratory Press.

Schaer DJ, Alayash AI. 2009. Clearance and control mechanisms of hemoglobin from cradle to grave. *Antioxidants and Redox Signalling* 12(2):181-4.

Schechter AN. 2008. Hemoglobin research and the origins of molecular medicine. *Blood* 112:3927-38.

Schoenly KG, Hall RD. 2002. Testing reliability of animal models in research and training programs in forensic entomology. Part II. In: Final report. National institute of Justice Journal. US department of Justice, Office of Justice Programs; National Institute of Justice, Washington, DC. 1-34.

Schricker BR, Miller DD. 2006. Effects of cooking and chemical treatment on heme and nonheme iron in meat. *Journal of Food Science* 48(4):1340-3.

Schweet RS. 1953. The quantitative determination of proline and pipecolic acid with ninhydrin. *Journal of Biological Chemistry* 60:3-3.

Shepherd M, Daily HA. 2005. A continuous fluorometric assay for protoporphyrinogen oxidase by monitoring porphyrin accumulation. *Analytical Biochemistry* 334(1):115-121.

Shiroma CY, Fielding CG, Lewis JA, Gleisner MR, Dunn KN. 2004. A minimally destructive technique for sampling dentin powder for mitochondrial DNA testing. *Journal of Forensic Sciences* 49:791-5.

Sorensen AD, Sorensen H, Sondergaard I, Bulchav K. 2007. Non-heme iron availability from pork meat: Impact of heat treatments and meat protein dose. *Meat Science* 76:29-37.

Stadler AM, Digel I, Artmann GM, Embs JP, Zaccai G, Buldt G. 2008. Hemoglobin dynamics in red blood cells: Correlation to body temperature. *Biophysical Journal* 95(11):5449-61.

Stavrianos C, Eldiades A, Kokkas A. 2010. The role of DNA in Forensic Odontology: Part II. *Research Journal of Medical Sciences* 4(5):309-14.

Stevens RE, Hedges REM. 2004. Carbon and nitrogen stable isotope analysis of northwest European horse bone and tooth collagen, 40,000 BP-present: Palaeoclimatic interpretations. *Quaternary Science Review* 23:977-91.

Swann LM, Forbes SL, Lewis SW. 2010. Analytical separations of mammalian decomposition products for forensic science: A review. *Analytica Chimica Acta* 682(1-2):9-22.

Ten Cate AR. 1994. Structure of oral tissues. In: AR Ten Cate, eds. *Oral Histology: Development, structure, and function*. St Louis: Mosby:45-52.

Troll W, Cannan RK. 1953. A modified photometric ninhydrin method for the analysis of amino and imino acids. *Journal Biological Chemistry* 200(2):803-11.

Tudek B. 2003. Imidazole ring-opened DNA purines and their biological significance. *Journal of Biochemical and Molecular Biology* 36(1):12-9.

Ussery DW. 2001. DNA denaturation. *Encyclopedia of Genetics* 1-3.

Van Belle LE, Carter DO, Forbes SL. 2009. Measurement of ninhydrin reactive nitrogen influx into gravesoil during aboveground and belowground carcass (*Sus domesticus*) decomposition. *Forensic Science International* 193:37-41.

Vass AA, Barshick S, Sega G, Caton J, Skeen JT, Love JC, Synsteliën JA. 2002. Decomposition chemistry of human remains: A new methodology for determining the postmortem interval. *Journal of Forensic Sciences* 47(3):542-53.

Vass AA, Bass WM, Wolt JD, Foss JE, Ammons JT. 1992. Time since death determinations of human cadavers using soil solution. *Journal of Forensic Sciences* 33:1236-53.

Virkler K, Lednev IK. 2009. Analysis of body fluids for forensic purposes: From laboratory testing to non-destructive rapid confirmatory identification at a crime scene. *Forensic Science International* 188:1-17.

Von Wurmb-Schwark N, Harbeck M, Wiesbrock U, Schroeder I, Ritz-Timme S, Oehmichen M. 2003. Extraction and amplification of nuclear and mitochondrial DNA from ancient and artificially aged bones. *Legal Medicine* 5:169-72.

Von Wurmb-Schwark N, Simeoni E, Ringleb A, Oehmichen M. 2004. Genetic investigation of modern burned corpses. *International Congress Series* 1261:50-2.

Voss S, Forbes SL, Dadour IR. 2008. Decomposition and insect succession on cadavers inside a vehicle environment. *Forensic Sciences and Medical Pathology* 4:22-32.

Wess TJ, Orgel JP. 2000. Changes in collagen structure: Drying, dehydrothermal treatment and relation to long term deterioration. *Thermochimica acta* 365:119-28.

Wiberg E, Wiberg N, Holleman AF. 2001. Inorganic Chemistry. Academic Press :1440-1.

Williamson B. 2000. Direct testing of rock painting pigments for traces of haemoglobin at Rose Cottage Cave, South Africa. *Journal of Archaeological Sciences* 27:755-62.

Wu G. 1997. Synthesis of citrulline and arginine from proline in enterocytes of postnatal pigs. *American Journal of Physiology–Gastrointestinal and Liver Physiology* 272(6):G1382-90.

Yang DY, Eng B, Waye JS, Dudar JC, Saunders SR. 1998. Improved DNA extraction from ancient bones using silica-based spin columns. *American Journal of Physical Anthropology* 105:539-43.

Ye J, Ji A, Parra EJ, Zheng X, Jiang C, Zhao X, Hu L, Tu Z. 2004. A simple and efficient method for extracting DNA from old and burned bone. *Journal of Forensic Sciences* 4(49):1-6.

Zehner R, Zimmermann S, Mebs D. 1998. RFLP and sequence analysis of the cytochrome *b* gene of selected animals and man: methodology and forensic application. *International Journal of Legal Medicine* 111:323-7.

Zhou P, Regenstein JM. 2006. Determination of total protein content in gelatine solutions with the Biuret or Lowry assay. *Journal of Food Science* 71(8):747-9.